Temporal and Spatial Patterns of Growth and Photosynthesis in Leaves of Dicotyledonous Plants Under Long-Term CO_2- and O_3-Exposure

Inaugural Dissertation

zur

Erlangung des Doktorgrades der

Mathematisch-Naturwissenschaftlichen Fakultät der

Heinrich-Heine-Universität Düsseldorf

vorgelegt von

Diplom-Biologin

Maja Mareike Christ

aus Hannover

2005

Gedruckt mit der Genehmigung der Mathematisch-Naturwissenschaftlichen
Fakultät der Heinrich-Heine-Universität Düsseldorf

Referent: Prof. Dr. Ulrich Schurr
Korreferent: PD. Dr. Dirk Gansert
Tag der mündlichen Prüfung: 22.06.2005

para Andrés

Abstract

The aim of this Ph.D. thesis was to investigate spatio-temporal effects of elevated $[CO_2]$ and $[O_3]$ on leaf growth and photosynthesis in dicotyledonous plants. High-resolution spatio-temporal patterns of leaf growth were measured with a digital image sequence processing method (DISP). For further analysis with the DISP method, the accuracy and resolution was estimated. The results led to the conclusion that temporal courses of leaf RGR could be analyzed with a resolution of at least 1-h-means, while 24-h-means could be used for heterogeneity determination, that requires a high spatial resolution.

Effects of elevated $[CO_2]$ were investigated on *Populus deltoides* trees at Biosphere 2 Center, AZ, USA. After four years in elevated $[CO_2]$ (800 and 1200 ppm), *Populus deltoides* did not show acclimation. In 1200 ppm, net CO_2 exchange rate was stimulated by a factor of 2–3 in growing leaves, accompanied by reduced stomatal conductance and transpiration rate, resulting in increased water use efficiency (WUE) by a factor of 2. Dark respiration was increased by a factor of ca. 1.5 in growing leaves. In high light, photosynthesis did not become CO_2-limited in elevated $[CO_2]$. Excess photosynthate was not completely used for leaf growth, which was accelerated but finally stimulated only by a factor of 1.2, resulting in an accumulation of starch in elevated $[CO_2]$. Relative leaf growth rate (RGR), which showed a clear diel rhythm, was reduced in the afternoon compared to ambient $[CO_2]$, accompanied with a reduced concentration of glucose, the main carbohydrate for growth processes. Results indicate that glucose availability plays an important role in the control of decelerating growth stimulation in elevated $[CO_2]$. Furthermore, elevated $[CO_2]$ increased heterogeneity of leaf RGR, presumably caused by reduced stomatal conductance, as an altered transpiration rate affects turgor and as such, growth. Increased patchiness of growth was accompanied by increased spatial heterogeneity of carbohydrate distribution, which is a further indication for the role of carbohydrates in growth processes.

Experiments on the effects of elevated ozone ($[O_3]$) were performed on *Glycine max* at SoyFACE, IL, USA. Season-long elevation of $[O_3]$ by 20 % above ambient concentration in the field led to a decreased leaf net CO_2 exchange rate of *Glycine max* of up to 30 % at the time of pod-fill, accompanied by a reduction of stomatal conductance. Effects were similar in growing and mature leaves, and leaf growth was slightly reduced, while yield remained unchanged. This might be explained by a shift of assimilates from vegetative to reproductive growth, as soluble carbohydrates were reduced in growing leaves by the end of the growing season. In mature leaves, however, starch accumulated, indicating altered sugar transport in elevated $[CO_2]$. In the growth chamber it could be shown that mild ozone stress (70 ppb, 6 h daily) increased the heterogeneity of leaf growth, which could have been caused by local damage of O_3, which entered the leaf through the stomata and likewise by the altered stomatal conductance.

Experiments on cuttings of *Populus deltoides* showed that fluctuating environmental conditions increased spatial heterogeneity of leaf growth, and could alter the diel course of the leaf RGR, but did not change phasing completely. For *Populus deltoides*, it could further be shown by growth and photosynthesis measurements, that veinal and vein-surrounding tissue develops faster than interveinal tissue.

I

II

Zusammenfassung

Ziel dieser Arbeit war es, raum-zeitliche Effekte unter erhöhtem $[CO_2]$ und $[O_3]$ auf Blattwachstum und Photosynthese dikotyler Pflanzen zu untersuchen. Hoch auflösende raum-zeitliche Blattwachstumsmuster wurden dabei mit einer digitalen Bildverarbeitungsmethode (Digital Image Sequence Processing, DISP) ermittelt. Zunächst wurde die Auflösung und Genauigkeit dieser DISP-Methode bestimmt. Zeitliche Wachtumskurven können mit mindestens 1-h-Mittelwerten dargestellt werden, während Heterogenitätsbestimmungen, die eine hohe räumliche Auflösung benötigen, anhand von 24-h-Mittelwerten durchgeführt werden können.

Effekte von erhöhtem $[CO_2]$ wurden am Biosphere 2 Center in Arizona, USA, an *Populus deltoides* untersucht. Nach vier Jahren in erhöhtem $[CO_2]$ (800 und 1200 ppm) zeigte *Populus deltoides* keine Akklimatisierungserscheinungen. In 1200 ppm war die Netto-CO_2-Austauschrate in wachsenden Blättern um einen Faktor 2–3 stimuliert, verbunden mit einer reduzierten stomatären Leitfähigkeit und Transpirationsrate, was wiederum zu einer erhöhten Wassernutzungseffizienz (water use efficiency, WUE) um einen Faktor 2 führte. Die Dunkelatmung war in wachsenden Blättern um einen Faktor 1.5 vergrößert. Überschüssige Assimilate wurden jedoch nicht vollständig in Blattwachstum umgesetzt. Die Entwicklung war zwar beschleunigt, dennoch war die Endblattfläche nur um einen Faktor 1.2 erhöht. Dies führte zu einer Akkumulation von Stärke in den Blättern. Im Vergleich zu ambientem $[CO_2]$ war die relative Blattwachstumsrate (RGR), die einen deutlichen Tagesgang zeigte, in erhöhtem $[CO_2]$ am Nachmittag leicht reduziert, verbunden mit einer reduzierten Konzentration an Glucose, dem Hauptsubstrat für Wachstum. Diese Ergebnisse deuten auf eine wichtige Rolle von Glucose bei der Kontrolle der Wachstumsregulierung in erhöhtem $[CO_2]$ hin. Des Weiteren führte erhöhtes $[CO_2]$ zu einer gesteigerten Heterogenität der räumlichen Blattwachstumsmuster, die u.a. auf die veränderte stomatäre Leitfähigkeit zurückzuführen ist, da eine veränderte Transpiration einen Einfluss auf den Turgor und somit Wachstumsprozesse haben kann. Die erhöhte Heterogenität des Blattwachstums war verbunden mit einer erhöhten Heterogenität in der Kohlenhydratverteilung im Blatt, was ein weiteres Indiz für die Rolle von Kohlenhydraten in Wachstumsprozessen ist.

Experimente zu Effekten von erhöhtem Ozon ($[O_3]$) wurden am SoyFACE in Illinois, USA, an *Glycine max* durchgeführt. Eine Erhöhung der Ozonkonzentration im Freiland um 20 % führte bei *Glycine max* zur Zeit der Hülsenbildung zu einer verminderten Netto-CO_2-Austauschrate von bis zu 30 %, verbunden mit einer reduzierten stomatären Leitfähigkeit. Die Effekte waren in wachsenden Blättern vergleichbar mit denen in ausgewachsenen. Das Blattwachstum war leicht reduziert, während der Ernteertrag nicht verändert war. Zurückzuführen sind diese Ergebnisse wahrscheinlich auf eine Verschiebung der Assimilate von generativem zu reproduktivem Wachstum, da am Ende der Wachstumsperiode lösliche Kohlenhydratgehalte in wachsenden Blättern reduziert waren. Stärke dagegen akkumulierte in ausgewachsenen Blättern, was auf einen veränderten Zuckertransport in erhöhtem $[O_3]$ schließen läßt. In der Klimakammer konnte gezeigt werden, dass ein leichter Ozonstress (70 ppb, 6 h täglich) eine erhöhte Heterogenität des Blattwachstums hervorrufen kann. Es ist anzunehmen, dass Ozon, das durch die Stomata in das Blatt eindringt, lokale Schäden verursacht, die wiederum die Wachstumsprozesse beeinträchtigt haben. Des Weiteren kann auch hier die veränderte stomatäre Leitfähigkeit einen Einfluss haben.

Experimente an Stecklingen von *Populus deltoides* zeigten, dass fluktuierende Umweltbedingungen sowohl die Heterogenität der räumlichen Blattwachstumsmuster erhöhen, als auch den Tagesgang leicht verändern können, nicht aber die Phase verschieben. Für Pappeln konnte des Weiteren gezeigt werden, dass sich Wachstum und Photosynthese in Adern und ader-umgebendem Gewebe schneller entwickelt als im Intercostalfeld.

IV

Contents

Abbreviations and Definitions

A	Net CO_2 exchange rate (μmol CO_2 m^{-2}s^{-1})
A$_{sat}$	Net CO_2 exchange rate at saturating light conditions (μmol CO_2 m^{-2}s^{-1})
A$_L$	Leaf area (mm^2 or cm^2)
AOI	Area of Interest
ATP	Adenosine triphosphate
B2C	Biosphere 2 Center, AZ, USA
c	Concentration $\left((\mu)\text{mol l}^{-1},\ \text{cm}^{-2}\text{ or g}^{-1}\right)$
c$_i$	Internal CO_2 concentration
CCD	Charge Coupled Device, chip for image acquisition in digital cameras
CMOS	Complementary Metal Oxide Semiconductor, chip for image acquisition in digital cameras
DISP	Digital Image Sequence Processing
DW	Dry weight (g, mg)
ε	Extinction coefficient (l cm^{-2} mol^{-1})
E	Transpiration rate (mol H_2O m^{-2}s^{-1})
e$^-$	Electron
E-Cup	Eppendorf micro reaction tube
EDTA	Ethylendiamintetraacetate
ETR	Apparent rate of photosynthetic electron transport of PS II
F	Steady state level of fluorescence
F$_0$	Minimum fluorescence of dark-adapted leaves
F$_m$	Maximum fluorescence of dark-adapted leaves
F$_m$**′**	Maximum fluorescence of light-adapted leaves
F$_v$	Variable fluorescence of dark-adapted leaves (F$_v$ = F$_m$ − F$_0$)
F$_v$**/F**$_m$	Potential quantum yield of PS II in dark-adapted leaves
ΔF	Variable fluorescence of light-adapted leaves (Δ F = F$_m$′ − F)
ΔF/F$_m$**′**	Effective quantum yield of PS II in light-adapted leaves
FACE	Free Air gas Concentration Enrichment
FLA	Final leaf area (cm^2)
Fru	Fructose
FFT	Fast Fourier Transformation
FW	Fresh weight (g, mg)
G6PDH	Glucose-6-phosphate dehydrogenase
GC	Growth chamber
Glc	Glucose
GR	Absolute Growth Rate (cm^2 d^{-1})
g$_S$	Stomatal conductance (mol H_2O m^{2}s^{-1})
HEPES	N-(2-Hydroxyethyl)-piperazine-N'-(2-ethansulfone acid)
HK	Hexokinase

IFB   Intensive Forestry Biome at Biosphere 2 Center
IR   Infra red
L   Leaf length (mm, cm)
λ   wave length (nm)
LWP   Leaf water potential (MPa)
m   Mass (g, mg)
NADP$^+$ Nicotinamide adenine dinucleotide phosphate
NADPH+H$^+$ Reduced form of NADP$^+$
NPQ   Non-photochemical quenching $\left(NPQ = (F_m - F_m\prime) \, / \, F_m \right)$
OD   Optical density
PAR   Photosynthetically active radiation
                   (λ = 380–710 nm, μmol photons m^{-2}s^{-1})
PGI   Phosphoglucoisomerase
ppb   parts per billion, nl l^{-1}
ppm   parts per million, μl l^{-1}
PS   Photosystem (I, II)
RLA   Actual part of the leaf area in relation to the
                   final leaf area (%)
RGR   Relative Growth Rate (% h^{-1} or % d^{-1})
                   $\left(RGR = \ln (A_2/A_1)/dt*100, A_2 = \text{area at point in time } t_2, \right.$
                   $\left. A_1 = \text{area at } t_1, dt = \text{time between } t_2 \text{ and } t_1 \right)$
ROS   Reactive oxygen species
Rubisco   Ribulose-1,5-bisphosphate carboxylase / oxygenase
RuBP   Ribulose-1,5-bisphosphate
RT   Room Temperature ($^{\circ}$C)
RWC   Relative Water Content
SD   Standard deviation, $SD = \sqrt{\frac{n\sum x^2 - (\sum x)^2}{n(n-1)}}$
SE   Standard error, $SE = \frac{SD}{\sqrt{n}}$
SLA   Specific Leaf Area (cm^2 g^{-1} FW)
SLW   Specific Leaf Weight (1/SLA, g FW cm^{-2})
SoyFACE   Soybean Free Air gas Concentration Enrichment
Suc   Sucrose
TNC   Total non-structural carbohydrates, sum of Glc, Fru, Suc and Starch
Tris   Tris-(hydroxymethyl)-aminomethane
UV   Ultra violette
U$_x$, U$_y$ Pixel velocity in x- or y-direction, respectively
W   Leaf width (mm or cm)
WUE   Water use efficiency (WUE = A/E)

Chapter 1

Introduction

1.1 Plant Growth and Photosynthesis

Growth is one of the most central processes in plants. It is of crucial importance for plant development and for plant performance in variable environments. Growth is dependent on carbon gain of plants by photosynthesis. Thus, the interaction between both, growth and photosynthesis, is of central relevance for plant performance in general.

1.1.1 Leaf Growth: Definition and Relevance

Plant growth is defined as an irreversible increase of biomass and is the result of cell division and elongation (Schurr, 1998). Dicot leaf growth is a spatio-temporal process which is organized in a complex manner (Schurr, 1998). Temporal variations range from small-scale oscillations to diel rhythms (Boyer, 1968; Bunce, 1977; Kemp, 1980; Christ, 2001; Walter et al., 2002a) or dampening of patterns with time when leaves mature (Seneweera et al., 1995). Spatial patterns include heterogeneities that are present only for a short time, differences between veinal and interveinal tissue or base-to-tip gradients (Avery, 1933; Walter and Schurr, 2005). Spatio-temporal considerations are advancing our understanding of development and rhythmicity of biological processes (Rascher et al., 2001). However, complex dynamic processes remain a central enigma (Golden et al., 1997), despite the increasingly precise genetic characterization of oscillating units and their components (Harmer et al., 2000).

Functionally, leaves can be considered as "iterated green antennae" specialized for trapping light energy, absorbing carbon dioxide (CO_2), transpiring water, and monitoring the environment (van Volkenburgh, 1999). Thus, leaf growth has to be coupled to photosynthesis as photosynthesis produces the assimilates that are necessary for growth, but is itself determined by leaf area and morphology. During development, a plant has to optimize its leaves in function as primary photosynthetic organs, and at the same time guarantee water availability (Farquhar and Sharkey, 1982).

Plant growth is heavily dependent on environmental factors, of which water and light are deemed to be the main determinants (Dale, 1988). As plants cannot move to evade stress factors, they have to adapt or acclimate to changing environmental conditions. Up to now, relatively little is known about the physiology of leaf growth and the controlling mechanisms that induce the adaptation to environmental constraints as well as the connections to photosynthesis (Walter and Schurr, 2005).

1.1.2 Analyzing Leaf Growth

Leaf growth can be measured as an increase in length or area. Either the absolute or relative growth rate can be used:

Absolute Growth Rate (GR):   Absolute increase of length or area per time, given in e.g. $cm^2 \, d^{-1}$

Relative Growth Rate (RGR):   Relative increase of length or area per time, given in $\% \, h^{-1}$ or $\% \, d^{-1}$

Leaf area can be determined easily invasively by e.g. scanning detached leaves or non-invasively by e.g. measuring leaf length (and width) of attached leaves with a ruler and calculating area on the basis of a calibration. However, with these methods no high spatio-temporal resolution of growth patterns can be achieved, which is necessary for a better understanding of underlying processes. Until recently, leaf growth could only be examined with relatively low spatial or temporal resolution; for higher resolution a high effort was needed (Maksymowych, 1973; Wolf et al., 1986). LVDTs (linear variable displacement transducers) offer a good temporal resolution but they do not provide any spatial information. Growth analyzing methods with spatial information were either time consuming (Avery, 1933) or did not offer an adequate high resolution (e.g. Taylor et al., 2003).

Schmundt et al. (1998) developed a method that is based on Digital Image Sequence Processing (DISP), with which the RGR of leaves and roots can be analyzed with a high temporal or spatial resolution (see also Walter et al., 2002a,b). Structures in acquired grey-value image sequences are tracked with time via a structure tensor method. The determined velocity fields are used to calculate RGR maps. This method was highly improved during the last three years (e.g. Lai et al., 2005; Matsubara et al., 2005; Scharr, 2005), and resolution and accuracy could be increased (see also Fig. 1.1). Thus, it provides a powerful tool to study spatio-temporal patterns of leaf growth, such as diel cycles, base-tip-gradients or the degree of spatial heterogeneity. Recently, van der Weele et al. (2003) published a similar method for root growth, which shows the importance of comparable methods to understand the complicity of spatio-temporal growth patterns and their relation to physiological and molecular processes.

Figure 1.1: Color-coded map of the relative growth rate (RGR) of a *Populus deltoides* leaf: 24h-mean of the RGR ($\% \, h^{-1}$). Blue color: $0 \, \% \, h^{-1}$ or 'outflow' (the part of the leaf that grew out of the image during the acquisition), red color: $1 \, \% \, h^{-1}$.
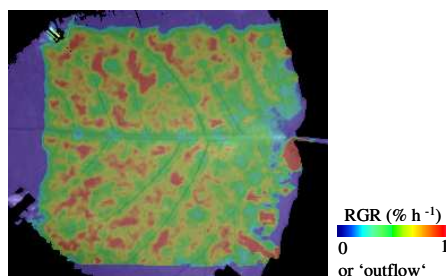
1.1.3 Analyzing Photosynthesis

Photosynthesis consists of two primary processes, the light reactions and the dark reaction (Lambers et al., 1998). During the light reactions of photosynthesis, photons are absorbed, and the excitation energy is transferred to the reaction centers to produce ATP and NADPH+H^+ via the electron transport chain. The dark reaction comprises CO_2 assimilation via the photosynthetic carbon-reduction cycle (Calvin cycle). Photosynthetic processes can be measured in different ways, the most common are analyses of *gas exchange* and *chlorophyll fluorescence*.
Gas exchange comprises the exchange of gases like carbon dioxide (CO_2), oxygen (O_2) and water vapor (H_2O) between the plant and the environment (Lambers et al., 1998). Gas exchange systems measure the *net CO_2 exchange*, which is determined by CO_2 fixating processes as the photosynthetic

CO_2 fixation (CO_2 assimilation) and CO_2 releasing processes as mitochondrial respiration and photo-respiration.

A small proportion of light absorbed by chlorophyll is emitted as fluorescence at approximately 680–760 nm. This fluorescence originates mainly from chlorophyll a (Chl a), associated with photosystem II (PS II). The measurement of the kinetics of *chlorophyll fluorescence* has been developed into a sensitive tool for probing state variables of the photosynthetic apparatus *in vivo* (Krause and Weis, 1991; Lambers et al., 1998; Maxwell and Johnson, 2000).

1.2   Plant Growth and Global Change

The global environment is changing. *Global change* comprises land use and the change of atmo-spheric chemistry, which may induce secondary effects, including climatic changes (Körner, 2003a). Increases in atmospheric concentrations of greenhouse gases might cause rising temperatures, altered precipitation patterns, as well as numerous other potential changes in global climate (Norby et al., 2001; Körner, 2003b) and these changes will also affect plants. Throughout the last decades, much work was done in the field of global change and its impact on plant processes. A high number of pub-lications exist that deal with the effect of elevated [CO_2] on plant growth (Ferris et al., 2001; Taylor et al., 2003; Ceulemans et al., 1994, 1995; Hättenschwiler et al., 2002), photosynthesis (Gunderson and Wullschleger, 1994; Norby et al., 1999; Long et al., 2004; Rogers et al., 2004) and carbohydrate contents (Kehr et al., 1998; Masle, 2000). More recently, also the effect of elevated ozone ([O_3]) on plants was investigated (Mulchi et al., 1992; Morgan et al., 2003, 2004), as well as the combination of elevated [CO_2] and [O_3] (Grams et al., 1999; Noormets et al., 2001; Lui et al., 2004).

Most studies focused on mature leaves or whole plant biomass, and little effort was put on the effects on growing leaves (Pearson and Brooks, 1995; Miller et al., 1997; Wait et al., 1999), although grow-ing tissue comprises a large part of the whole plant and analysis of mechanisms of growing leaves in response to a changing environment is necessary to understand how plants will cope with the altered conditions, in particular if one considers that [CO_2] affects the transition of *sink* to *source* leaves (Stitt, 1991). Furthermore, a change of function always requires a change of structure, i.e. development of new leaves (*structure-function relationship*).

First experiments with elevated [CO_2] or [O_3] were performed on single plants in pots that were culti-vated in closed chambers or closed glasshouse cabinets (GHCs, e.g. Ceulemans et al., 1997). Open top chambers (OTCs) were established to test whether the short-term responses of tree seedlings described in controlled environments would be sustained over several growing seasons under field conditions (Norby et al., 1999), but they could not predict how e.g. canopy closure would influence growth and competition (Gielen and Ceulemans, 2001). Enclosure studies have some major limitations and results cannot be transferred directly to the open field. Effects of elevated [O_3], for example, would be over-estimated in a closed chamber compared to the field. Stomatal conductance is often higher in growth chambers as plants are normally well watered, and air is continuously mixed and forced through the plant canopy, both resulting in higher uptake rates in closed chambers.

FACE (Free Air gas Concentration Enrichment) technologies overcome these limitations and provide a means to investigate the effects of elevated [CO_2] and [O_3] on vegetation without altering atmospheric coupling (McLeod and Long, 1999) as they allow controlled [CO_2] and [O_3] enrichment of large plots within a field without any enclosure. Moreover, changes of the micro-environment imposed by cham-bers are avoided.

1.2.1   Effects of Rising CO_2 on Plant Growth and Photosynthesis

Atmospheric CO_2 concentration [CO_2] rose from a preindustrial value of approximately 280 ppm (μl l^{-1}, Houghton et al., 2001) to a current concentration of 372 ppm (Fig. 1.2 A; Keeling and Whorf,

2002). Dependent on assumptions about economic growth, technological advances and carbon seques-tration by biological and geological processes, $[CO_2]$ is expected to reach $540 – 970$ ppm by the end of this century (Fig. 1.2 B; Prentice, 2001; Houghton et al., 2001).
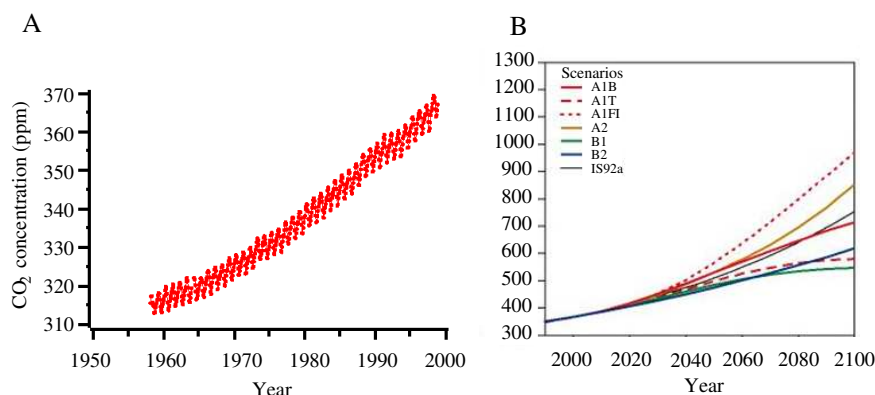

Figure 1.2: Rising $[CO_2]$ from 1958–2000, measured in Mauna Loa, Hawaii, USA (A, source: C. D. Keeling and T. P. Whorf, Scripps Institution of Oceanography, HW, USA, http://cdiac.ornl.gov/ftp/trends/co2/maunaloa.co2), and predicted $[CO_2]$ for this century, calculated with different models (B, source: IPCC, 2001).

Elevated atmospheric $[CO_2]$ has interested biological scientists, especially ecologists and plant phys-iologists, because of the potential biological impacts from CO_2-induced global warming and from direct effects of elevated $[CO_2]$ on vegetation that are independent of global warming (Nowak et al., 2004).

The effects of elevated $[CO_2]$ on plants can be divided in two groups, primary and secondary effects (Ceulemans et al., 1995). Primary effects comprise increasing net photosynthesis (Stitt, 1991; Long and Drake, 1992), decreasing stomatal conductance (Mousseau and Saugier, 1992; Gonzalez-Mehler et al., 1997) and effects on dark respiration (e.g. Curtis and Wang, 1998; Davey et al., 2004), while secondary effects include growth, morphology and development (Ceulemans and Mousseau, 1994).
Photosynthesis of C_3 plants is stimulated by elevated $[CO_2]$, mainly because present $[CO_2]$ is insuffi-cient to saturate Rubisco and because CO_2 inhibits the competing process of photorespiration (Long and Drake, 1992; Drake et al., 1997). However, interactions with other factors such as temperature (Turnbull et al., 2002) and nutrient availability (Kruse et al., 2003) can alter the degree of photosyn-thetic enhancement. Thus, it is discussed whether the photosynthetic stimulation can be maintained in the long-term. A possible decrease of photosynthetic stimulation after a (relatively) long-term $[CO_2]$ exposure has been ascribed to acclimation processes considered to improve plant performance through increased resource use efficiency (Sage, 1994), or as a result of an accumulation of excess carbohy-drates. Thus, $[CO_2]$ responses may be related to growth rate and sink strength (Stitt, 1991). The hypothesis that fast growing species (e.g. poplar) may take more advantage of a $[CO_2]$ enrichment compared to slower growing species, has therefore been examined by a number of researchers (e.g. Tjoelker et al., 1998).

Leaf expansion and cell production are sensitive to CO_2 (Taylor et al., 1994), and leaf growth is often stimulated by elevated $[CO_2]$ (e.g. Taylor et al., 2003), but the response of plant growth is usually smaller than the response of photosynthesis might suggest (Poorter and Navas, 2003). Furthermore, it is likely that growth processes respond to additional carbohydrates from photosynthesis and, as such, altered atmospheric $[CO_2]$ concentration provides a critical insight into how carbon regulates plant development and growth (Masle, 2000).

For tree species a mean photosynthetic stimulation of 40 – 60 % was found in experiments over 1 to 2 growing seasons with an [CO_2] elevation as predicted for the end of this century (Gunderson and Wullschleger, 1994; Curtis and Wang, 1998; Norby et al., 1999). In developing leaves, assimilation was often more strongly stimulated under elevated [CO_2] than in mature leaves (Pearson and Brooks, 1995; Miller et al., 1997; Wait et al., 1999). Although species vary concerning their velocity of leaf development, assimilation changes generally in more or less the same way in all species: photosynthetic capacity increases as leaves develop, becomes maximal at or around full expansion, and then declines later in maturity (Kozlowski et al., 1991). Young leaves are typically strong *sinks* for photosynthates, whereas mature leaves are typically strong *sources* (Vogelmann et al., 1982). Because most studies have been conducted on a limited number of leaf developmental stages, we do not know in general, whether elevated [CO_2] differentially affects photosynthetic capacity as leaves develop.

It is a common observation that plants grown in elevated [CO_2] accumulate more starch in leaves than plants from ambient [CO_2]. The proportion of non-structural carbohydrate increases continuously in leaves from elevated [CO_2] and leads to a higher residence time of freshly assimilated carbon in the mesophyll (Wong, 1990; Vessey et al., 1990). Grimmer et al. (1999) therefore concluded that the stimulation of primary carbon assimilation at elevated [CO_2] could be fully exploited by the plants because of the lack of a similar increase in carbon export or in carbon consumption.

According to Stitt (1991), enhanced [CO_2] should lead to a change in the sink-source balance of the plant. (1.) Carbohydrates accumulate in the source leaves if the rate of photosynthesis exceeds the capacity of the sinks to utilize the photosynthates for growth. Accumulation of carbohydrates has been seen in almost all studies (for references see Stitt, 1991), either as starch or soluble sugars, depending on the normal storage strategy of the plants. Indeterminate plants like cotton, soybean and potato seem to respond better to enhanced [CO_2] than determinate plants like tomato or tobacco (Kramer, 1981). (2.) Variability in the response to [CO_2] in different species, developmental stages or environmental conditions can be explained in terms of the differing sink-strength of the plants (Stitt, 1991). (3.) Some of the morphological changes can be explained in terms of an increased supply of photosynthate which forces the development of new sinks (like bushiness, caused by secondary shoots, Kramer, 1981). An increased leaf area would interact with higher photosynthetic rates to increase the production of photosynthate even further, but this effect is often counteracted at the whole plant level, either because of self-shading or because the rate of photosynthesis on a leaf area basis declines (for references see Stitt, 1991). Non-productive accumulation of large amounts of storage carbohydrates, which are not being turned over, will also reduce the potential response of growth at the whole plant level (for discussion see Wong, 1990). Thus, effects of elevated [CO_2] on plants will be highly complex and diverse.

Forest ecosystems cover approximately 35 % of the world's land surface (Meyer and Turner, 1992; Melillo et al., 1993). They have been estimated to contain up to 80 % of all aboveground and approximately 40 % of all belowground (i.e. soils, roots, and litter) terrestrial organic C (Dixon et al., 1994). Furthermore, they may account for approximately 70 % of the terrestrial net primary productivity (Meyer and Turner, 1992; Melillo et al., 1993). Thus, forests play an important role in global carbon cycle and also in the control of [CO_2] in the atmosphere. They do not undergo global climate changes passively but are also driving factors that may influence the course of climate change (Calfapietra et al., 2003).
A facility that enabled studies on stand-level at near-ecosystem scale in a controlled environment was the Biosphere 2 Center (B2C), AZ, USA (see also Sect. 2.1.2, Fig. 2.4). B2C, originally built to test whether life would be possible in an artificial environment, served as a tool for global change biology on various complex mesocosms from 1996–2003, in particular for the influence of elevated [CO_2] (Walter and Lambrecht, 2004).

The large semi-closed space of B2C uniquely enabled precise $[CO_2]$ exchange measurements at the near ecosystem scale. Highly controllable climatic conditions within B2C also allowed for reproducible examination of CO_2 exchange under different scales in space and time (Barron-Gafford et al., 2005). Advantage over other systems for community level research were the higher suitability to address mass balance issues because the mesocosms could be operated as closed systems and CO_2 fluxes could be measured on the community level. Furthermore, a greater control of environmental parameters over the entire community allowed to study responses to small perturbations (Murthy et al., 2003). Unfortunately, due to political reasons, B2C was closed at the end of 2003 for research, making further experiments impossible.

From 1998–2003, three bays, which were planted with *Populus deltoides* (see also Fig. 2.1), were run with 400, 800 and 1200 ppm CO_2, respectively. *Populus* is well known for its dynamic responses to different environmental factors, and therefore provides a useful study object or even model system in global change research (Gielen and Ceulemans, 2001). *Populus* is characterized by a high growth rate, high plasticity, and unusually high sink strength (Scarascia-Mugnozza et al., 1997), related to an indeterminate growth pattern and to the continuous production of sylleptic branches during periods of active growth. Thus, for poplar a sustained photosynthetic enhancement under elevated $[CO_2]$ may be expected (Gielen and Ceulemans, 2001).

1.2.2   Effects of Rising O_3 on Plant Growth and Photosynthesis

Surface ozone concentration ($[O_3]$) has risen from an estimated pre-industrial concentration of 10 ppb to an average regional concentration of approximately 60 ppb in the middle latitudes of the northern hemisphere and is predicted to rise by 20 % in the next 50 years (Chameides et al., 1994; Prather and Ehhalt, 2001, see also Fig. 1.3). The current mean global ozone concentration of approximately 60 ppb exceeds the threshold for damage to sensitive plant species of approximately 40 ppb (Fuhrer et al., 1997; Mills et al., 2000). In Europe, summer values of 35–55 ppb were reported at the end of the last century (Stockwell et al., 1997), but on sunny days, peak $[O_3]$ in air could be 200 ppb or more in Germany (Umweltbundesamt, 1991).

Ozone appears to affect plant health in two ways: low doses over a long time affect mainly physiological processes and metabolism without causing visible injuries (reviewed by Darrall, 1989), while short periods of moderate to high doses can cause visible injuries and can be even more harmful than long-term exposure to low doses (Kohut et al., 1987; Mehlhorn et al., 1991). Both effects reduce photosynthesis, may enhance premature senescence (Pell and Dann, 1991) and can thereby lead to crop losses (Dann and Pell, 1989). Ozone enters plants through open stomata. Inside the leaf, radicals can be produced from O_3 (Lee, 1968). As it reacts with the components of the cell walls and plasma membranes, reduced oxygen species such as superoxide radicals (O_2^-), hydroxyl radicals ($OH^.$) and hydrogen peroxide are formed (Kangasjärvi et al., 1994). Ozone is thought to cause more damage to vegetation than all other atmospheric pollutants combined (Kley et al., 1999).

Most studies on the effects of elevated $[O_3]$ were conducted in controlled environments and open-top chambers (reviewed in Ashmore, 2002; Morgan et al., 2003). However, as mentioned before, these studies have some major limitations, that can be overcome to some extent by FACE studies, which allow the study of effects of elevated $[O_3]$ on crops grown under field conditions without any enclosure. Large areas of undisturbed canopy are available, where edge effects and other unnatural disturbances to the growing environment can be avoided.

The soybean FACE facility (SoyFACE, Sect. 2.1.2) is situated on 32 hectares of Illinois farmland within the Experimental Research Station of the University of Illinois at Urbana-Champaign (http://
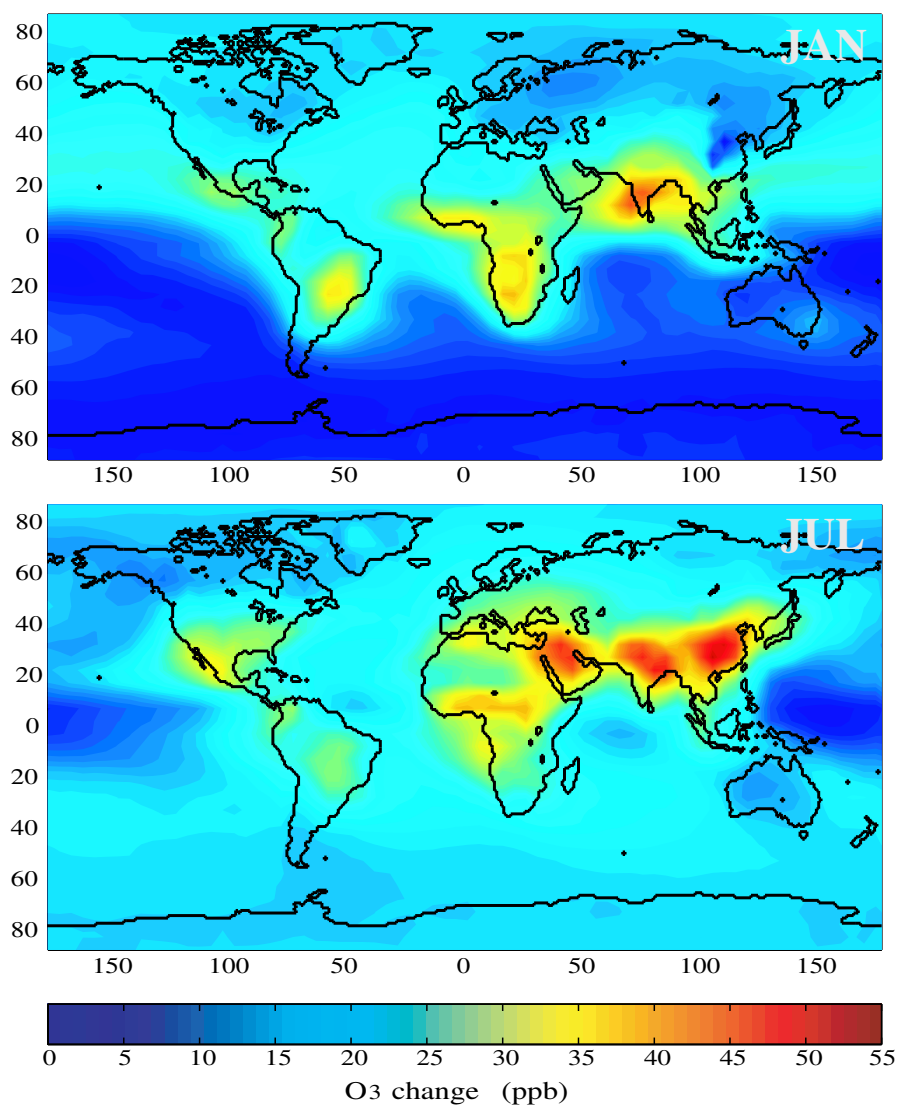
Figure 1.3: Monthly mean surface [O_3] increase (ppb) for January and July from year 2000 to 2100 following scenario A2x. Results are the average of 10 models (Prather and Ehhalt, 2001, HGIS, IASB, KNMI, MOZ1, MOZ2, UCAM, UCI, UIO1, UKMO, ULAQ). Figure taken from Prather et al. (2003), copyright 2003 American Geophysical Union, reproduced by permission of American Geophysical Union.

www.soyface.uiuc.edu). Soybean and maize were each cultivated on one half of the site with annual rotation. Elevated $[O_3]$ was based on projected future mean global tropospheric concentrations, predicted to be increased by 20% in 2050 (Prather and Ehhalt, 2001; Prather et al., 2003).

Soybean (*Glycine max*) is the most widely grown dicotyledonous crop in terms of area planted and a key source of protein. The plant is among the more sensitive species to tropospheric ozone (Fiscus et al., 1997; Ashmore, 2002). Thus, the response of its seed yield to elevated $[O_3]$ and underlying factors are of great interest (Morgan et al., 2003).

1.3   Aim of This Thesis

The aim of this Ph.D. thesis was to investigate the effect of elevated $[CO_2]$ and $[O_3]$ on spatio-temporal patterns of leaf growth and photosynthesis. Leaf growth is stimulated by elevated $[CO_2]$, but not to the same extent as photosynthesis. $[CO_2]$ stimulates cell division and expansion (Taylor et al., 1994) and affects metabolic processes, of which many show diel cycles (Geiger et al., 1998; Matt et al., 2001). Thus, elevated $[CO_2]$ may affect the diel growth cycle.

Furthermore, small-scale spatial heterogeneities were found for stomata movements (Küppers et al., 1999; Osmond et al., 1999) and photosynthesis (Rascher et al., 2001), and as these processes are known to be affected by elevated $[CO_2]$ and $[O_3]$, it is likely that also spatial heterogeneity of leaf growth is affected by these atmospheric gases.

To test these hypotheses, foremost the spatio-temporal resolution of the Digital Image Sequence Processing (DISP) method had to be estimated, and a more general classification of spatio-temporal patterns of growth, photosynthesis and assimilates was made.

Chapter 2

Material and Methods

2.1 Growth Conditions and Plant Material

2.1.1 Plant Material

Experiments were performed on two different model species: *Populus deltoides* (eastern cottonwood, a fast-growing model species for woody plants) and *Glycine max* (soybean, an important crop plant).

Populus deltoides

Populus deltoides Bartr. ex. Marsh (eastern cottonwood, Fig. 2.1) belongs to the Salicaceae and is a deciduous bottomland hardwood that is native in Northern America. Experiments were performed on clone S7c8, which descended from a production fiber farm (Westvaco, Summerville, SC, USA). Height of *P. deltoides* ranges from 10–60 m, maturity occurs with approximately 35 years, life expectancy is 100–200 years. Because of its fast growth, easy handling and small genome, poplar became a model species for woody plants in plant physiology. During the last years a broad genetic database was developed (https://genome.jgi-psf.org/poplar).
The lamina of young, growing leaves of *P. deltoides* is convoluted. In the context of this thesis, unrolling of the leaf was defined as 'leaf emergence'. As measurements were performed on trees, leaves of *P. deltoides* were defined as follows at the beginning of an experiment (Fig. 2.1, B):

- *Mature*: leaf 1,
  (10th leaf downstream of the latest unrolled leaf)
- *Growing, fully unrolled* usually leaf 10
  (latest unrolled leaf, RGR ca. 30 ± 10 % d^{-1} in typical IFB conditions)
- *Growing, still unrolling* usually leaf 12
  (used for chlorophyll fluorescence)

Glycine max

Glycine max L. Merr. (soybean, Fig. 2.2) belongs to the legumes. Experiments were performed on cultivar 'Spencer' that is ozone-sensitive (R. Nelson, personal communication). The plant has flat trifoliates that sprout after two primary leaves and grow relatively fast. Emerging leaves are folded and unfold with a length of approximately 3 cm. For the experiments, leaves were numerated in early August. As some of the first leaves were already wilted or eaten by insects, the 3rd leaf downstream of the latest unfolded leaf was labelled as Leaf '1'. This leaf was already fully expanded. As a result, the latest unfolded leaf at the beginning of August was leaf '4' (Fig. 2.2, B).
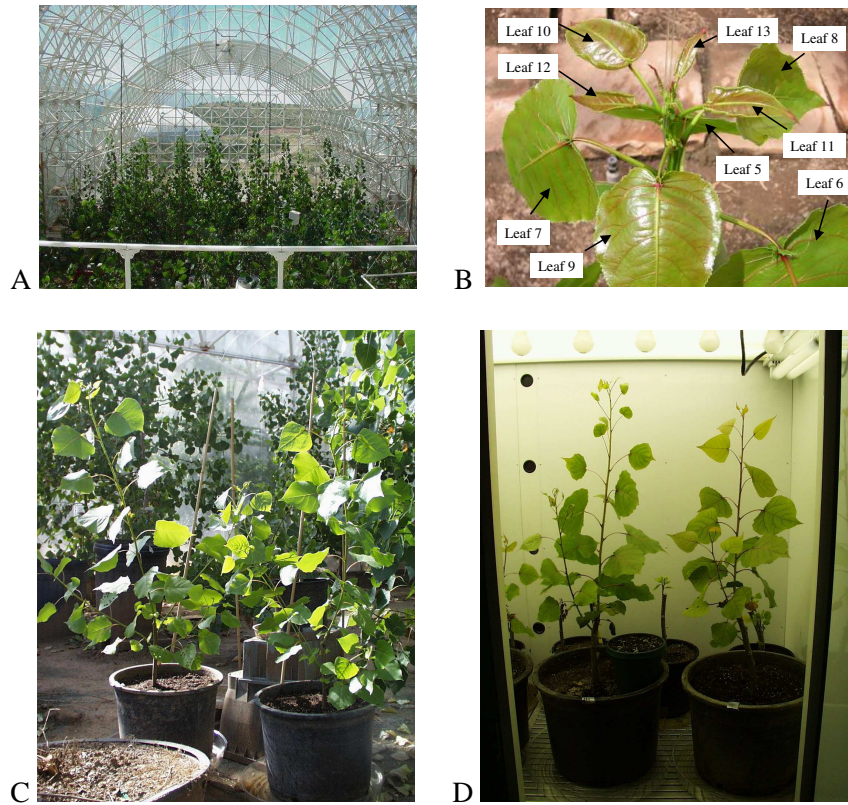
Figure 2.1: *Populus deltoides* trees and cuttings in the Intensive Forestry Biome (IFB) and growth chamber (GC) at Biosphere 2 Center (B2C). Trees in the IFB (A), young shoot of *P. deltoides* (B, photograph courtesy of A. Walter, modified), cuttings in the IFB (C) and in the growth chamber (D) in June 2003.
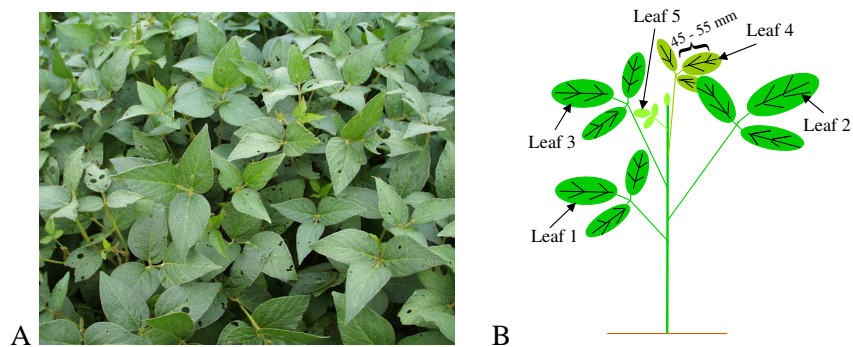

Figure 2.2: *Glycine max* (soybean): field at the SoyFACE facility in Champaign, IL, USA (A), and schematic single plant with numeration of the leaves (B).

2.1.2 Experimental Sites

Experiments with field or greenhouse conditions were performed in the greenhouse (PhyTec) of the Institute of Phytosphere Research (ICG III, Jülich, Germany), in Biosphere 2 Center (Oracle, AZ, USA), and at the SoyFACE facility (Champaign, IL, USA).

Controlled conditions were achieved in growth chambers and cultivation rooms of the Heidelberg Institute of Plant Sciences (HIP, University Heidelberg, Germany), the ICG III, Biosphere 2 Center and the Edward R. Madigan Laboratory of the University of Illinois (Urbana, IL, USA).

Biosphere 2 and SoyFACE are specialized facilities to investigate global change biology and allowed experiments with elevated CO_2 and O_3 in free air or nearly-field conditions.

Experimental Plant Facility PhyTec

PhyTec, the greenhouse of the Institute of Phytosphere Research (ICG III, Research Center Jülich, Germany, 50°54'23"N; 6°24'14"E, 80 m above see level) was developed to cultivate plants under controlled environmental conditions similar to field conditions (Fig. 2.3). To achieve a high transparency for PAR and UV-radiation (up to 97 % in visible light and up to 35 % UV-B transmittance), microstructured glass was installed which lead to a homogeneous illumination of the cultivation area.

The greenhouse that was built in 2003 consists of four compartments, of which two are fully air-conditioned. [CO_2] can be elevated up to 2000 ppm.

Figure 2.3: PhyTec, the greenhouse of the Institute of Phytosphere Research (ICG III, Research Center Jülich, Germany). The greenhouse consists of high PAR and UV permeable glass (photograph courtesy of U. Schurr).

Biosphere 2 Center (B2C)

Biosphere 2 Center (B2C), located at Oracle, AZ, USA (32°35'N, 110°51'W, 1200 m above see level) consists of five separated biomes in which climate could be controlled separately from each other: a rain forest, an ocean, a savanna, a desert and the Intensive Forestry Biome (IFB, former agro-forestry biome, Fig. 2.4; for more information see Dempster, 1999; Zabel et al., 1999; Griffin et al., 2002; Murthy et al., 2003).

Experiments for this thesis were performed in the 2000 m^2 comprising IFB (Fig. 2.1, A). It was physically isolated from the remainder of B2C and separated into three distinct bays by transparent polyvinyl chloride (PVC) curtains. Each bay was approximately 42 m long in a north-south orientation, 18 m wide and maximally 24 m high, with a volume of approximately 12,000 m^3 and a soil depth of approximately 1 m. Based on their orientation, the bays were referred to as *East Bay*, *Center Bay* and *West Bay* (Fig. 2.4).

The bays were kept at daytime CO_2 levels of 400 ppm, 800 ppm and 1200 ppm (see Fig. 2.6), by controlled CO_2 injection via Sierra mass flow controllers (60 l min^{-1}) using LiCor 'Gashound' infrared gas analyzers (LiCor, Lincoln, NE, USA). Well water purified by reverse osmosis was used for irrigation via rotary sprinkler heads mounted high in the roof-support system (space frame). The space frame structure and the laminated glass reduced the irradiation in the biomes to about 50 % of the incident irradiation and blocked out UV radiation completely.
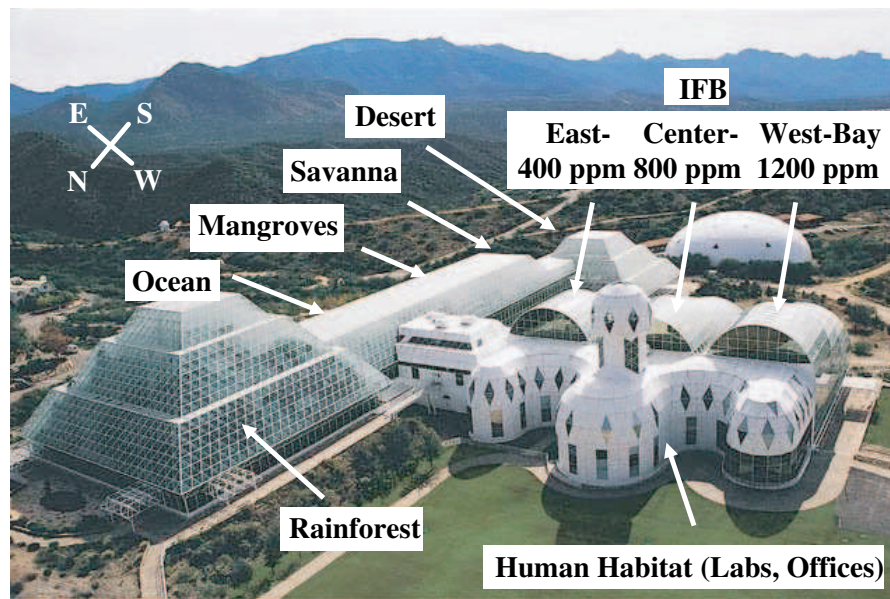
Figure 2.4: Overview of the Biosphere 2 Center, Oracle, AZ, USA: human habitat, rain forest, ocean, mangrove forest, savanna, desert and agro-forestry (Intensive Forestry Biome, IFB) with different CO_2 concentrations. Photograph taken from http://www.bio2.com (modified).

SoyFACE

The soybean FACE facility (SoyFACE) is situated on a 32 ha field within the Experimental Research Station of the University of Illinois at Urbana-Champaign, USA (40°03'21.3"N, 88°12'3.4"W, 230 m above see level). Soybean and maize were each cultivated on one half of the field, with annual rotation and typical Illinois agricultural practices (Long et al., 2004; Rogers et al., 2004).

In the 16 ha that were planted with soybean four blocks were situated, each containing one control, one elevated $[CO_2]$ (current $[CO_2]$ x 1.5), one elevated $[O_3]$ (current $[O_3]$ x 1.2) and one combination treatment plot (Fig. 2.5). Arrangement of the plots was randomized, and they were separated by at least 100 m to avoid cross-contamination. Plots were subdivided into 52 subplots (Fig. 2.5, A) that were planted with different soybean cultivars.
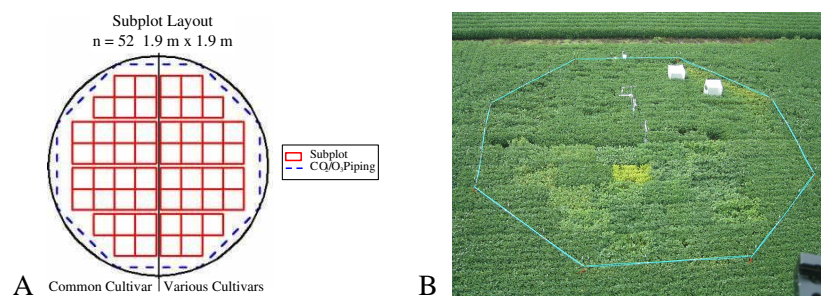

Figure 2.5: SoyFACE facility in Champaign, IL, USA. Schematic overview of the subplot layout (A), and one plot in August 2004 (B). Figure (A) taken from http://www.soyface.uiuc.edu, photograph (B) courtesy of A. Walter and U. Rascher.

Wind direction and velocity were measured in the center of the plot, a computer controlled the release of gases. Micro-pores in a segmented tube around the circumference released CO_2 or/and O_3 according to the wind direction. Elevation of the gas concentration was achieved by the method of Miglietta et al. (2001), in case of the ozone treatment with compressed air enriched in O_3 replacing compressed CO_2 of the original design. Each plot was defined by an octagon (diameter 21 m) of horizontal pipes that released O_3 at approximately 10 cm above the soybean canopy to assure a constant increase above the current ozone level. Ozone was generated as described by Morgan et al. (2004) and was injected into the wind and carried over the crop. Rate and position of gas release needed to maintain the enrichment within the ring was achieved via an anemometer and wind vane in the center of each plot. In 2004, fumigation began in June and continued throughout the daylight hours until harvest.

2.1.3 Growth Conditions

Populus deltoides – Greenhouse

P. deltoides cuttings derived from lower side branches of trees of the IFB at Biosphere 2 and were planted directly into soil after a cold period and let to grow in a cultivation room. They were transferred to 12 l-pots in the greenhouse and coppiced approximately every 4 months. Plants were watered automatically with tap water and additionally once a week with 0.5 l/pot 'HakaPhos' nutrient solution (30 ml/l, 10 %, N:P:K:Mg = 8:12:24:4 %, Compo GmbH & Co. KG, Münster, Germany).
When experiments were performed, mean midday PAR was in average 800 μmol m^{-2} s^{-1} with maximal values of 1200 μmol m^{-2} s^{-1}, temperature was set to 21/19°C day/night, reaching 30°C on sunny summer days, relative humidity was 60 %. When sunlight was lower than 130 μmol m^{-2} s^{-1}, artificial illumination was switched on (SON-T, Philips, Köln, Germany; HQI-Lamps, Osram, München, Germany; approximately 400–450 μmol m^{-2} s^{-1} at the tip of the cuttings).

Populus deltoides – Biosphere 2 Center: Trees

Approximately 50 cuttings of *P. deltoides* were planted in each bay of the Intensive Forestry Biome (IFB) in Biosphere 2 Center in 1998 (Murthy et al., 2003; Walter and Lambrecht, 2004). From 1999 to 2002 the plants were coppiced prior to the growing season with roots and trunk base remaining in the soil. In winter 2002/2003 they were not coppiced but forced into dormancy. Experiments on these trees were performed in the growing seasons of 2002 and 2003.

Within each bay the atmospheric CO_2 concentration, air and soil temperature, soil water and humidity levels could be independently manipulated (Rosenthal et al., 1999). From 1999 to 2003 the bays were kept at three different daytime CO_2 concentrations: 400 ppm (East Bay), 800 ppm (Center Bay) and 1200 ppm (West Bay). Meteorological data were captured every 15 minutes. Table 2.1 shows mean day and night temperature and midday mean light intensities of September 2002 and from May to July 2003. A typical diel course of [CO_2], light intensity and temperature over two days (May 1st and 2nd) is given in Fig. 2.6. Although [CO_2] changed diurnally by several hundred ppm due to the large phytomass:airmass ratio inside B2C, diel mesocosm gas exchange characteristics inside B2C were comparable to field situations (Rosenthal et al., 1999).

Populus deltoides – Biosphere 2 Center: Cuttings

Cuttings (length approximately 30 cm, Fig. 2.1, bottom) derived from lower side branches of 4-year-old trees grown in the IFB. They were cut in February 2003 and let to root in water/rooting solution (Greenhouse Professional Root Stimulator, Schultz, Bridgeton, MO, USA) in the growth chamber. After one month they were planted in pots (first 20 cm, later 40 cm diameter) with a soil/sand mixture, two weeks later five pots were transferred to the IFB, and five pots remained in the growth chamber.

Table 2.1: Meteorological data of the Intensive Forestry Biome (IFB) in September 2002 and May – July 2003: means of daytime maximum and nighttime minimum temperature in °C and midday mean photosynthetically active radiation (PAR) in μmol m^{-2}s^{-1}.

Bay	[CO$_2$]	Month Year	Temperature day (max, °C)	Temperature night (min, °C)	PAR μmol m^{-2}s^{-1}
		Sep 2002	38	20	878
East	400	May 2003	32	21	970
	ppm	Jun 2003	32	21	1111
		Jul 2003	31	23	1051
		Sep 2002	37	18	929
Center	800	May 2003	34	21	880
	ppm	Jun 2003	37	22	993
		Jul 2003	39	23	921
		Sep 2002	39	19	773
West	1200	May 2003	34	21	826
	ppm	Jun 2003	33	22	821
		Jul 2003	32	24	869

Figure 2.6: Meteorological data of the Intensive Forestry Biome (IFB) of two days in May (1st and 2nd): [CO$_2$] in ppm (A), photosynthetically active radiation (PAR) in μmol m^{-2}s^{-1} (B) and temperature in °C (C) in all three bays.
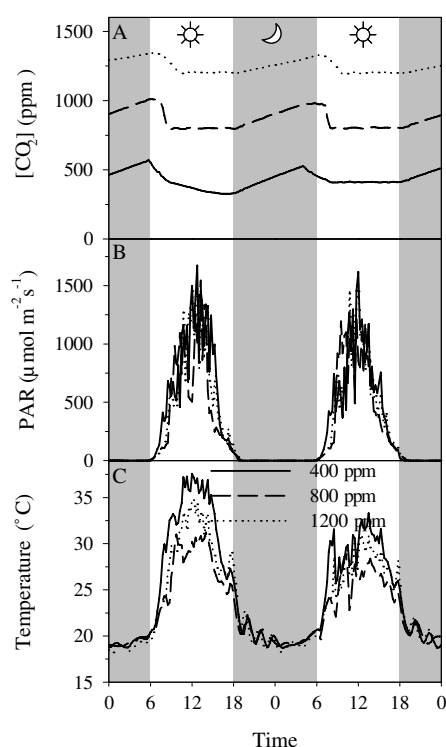
The growth chamber at B2C (E15, Conviron, Winnipeg, Manitoba Canada) was kept at 25/20°C day/night, 60 % relative humidity, 12/12 h day/night, 600 μmol m^{-2} s^{-1}. Lights were switched on from 12 pm to 12 am, this time was converted for the figures for a better comparison with cuttings in the IFB (12 pm was set to 8 am). Throughout the experimental period, day temperature in the IFB rose up to 35°C, night temperature was approximately 20°C. Light intensities were maximally 1500 μmol m^{-2} s^{-1}, with high fluctuations. Fig. 2.7 shows a comparison of temperature and light intensity in the East Bay of the IFB and in the growth chamber on May 4th and 5th, 2003.
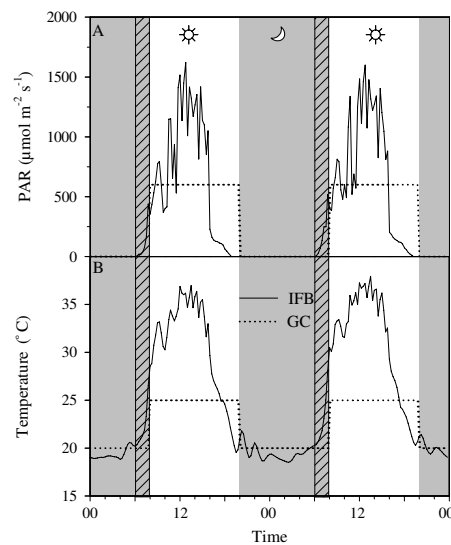
Figure 2.7: Diel photosynthetically active radiation (PAR, A) and temperature (B) in the East Bay of the Intensive Forestry Biome (IFB, solid line) and the growth chamber (GC, dotted line) at Biosphere 2 Center.

Glycine max – SoyFACE facility

G. max L. Merr. cv. Spencer was planted in May 2004 at the SoyFACE facility (Sect. 2.1.2). Row spacing was 0.38 m. Three out of the four blocks were chosen (n = 3). In each plot (ambient and elevated ozone) four plants were selected as sub-replicates. Leaves used for measurements, especially fully expanded ones, were exposed to full sunlight. Experiments were performed late in the growing season in August 2004. Meteorological data during this time are shown in Fig. 2.8.

Glycine max – Growth Chamber

G. max L. Merr. cv. Spencer was planted in pots in July 2004. Plants were grown under controlled conditions (14/10 h day/night, 25/20°C, 60 % relative humidity, approximately 600 μmol m^{-2} s^{-1} light intensity in an ambient and an ozone chamber (E15, Conviron, Winnipeg, Manitoba Canada). In the ozone chamber, ozone fumigation was kept at 70 ppb $\pm$ 10 % for six hours, starting three hours after lights were switched on. When ozone fumigation started, plants were 6 weeks old and in the 6-trifoliate-stadium.
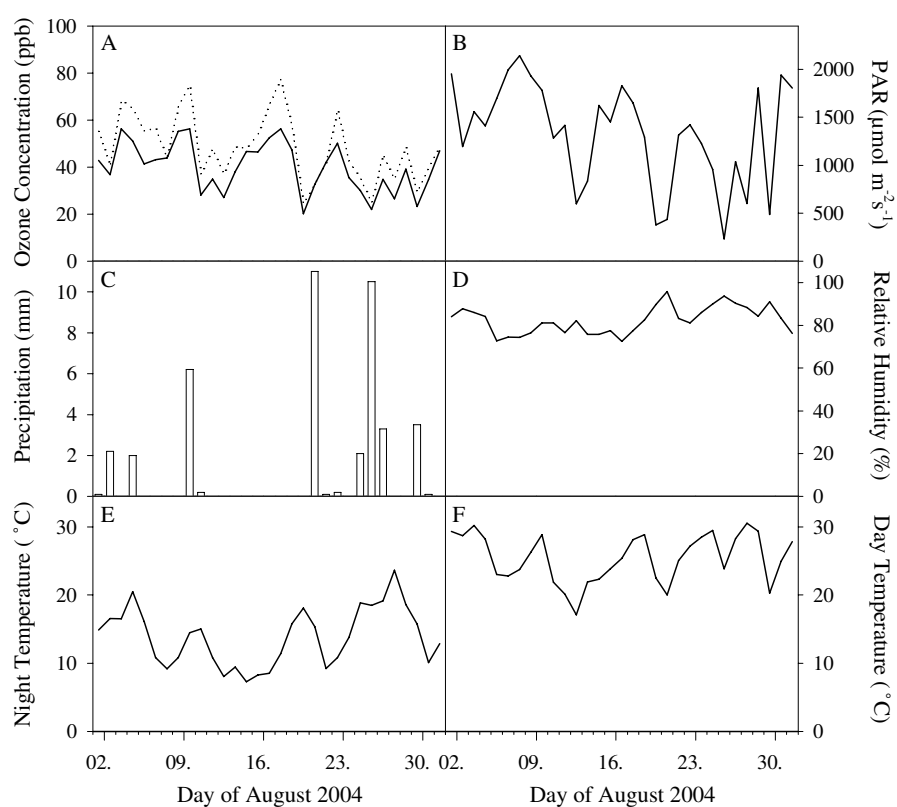
Figure 2.8: Meteorological data at the SoyFACE facility in August 2004. Ambient (bold line) and elevated (dotted line) ozone concentration (ppb, A), midday mean photosynthetically active radiation (PAR, μmol m^{-2}s^{-1}, B), daily precipitation (mm, C), mean relative humidity (%, D), nighttime minimum temperature ($^\circ$C, E) and daytime maximum temperature ($^\circ$C, F).

2.2 Measurement of Leaf Growth

A range of different methods was used to analyze leaf growth. They include classical methods, i.e. measuring leaf length or fresh weight, as well as the Digital Image Sequence Processing (DISP) method. Classical methods are useful to record growth in the long-term, while the DISP method provides a powerful tool to analyze short-term reactions with a high spatio-temporal resolution.

2.2.1 Classical Leaf Growth Measurements

Leaf Area A_L

Single leaf area (A_L) is proportional to the product of leaf length L and width W (Fig. 2.9):

$$A_L = f \cdot L \cdot W \tag{2.1}$$

where the 'form factor' f is dependent on the species, and sometimes also on the developmental stage. Values for f were determined as:

P. deltoides	:	0.61	(unrolled leaves, Fig. 2.9, B)
G. max	:	0.74	(field, independent of development, E.A. Ainsworth, personal communication)
N. tabacum	:	0.75	(independent of development, Walter, 1997)

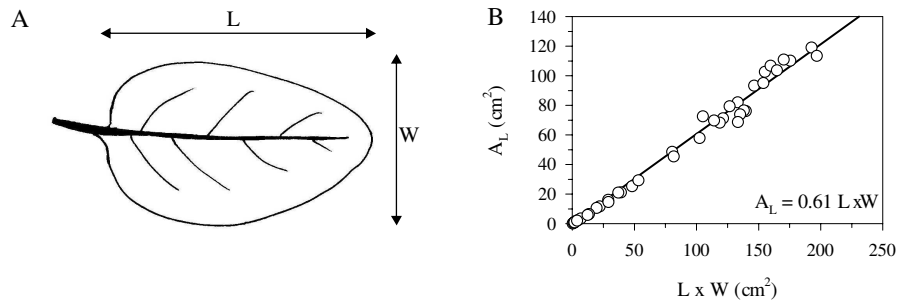L and W were measured non-destructively with a ruler.

Figure 2.9: Definition of leaf length L and width W for single leaf area calculation (A) and relationship between $L \cdot W$ and leaf area A_L for *Populus deltoides* (B).

Absolute Growth Rate (GR)

Absolute growth rate (GR) is defined as:

$$GR \ (cm^2 \ d^{-1}) = \bigl(A_L(t_2) - A_L(t_1)\bigr)\Delta t \tag{2.2}$$

with the difference of the leaf areas $A_L(t_1)$ and $A_L(t_2)$ at the points in time t_1 and t_2 and $\Delta t = t_2 - t_1$.

Relative Growth Rate (RGR)

Relative growth rate (RGR) is defined as:

$$RGR = \frac{1}{A_L}\frac{dA_L}{dt} \tag{2.3}$$

and is calculated by the integral of Eq. 2.3:

$$RGR\ (\%\ d^{-1}) = \frac{100}{\Delta t} ln \frac{A_L(t_2)}{A_L(t_1)} \tag{2.4}$$

where $A_L(t_1)$ and $A_L(t_2)$ are the leaf areas at the points in time t_1 and t_2, respectively (Walter and Schurr, 1999).

Relative Leaf Area (RLA)

The relative leaf area (RLA) is an important developmental index and is defined as the part of the leaf area at a certain point in time compared to the final leaf area (FLA, Walter, 1997; Christ, 2001). The RLA plotted against the RGR at a specific point in time reveals information about the growth behavior of leaves.

Fresh and Dry Weight

Leaf fresh weight (FW) was determined by weighing leaf disks immediately after harvest with an analytical balance (accuracy 0.1 mg). After drying the leaf disks at 80°C until their weight was constant, dry weight (DW) was determined. Fresh weight of midveins was determined immediately after cutting the veins off with a scalpel.

2.2.2   Digital Image Sequence Processing (DISP)

With the Digital Image Sequence Processing method (DISP), leaf growth is analyzed via algorithms that calculate the RGR from the pixel velocities of a sequence of grey value images captured by a CCD or CMOS camera (structure tensor method, see e.g. Schmundt et al., 1998; Scharr, 2005). This method is used to analyze spatial and temporal patterns of single leaf growth.

Image Acquisition

For image acquisition standard CCD or CMOS cameras were used (Sony XC55, Sony XC75 or Point Grey Flea BW, Fig. 2.10, resolution: 640x480 pixel). To obtain a constant illumination during day and night without affecting the plant growth behavior, near infrared light ($\lambda = 880$ or 940 nm) was used. In a two-dimensional (2D) setup the leaf had to be fixed in the focal plane to prevent movements. A set of small weights (3–5 x 12 g) was used to guarantee a growth pattern similar to that of a free moving leaf (Walter et al., 2002a). Grey value images were acquired every 60 or 120 seconds (*Aufnahme3.1* or *AufnahmeFire*). These images were composed of an average of 20 images, taken within 1 sec to diminish noise.

Image Analysis

In the obtained image sequences, local grey value structures are shifted with time because of the movement and growth of the object. The used data model assumes that there is no change in brightness between two following images (optical flow via brightness constancy constraint equation, BCCE). The first step of the calculation is the computation of displacement vector fields for each image. Any structure with a suitable grey value contrast to its neighborhood results in oriented grey value structures in piled-up image stacks (Figure 2.11). The orientation of trajectories in the spatio-temporal neighborhoods of the central pixel are analyzed by means of a structure tensor approach and lead to a velocity vector for the motion of the central pixel (see e.g. Schmundt et al., 1998).
After determination of velocities for all suitable pixels in the image stack, missing information is filled in by a regularization, based on normalized convolution (Jähne et al., 1999). Areal growth rates can be calculated as the divergence of the estimated velocity field (Figure 2.12).
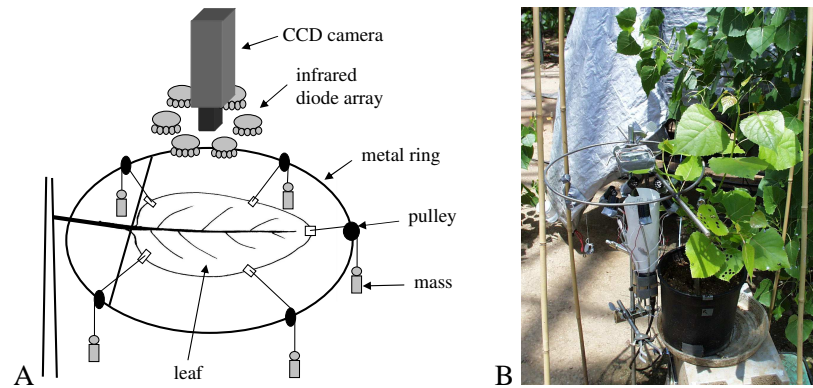
Figure 2.10: 2D DISP setup: Scheme of the acquisition (A) and fixed leaf of a cutting of *Populus deltoides* in the IFB (B).
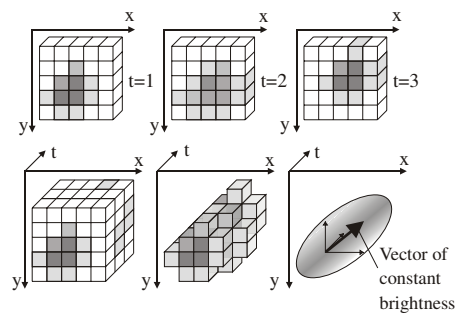

Figure 2.11: Scheme of the velocity calculation from moving grey value patterns by detection of the orientation of grey value gradients in image stacks (figure courtesy of A. Walter).
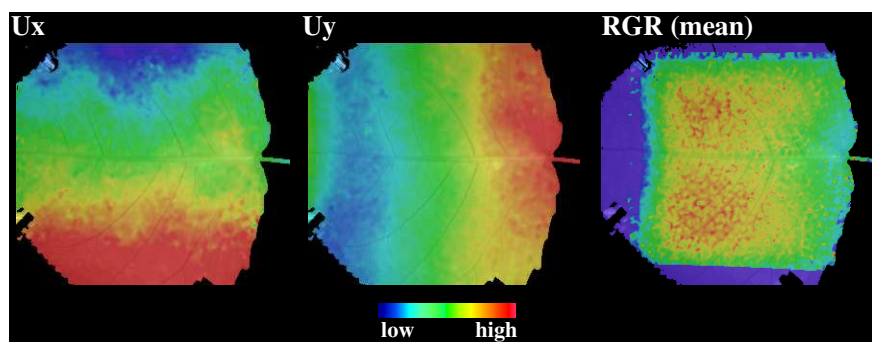

Figure 2.12: Color coded pixel velocities (U_x, U_y) and mean relative growth rate (RGR, 24 h) of a *Populus deltoides* leaf.

The data processing is divided into two parts: analysis of the pixel velocities and output of means of the RGR of a certain section or *Area Of Interest* (AOI). Analysis of pixel velocities is done with algorithms that are based on Schmundt et al. (1998) and Scharr (2005). The parameters typically used are given in the Appendix (p. 125).

The DISP method provides either a high temporal or a high spatial resolution at the expense of some information of the other variable:

- **GrowFlow**   high temporal resolution
  output: time course of spatially averaged RGR
- **RGRFlow**   high spatial resolution
  output: single image of temporally averaged RGR

Temporal information of the RGR is estimated from the pixel velocity maps with the program *GrowFlow* (Fig. 2.13). An AOI is chosen on the leaf and the average RGR of the AOI is estimated for every point in time. The spatial averaging works on a *Lagrange* basis, i.e. the structure is tracked and the selected area 'flows' with the growing area. In this program, also a slight temporally averaging occurs: for every point in time the RGR of neighboring points in time are taken into calculation of the short-term average (typically 5–20 points in time, corresponding to 5–40 minutes, depending on the acquisition frequency).
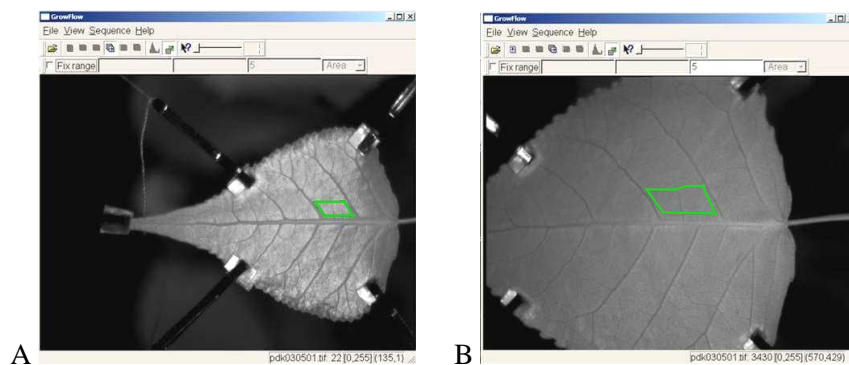

Figure 2.13: GrowFlow: *Populus deltoides* leaf at the beginning (A) and the end
(B) of an image sequence over a period of 6 days. The 'area of interest' (AOI, green)
is shifted with time.

Spatial information of the RGR can be obtained by averaging all images or a certain part of the sequence. This is done with the algorithm *RGRFlow*. After determination of the pixel velocities the mean RGR is calculated via a *Lagrange* description by tracking the structures. The result is one TIFF file with the mean RGR values for the leaf without short-time fluctuations and a TIFF file with information about the regions that flew out of the image.

Data Processing

For further analysis, RGR values lower than -2 % h^{-1} and higher than 6 % h^{-1} were discarded as outliers and hourly means were determined. For comparison of different diel courses, data were normalized as follows: the daily mean of the hourly averaged RGR was estimated and set to 100 %. Every RGR value was then expressed relative to the daily mean. Figure 2.14 shows the RGR course of a single *P. deltoides* leaf (A), the absolute hourly mean (B) and normalized hourly RGR (C), as well as the mean values of all measured days of one month in 2003 (D, E).
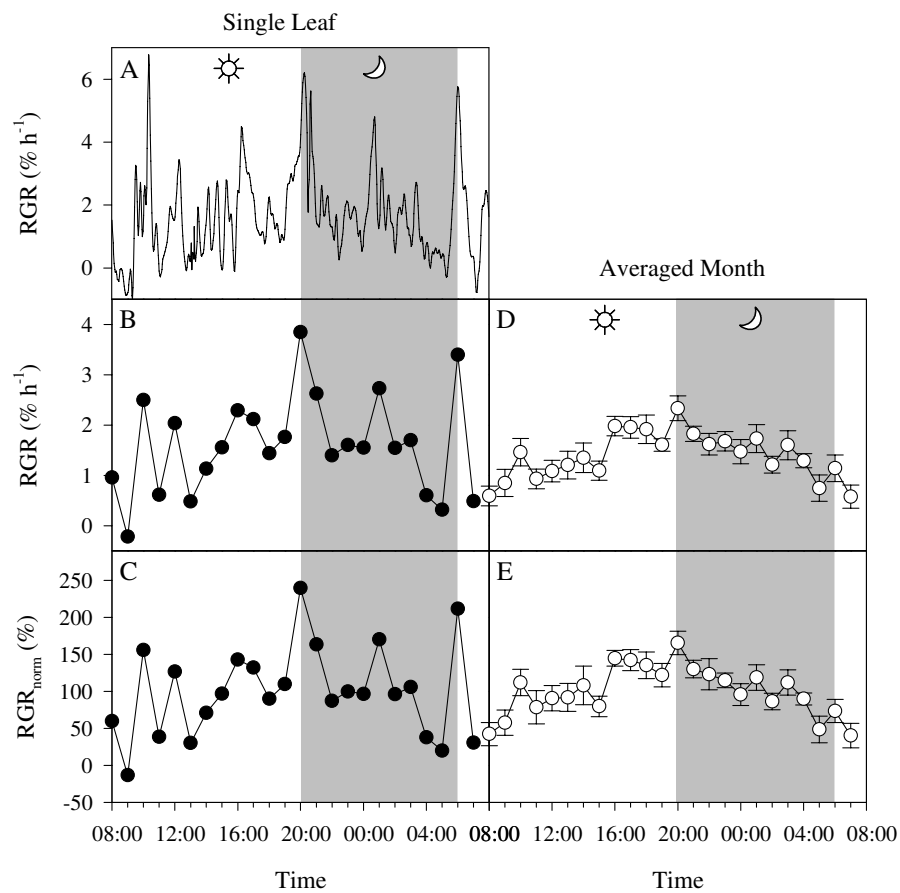
Figure 2.14: Diel relative growth rate (RGR) course of a single *Populus deltoides* leaf and mean of all measured leaves of one month in 2003: Raw data of a single leaf RGR in % h^{-1} (A), hourly mean in % h^{-1} (B), normalized hourly mean RGR in % of daily mean (C), and mean of 11 leaves $\pm$ SE for hourly mean (D) and normalized hourly mean (E).

Analysis of Heterogeneity

Spatio-temporal heterogeneity can be determined by different approaches (see e.g. Hütt and Neff, 2001). For this thesis, heterogeneity of RGR maps was determined with the program *energy* that utilizes the following principle. The energy functional

$$J = \int_\Omega |\nabla u|^2 dx \tag{2.5}$$

of a function *u* over a domain Ω measures how much *u* changes. A homogeneous function *u*, e.g. a constant, has a low energy *J*, while a fast oscillating (heterogeneous) *u* has a high energy. The energy functional is influenced by periodic as well as aperiodic components of heterogeneity. This fact is used to estimate the heterogeneity of the RGR. In a rectangular domain the function with minimal energy is determined for given boundary values. This function is the solution of the LaPlace equation:

$$\Delta u = 0 \ in \ \Omega \tag{2.6}$$
$$u = g \ on \ J \ \Omega, \tag{2.7}$$

where *g* is the boundary value function. The heterogeneity is now defined as:

$$\gamma = \frac{J(u_{measured}) - J(u_{LaPlace})}{\mu(\Omega)} \tag{2.8}$$

where $u_{measured}$ is the measured RGR, $u_{LaPlace}$ the minimal energy RGR for given boundary values (LaPlace solution) and $\mu(\Omega)$ the area of the rectangular. A high γ stands for more heterogeneity. Spatial heterogeneity was estimated for 24-h RGR maps. Care was taken to exclude the midvein and to include a comparable amount of side-veins in the AOIs. Two AOIs per leaf were used as sub-replicates.

Determination of Mean RGR of AOI Matrices

Mean RGR and variance of defined AOI matrices in RGR maps were calculated with the program *algotest*. It was used for the estimation of the accuracy of the DISP method and for determination of base-tip-gradients of leaf growth.

Fast Fourier Transformation

Discrete Fast Fourier Transformations (FFT) are a standard tool to analyze periodic time series. FFTs were performed with the program *fft*, which determines the amount of periodic wavelengths of a given time course.

2.3 Measurement of Photosynthesis

2.3.1 Chlorophyll Fluorescence

Spot measurements of chlorophyll a (Chl a) fluorescence were performed with a portable pulse-amplitude modulated photosynthesis yield analyzer (Mini-PAM, Heinz Walz GmbH, Effeltrich, Germany), provided with a leaf-clip holder 2030-B (Fig. 2.15 A, see also Bilger et al., 1995; Rascher et al., 2000). Spatially resolved measurements of chlorophyll fluorescence were performed with a kinetic imaging fluorometer (Open FluorCam, Photon Systems Instruments, Brno, Czech Republic, Fig. 2.15 B, see also Nedbal et al., 2000). The fluorometer was equipped with a CCD camera and a standard 25 mm lens (Cosmicar/Pentax, Japan) instead of the provided fisheye lens.

The definitions of the fluorescence parameters are outlined in Tab. 2.2 (for more details see Krause and Weis, 1991; Maxwell and Johnson, 2000). Potential quantum yield of photosystem (PS) II, F_v/F_m, was measured at predawn after a minimum dark adaptation time of 5 hours. The effective quantum yield of PS II, $\Delta F/F_m'$, was measured at midday. For spot measurements special care was taken not to change the ambient conditions (e.g. the angle of the measured leaf, shading). Measurements with the imaging fluorometer were performed on detached leaves immediately after cutting.

Table 2.2: Parameters of chlorophyll fluorescence.

Parameter	Definition
F	Steady state level of fluorescence [a]
F_0	Minimum fluorescence of dark-adapted leaves [a]
F_m	Maximum fluorescence of dark-adapted leaves [a]
F_m'	Maximum fluorescence of light-adapted leaves [a]
F_v	Variable fluorescence of dark-adapted leaves ($F_v = F_m - F_0$) [a]
F_v/F_m	Potential quantum yield of PS II in dark-adapted leaves [b]
ΔF	Variable fluorescence of light-adapted leaves ($\Delta F = F_m' - F$) [a]
$\Delta F/F_m'$	Effective quantum yield of PS II in light-adapted leaves [c]
NPQ	Non-photochemical quenching (NPQ = $(F_m - F_m') / F_m$) [d]

[a] van Kooten and Snel (1990), [b] Björkman and Demmig (1987), [c] Genty et al. (1989), [d] Bilger and Björkman (1990).
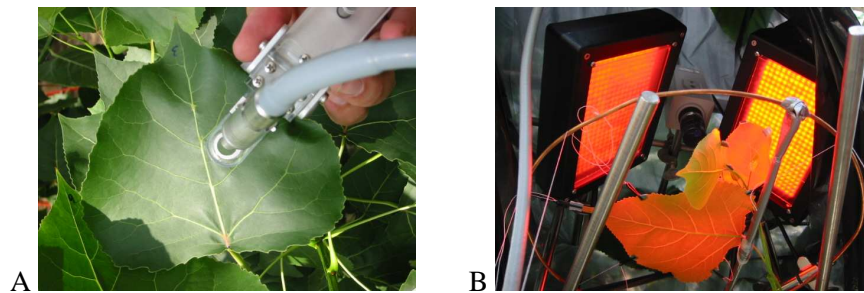

Figure 2.15: Chlorophyll fluorescence measurements: Mini-PAM for spot measurements (A); FluorCam with actinic light LEDs (B).

Fluorescence Induction Kinetic

Fluorescence induction kinetic was analyzed in 2003 on *P. deltoides* leaves at B2C with the FluorCam. After a minimum dark adaptation time of 5 hours, F_v/F_m was measured. Subsequently, actinic light was switched on (150 μmol m^2 s^{-1}) and a saturating light pulse was triggered every 30 sec for 20 min to determine $\Delta F/F_m'$ and NPQ (Fig. 2.16).

The slope of $\Delta F/F_m'$ and NPQ induction is a measure for processes like formation of a proton concentration gradient across the thylakoid membrane. The first three values were used for calculation of the slope (see Fig. 2.16). The last three values at the end of the measurement were used to calculate steady-state levels of $\Delta F/F_m'$ and NPQ as a measure for slow processes.
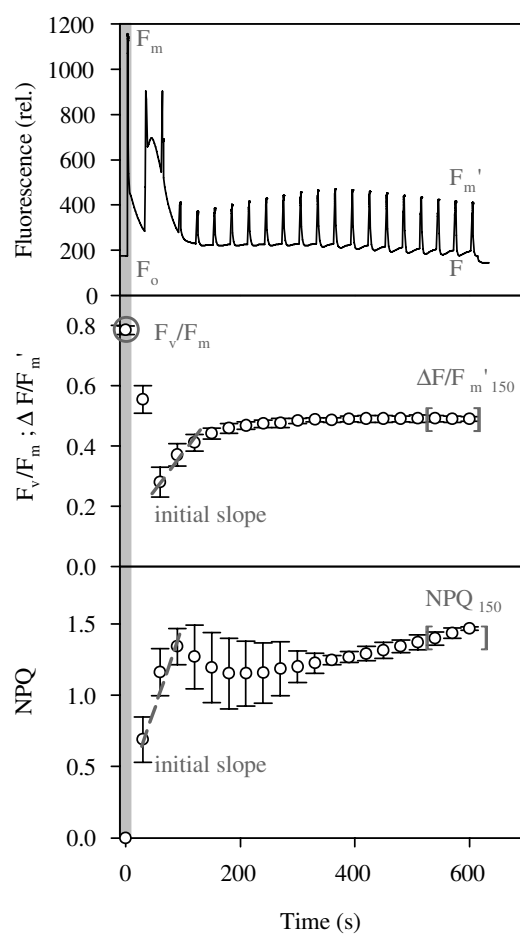
Figure 2.16: Typical fluorescence induction kinetic (A), PS II efficiency F_v/F_m and $\Delta F/F_{m}\prime$ (B) and NPQ (C). The initial slope (dashed line) and end values (square brackets) were used for further analysis.

2.3.2 Gas Exchange

Leaf gas exchange was measured with a portable open-flow gas exchange system (LiCor 6400, LiCor, Lincoln, USA). At B2C, a standard leaf chamber (using ambient light) or a closed leaf chamber with an internal light source (6400-02B LED Light Source) was used. CO_2 concentration, humidity and temperature were maintained at ambient conditions within each bay. From April to July 2003, net CO_2 exchange rate, A, and stomatal conductance, g_S, was measured on a leaf clamped with the standard leaf chamber for 24 hours, while the measurements in October 2003 were performed with the closed leaf chamber. Here, five time points (8:00, 11:00, 13:00, 15:00 and 17:00) were chosen over the day. Based on the mean light intensity at each point in time (400, 1200, 1100, 675 and 100 μmol m^{2}s^{-1}, respectively), an identical light intensity was used for measurements.

At SoyFACE, net CO_2 exchange rate at saturating light conditions, A_{sat}, and stomatal conductance, g_S, were measured at two days (August 15th and 31st, 2004) with an integrated fluorescence chamber head (LI-6400-40 leaf chamber fluorometer). Light was set to maximum light intensities of that day (1500 and 1800 μmol m^{2}s^{-1}, respectively), chamber CO_2 concentration to 380 ppm and leaf temperature to 26 and 28°C, respectively.

Water use efficiency (WUE) is defined as the proportion of net CO_2 exchange rate A to transpiration E:

$$WUE = \frac{A}{E} \tag{2.9}$$

2.4 Measurement of Stomatal Density

Leaf disks of soybean (10 mm diameter) were sampled on Aug 12th, 2004 at the SoyFACE facility (leaves 1 to 5, two sub-replicates per ring), and stored in fixation buffer (PBS buffer, 2 % formaldehyde and 10 % dimethylsulfoxide) at 4°C until bleaching (90 % phenol, 16 h). After bleaching, leaf disks were washed 3 times with 4 M KOH and 3 times with PBS buffer (140 mM NaCl, 2.6 mM KCl, 8 mM Na$_2$HPO$_4$, 1.4 mM KH$_2$PO$_4$; pH 7.2). Number of stomata was determined with a light microscope (Olympus BX 40, Olympus America Inc., Melville, NY, USA) in five sections on the adaxial and abaxial side of each leaf disk (see Fig. 2.17).
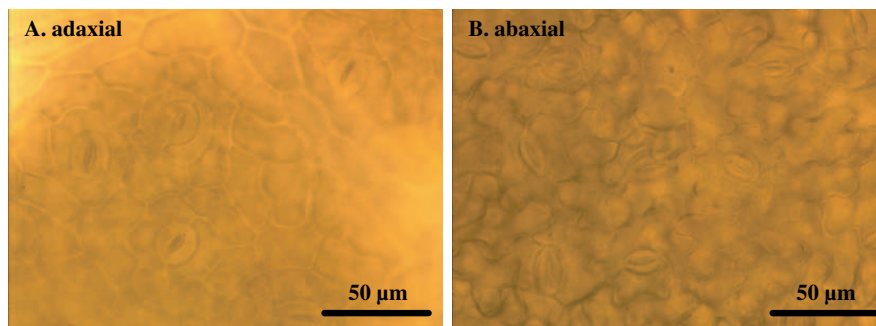

Figure 2.17: Microscopical image of the adaxial (A) and abaxial (B) epidermis with stomata of leaves of *Glycine max*.

2.5   Measurement of Leaf Water Potential

Leaf water potential (LWP) was measured in 2003 on growing and mature leaves of *P. deltoides* at B2C with a scholander pressure bomb (Model 600, PMS Instruments, Corvallis, OR, USA). The detached leaf was clamped into the pressure bomb immediately after cutting from the tree and set under pressure until xylem sap leaked at the cutting area of the petiole. The required pressure in MPa was recorded as the LWP.

2.6   Chlorophyll and Carbohydrate Analysis

Samples for chlorophyll and carbohydrate analysis were taken as follows:

Interveinal tissue: Leaf disks were taken with a cork borer (diameter 5–10 mm),

Veinal tissue: Veins (length 5–10 mm) were cut out with a scalpel or a razor blade.

Detailed description of sampling for each experiment is given in Chapter 3. Samples were frozen in liquid nitrogen after determining the fresh weight (FW) and stored at -80°C until extraction. The sampling scheme for spatial analysis of leaf carbohydrates is given in Fig. 2.18.
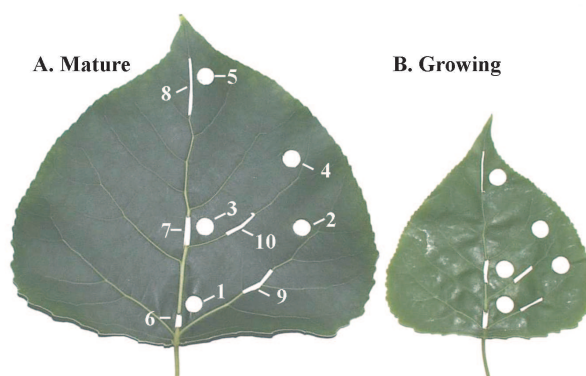

Figure 2.18: Scheme of sampling for spatial carbohydrate analysis of mature (A) and growing (B) leaves of *P. deltoides* trees at Biosphere 2 Center. Numbers of samples are used in the figures of the respective section.

2.6.1   Extraction

Chlorophyll and soluble sugars were extracted from frozen leaf material in 400 μl 80°C ethanol/water (80:20 v/v, 5 mM HEPES) for 20 min according to Arnon (1949). The supernatant was stored at 4°C and the extraction was repeated with 400 μl 80°C ethanol/water (50:50 v/v, 5 mM HEPES) and 200 μl 80°C ethanol/water (80:20 v/v, 5 mM HEPES). If leaf disks were not pale, another step with 200 μl 80:20 v/v ethanol/water, 5 mM HEPES was added. The combined supernatant was filled to 1 ml with ethanol. Leaf material with a mass of less than 10 mg was extracted sequentially with 200–200–100 μl ethanol/water (total volume 500 μl), material with more than 40 mg with 600–600–300 μl ethanol/water (total volume 1.5 ml).

The extracted and pale leaf material was prepared for starch analysis by grinding it in 300 μl distilled water using a mixer mill (MM200, Retsch GmbH & Co. KG, Haan, Germany) with a stainless

steel ball (diameter 7 mm). The ball was washed with additional 200 μl distilled water. The samples were autoclaved for 2h at 120°C, 1 bar. 100 μl of the autoclaved sample were incubated in 400 μl Na-acetate buffer (50 mM, pH 4.9 with 1.4 U amyloglucosidase and 1 U α-amylase, Sigma-Aldrich, Taufkirchen, Germany) for 16 h at 37°C. After extraction, samples were stored at -20°C or -80°C until further analysis.

2.6.2 Chlorophyll

Chlorophyll concentration was measured according to Arnon (1949) immediately after extraction. After vortexing, 400 μl of the extract were diluted 1:1 or 1:2 with ethanol p.a., centrifuged for 4 min at 13000 rpm, RT (room temperature), and analyzed using a photometer at $\lambda = 652$ nm against 100% ethanol. Chlorophyll concentration was estimated from the optical density (OD) using the law of Lambert-Beer:

$$OD = \varepsilon \cdot d \cdot c \qquad \Longrightarrow \qquad c = \frac{OD}{\varepsilon \cdot d} \tag{2.10}$$

with the extinction coefficient ε (l cm^{-1}mol^{-1}), the concentration c (mol l^{-1}) and cuvette width $d = 1$ cm.

With 1 mg Chlorophyll ml^{-1} having an OD of 34.4 the chlorophyll concentration was estimated as follows:

$$c_{Chl}(mg\ g^{-1}FW) = \frac{OD \cdot \frac{V_{extract}}{V_{aliquot}} \cdot V_{cuvette}}{34.4\ ml\ mg^{-1} \cdot m_{FW}} \tag{2.11}$$

with the volume of the extract $V_{extract}$, the used aliquot $V_{aliquot}$ and the cuvette $V_{cuvette}$ in μl, and the fresh weight of the plant material m_{FW} in mg. Alternatively, the concentration was given in mg cm^{-2}.

2.6.3 Soluble Carbohydrates

Glucose (Glc), fructose (Fru) and sucrose (Suc) concentrations were analyzed with a coupled enzyme assay according to Jones et al. (1977). The reaction from NADP$^+$ to NADPH+H$^+$ is detected quantitatively via the increase of the optical density at $\lambda = 334$ nm (1 μmol NADPH+H$^+$ ml^{-1} = 6,22 OD) and is catalyzed by the starting enzyme glucose-6-phosphate dehydrogenase (G6PDH, Fig. 2.19). Successively, the enzymes hexokinase (HK), phosphoglucoisomerase (PGI) and invertase (INV) are given to the extract so that glucose, fructose and sucrose can be measured (Fig. 2.19).
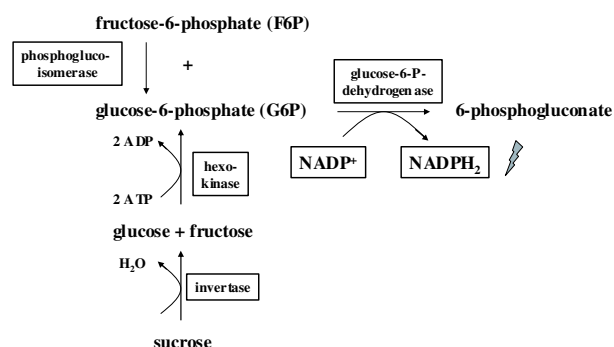

Figure 2.19: Scheme of the coupled enzyme assay for determination of hexose and sucrose concentration.

One molecule of hexoses corresponds to one produced molecule of NADPH+H$^+$, one molecule sucrose to two NADPH+H$^+$.

G6PDH (5.6 U), HK (6 U) and PGI (10 U, Roche Diagnostics GmbH, Mannheim, Germany,) were centrifuged (4 min, 13000 rpm, RT). The pellet was dissolved in 200 μl TRIS buffer (100 mM, 10 mM MgCl$_2$, pH 8.1). 1/4 of a microcentrifuge tube of Invertase (Sigma-Adlrich, Taufkirchen, Germany)

was dissolved in 100 μl TRIS buffer (ca. 5 U).

Analysis was made using a multiplate photometer (ht II, Anthos Mikrosysteme GmbH, Krefeld, Germany). For one 96-well-microtiter plate the following master mix was used (160 μl master mix and 20 μl extract per well):

> 15.5 ml imidazole buffer (100 mM, 5 mM $MgCl_2$, pH 6.9)
> 480 μl ATP (60 mg ml^{-1})
> 480 μl NADP$^+$(36 mg ml^{-1})
> 200 μl G6PDH

After finished reaction, 2 μl of the next enzyme per well was added successively (Fig. 2.19). Soluble carbohydrate concentration was determined as follows:

$$c_{hexose}(\mu mol\ g^{-1}FW) = \frac{\Delta OD \cdot \frac{V_{extract}}{V_{aliquot}}}{6.22\,ml\,\mu mol^{-1}cm^{-1} \cdot 2.85\ cm \cdot m_{FW}} \tag{2.12}$$

with the volume of the ethanolic extract $V_{extract}$ and of the aliquot $V_{aliquot}$ in μl, and the fresh weight of the plant material m_{FW} in mg. Alternatively, the concentration was given in μmol cm^{-2}. Sucrose concentration was calculated by dividing c_{hexose} by a factor of 2.

2.6.4   Starch

Starch concentration was determined enzymatically in glucose equivalents using the same procedure described above for soluble sugars, with TRIS instead of imidazole buffer.

$$c_{starch(Glc)}(\mu mol\ g^{-1}FW) = \frac{\Delta OD \cdot \frac{V_{extract}}{V_{aliquot}} \cdot \frac{V_{inkub}}{V_{inkub-aliquot}}}{6.22\,ml\,\mu mol^{-1}cm^{-1} \cdot 2.85\ cm \cdot m_{FW}} \tag{2.13}$$

with the volume of the extract $V_{extract}$ and the aliquot $V_{aliquot}$, the incubation volume V_{inkub} and the incubated extract volume $V_{inkub-aliquot}$ in μl.

2.6.5   Carbohydrate Turnover

Daily carbohydrate turnover was calculated by:

$$Carbohydrate\ Turnover(\%) = \frac{value\ at\ sunset - value\ at\ sunrise}{value\ at\ sunset} * 100 \tag{2.14}$$

according to Turnbull et al. (2002).

Chapter 3

Results

3.1 Estimation of the Spatio-Temporal Resolution of the DISP Method

To check the accuracy of the Digital Image Sequence Processing (DISP) method and to identify suitable parameters for further analysis, it was necessary to estimate the spatial and temporal resolution of the DISP method and to test the used parameters. For this purpose, growth was simulated by moving a camera towards a non-moving object.

Setup

To simulate growth a CMOS-camera (Flea BW, Point Grey, Vancouver, Canada) was attached on a vertically fixed moving stage (VTM80, Owis GmbH Stauffen, Germany) and moved towards the object (Fig. 3.1). Measurements were performed under infrared illumination. The velocity of the moving stage and the acquisition time were chosen to achieve a pixel velocity comparable to that of growing leaves. Special care was taken to achieve accuracy in the shifting process by avoiding a movement of the camera at image acquisition.

Initial object–camera distance:	34 cm (print-out) and 31.5 cm (leaf)
Image frequency:	10 sec
Moving stage velocity:	0.04 mm frame^{-1} (14.4 mm h^{-1})
Image number:	360

It was assumed that the surface of the object expanded homogeneously, apart from border effects, due to the pinhole camera model (Fig. 3.1, B). Furthermore, a constant RGR could be assumed, if the shifting distance was short compared to the camera-object-distance (A. Chavarría-Krauser, personal communication).

A fully expanded, fixed tobacco leaf as well as a "synthetic" leaf (a printout of a leaf image) were tested. The surface of the synthetic leaf was flat, in contrast to the real leaf, whose surface was slightly uneven, in particular due to the veins. The analysis was performed with different parameters (Tab. 3.1). The parameters of the algorithms are described in more detail in the Appendix (Sect. A). The temporal resolution was tested by variation of the AOI size in GrowFlow (Sect. 2.2.2). A general analysis of the standard deviation (SD) of the RGR was performed with 10x10 – 540x240 pixel for parameter settings [1] and [2]. A closer look on the RGR time course was done with two AOIs: 35x32 ('small') and 150x150 pixel ('large' AOI). In addition, the influence of brightness fluctuations on the analysis was tested. The spatial resolution was tested via RGR maps (representing the average RGR over 2 – 360 images) which were achieved using RGRFlow (Sect. 2.2.2). The standard deviation among differently sized AOIs defined in the RGR maps was determined.
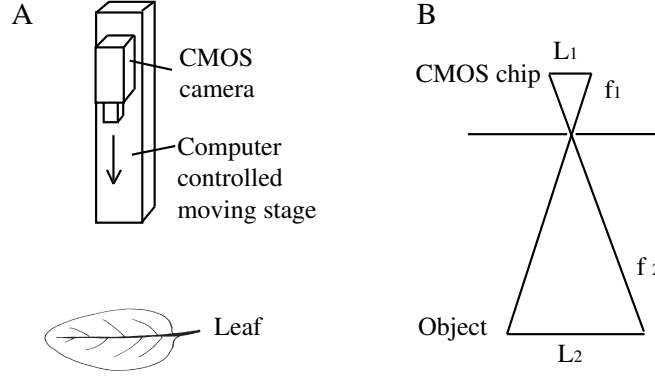
Figure 3.1: Setup for a test to simulate growing objects using a camera attached to a vertically fixed moving stage (A) and pinhole camera model with size of the CMOS chip L_1, distance chip-lens f_1, size of the object L_2 and distance lens-object f_2 (B).

Statistically, the relative standard deviation (SD$_{rel}$) should be proportional to $\frac{1}{\sqrt{N}}$ with N being the number of contributing data points (Landau and Lifschitz, 1987), hence $N = N_{frames} \cdot N_{pixel}$.

Table 3.1: Parameter settings to test the DISP method. Description of parameters and filter settings are given in the Appendix (Sect. A).

Case No.	Regularization B_{rec}	Iterations $Iter, Iter_{rec}$	Smoothing $Smooth$	Pyramid level Pyr	Filter
[1]	0.55 0.45	5, 10	1000	1	auto
[2]	0.80 0.20	5, 10	1000	1	auto
[3]	0.80 0.20	5, 10	10000	1	auto
[4]	0.80 0.20	5, 10	1000	1	small

GrowFlow: Variations in the RGR Time Course

In GrowFlow differently sized AOIs were defined (10x10 – 540x240 pixel) for both 'growing' objects (synthetic and real leaf), and the standard deviation (SD) of the RGR in time was determined (Fig. 3.2). The SD fell asymptotically with increasing AOI size to reach a minimal value different from zero in the range of possible AOI sizes. The value was achieved at an AOI size of approximately 10,000 (100x100) pixel. Independent from the parameter settings and for both the real leaf and the printout it was approximately $5 * 10^{-4}$ % frame^{-1}, if 20 images were smoothed in GrowFlow (Fig. 3.2, A, B, D). Less smoothing in GrowFlow led to a higher SD: if only 5 images were averaged, the minimal SD was 1.5 times larger as it was the case for 20 images (Fig. 3.2, C). As this value was independent of the parameter settings, it gives us the systematic error of the DISP method for the respective smoothing in GrowFlow.
Smaller AOIs led to a higher SD, in particular with less regularization (case [1], Fig. 3.2, D) and less smoothing with GrowFlow (Fig. 3.2, C).

These findings were confirmed by the results shown in Tab. 3.2. Here, the two AOI sizes used in the next section were investigated. The mean RGR and the SD were determined for all tested parameter settings and objects. The mean RGR (% frame^{-1}) of the non-growing leaf was approximately 0 with
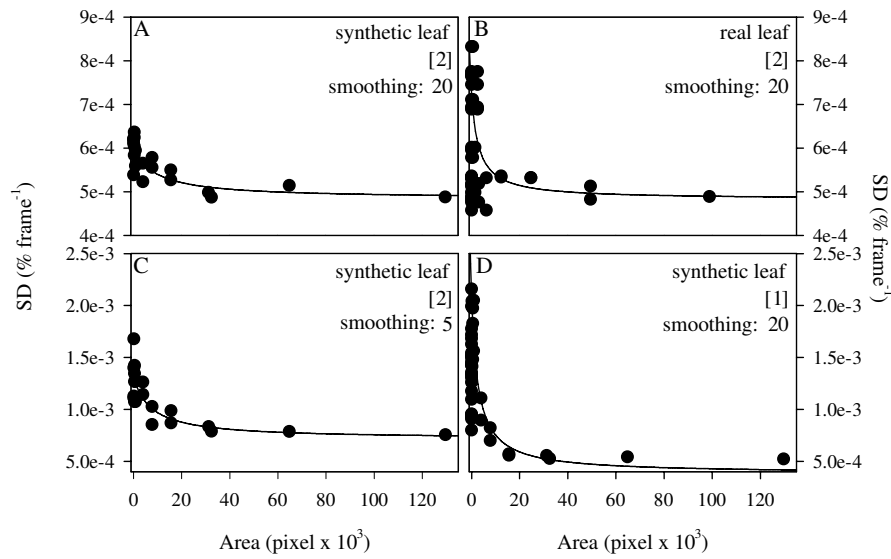
Figure 3.2: Effect of AOI size on the standard deviation (SD) of the relative growth rate (RGR). In GrowFlow, differently sized AOIs (10x10 – 540x240 pixel) were defined. The SD of the RGR in time was calculated. A synthetic and a real leaf were analyzed with parameter settings [1] and [2] (see Tab. 3.1). In GrowFlow, 5 or 20 images were averaged in time ("smoothing").

all tested parameter settings. The standard deviation (SD) was highly dependent on the parameters (Tab. 3.2). Again, a stronger regularization led to less fluctuations of the RGR (smaller SD), for the synthetic leaf as well as for the real leaf (Tab. 3.2, case [1] and [2]).

Table 3.2: Effect of analysis parameters and 'area of interest' (AOI) size on the mean relative growth rate (RGR): Mean RGR (% frame^{-1} x 10^{-2}) $\pm$ SD x 10^{-2} of three different tested leaves (synthetic, non-growing; synthetic, growing; and real, growing leaf) of a small (35x32 pixel) and a large AOI (150x150 pixel). Parameters (case [1]–[4]) were set as described in Tab. 3.1.

| case | synthetic, non-growing | | synthetic, growing | | real, growing | |
	35x32	150x150	35x32	150x150	35x32	150x150
[1]	-0.03 ± 0.29	0.00 ± 0.04	2.16 ± 0.17	2.14 ± 0.06	2.22 ± 0.36	1.99 ± 0.33
[2]	-0.01 ± 0.05	-0.01 ± 0.02	2.13 ± 0.06	2.13 ± 0.05	2.15 ± 0.24	2.01 ± 0.29
[3]	-0.01 ± 0.05	-0.01 ± 0.02	2.13 ± 0.06	2.14 ± 0.05	2.14 ± 0.25	2.01 ± 0.29
[4]	-0.02 ± 0.05	-0.01 ± 0.02	2.10 ± 0.06	2.14 ± 0.06	2.12 ± 0.25	1.98 ± 0.29

GrowFlow: Analysis of the RGR Time Course

In the next step, the evolvement of the RGR in time was tested. The RGR showed high fluctuations when the AOI and the regularization were small (Fig. 3.3, 3.4 and 3.5, A, parameter [1]). With an AOI of 150x150 pixel (more spatial averaging) the regularization parameters had less effect on the growth pattern. This was valid for all tested objects, also for the real leaf where the surface was uneven due to the veins (Fig. 3.3 – 3.6). Increased smoothing (case [3]) or other filter settings (case [4]) did not change the pattern of the RGR time course, neither with the small nor the larger AOI.
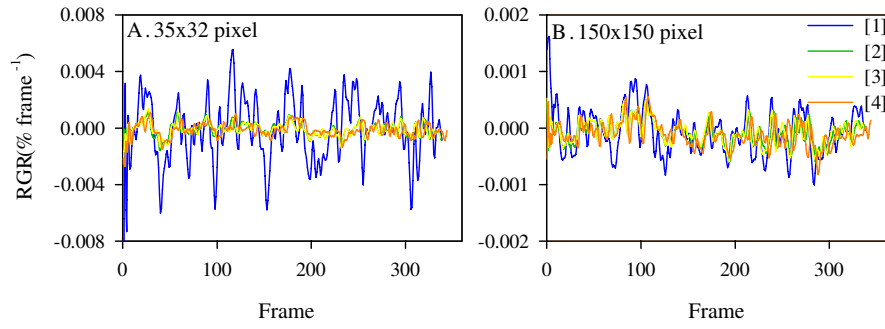
Figure 3.3: Effect of analysis parameters and 'area of interest' (AOI) size on the relative growth rate (RGR) of a synthetic, non-growing leaf: RGR of an AOI with 35x32 pixel (A) and 150x150 pixel (B) of the same sequence that was analyzed with four different parameter settings (Tab. 3.1).
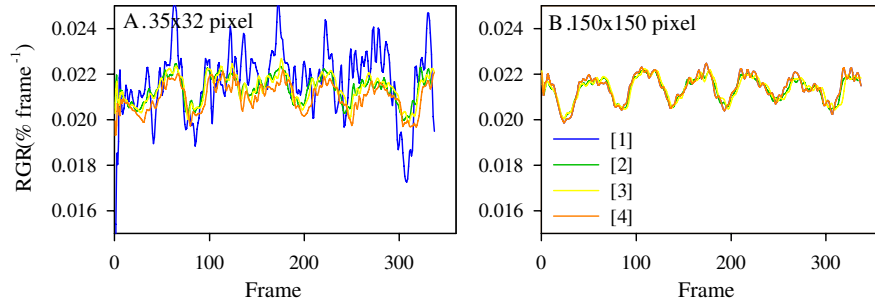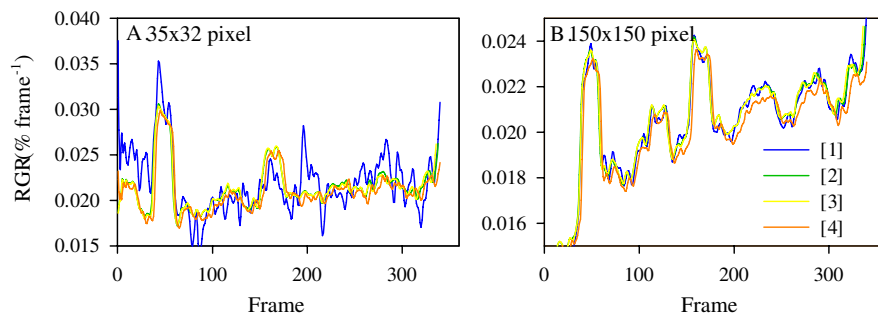

Figure 3.4: Effect of analysis parameters and 'area of interest' (AOI) size on the relative growth rate (RGR) of a synthetic, growing leaf: RGR of an AOI with 35x32 pixel (A) and 150x150 pixel (B) of the same sequence that was analyzed with four different parameter settings (Tab. 3.1).

Figure 3.5: Effect of analysis parameters and 'area of interest' (AOI) size on the relative growth rate (RGR) of a real leaf: RGR of an AOI with 35x32 pixel (A) and a 150x150 pixel (B) of the same sequence that was analyzed with four different parameter settings (Tab. 3.1).

In case of the growing objects (synthetic and real) periodic oscillations occurred (Fig. 3.4 and 3.5) with $\lambda = 60$ images. These oscillations were independent of the algorithms, as the pattern did not change if the analysis of the sequence was started at image 25 instead of the first image (Fig. 3.6, A, dotted line).

Furthermore, it was tested if brightness changes could be the reason for the oscillations of the RGR (Fig. 3.6, B). Infrared diodes and fluorescent lamps usually show oscillations, but no relationship between the RGR course and changes in light could be found.

The synthetic leaves were printouts of a real leaf. Prints show sharp borders, which depend on the printer resolution. When the camera moves towards the object, this periodic pattern can result in periodic oscillations, known as 'Moiré' patterns. However, as the periodicity was the same for the real leaf where no periodic borders are present, it could be assumed that the periodic pattern of the RGR course might have been caused by the shifting process and inaccuracy of the moving stage.
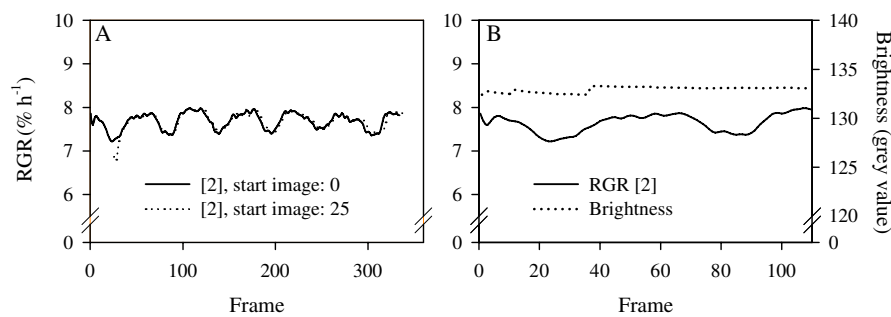
Figure 3.6: Effect of initial point of the analysis and brightness changes on the relative growth rate (RGR) of a synthetic leaf. Analysis was performed with parameter settings [2] (Tab. 3.1). The impact of the initial point (image 0 or image 25) on the oscillation of the RGR (A) and changes in brightness (B) was tested.

Spatial Information of Single Images

Single images showed a more noisy and patchy RGR distribution than averaged sequences, but, as expected, the noise was dependent on the regularization parameters. Less regularization caused patches with high negative growth rates that were located next to patches with high positive growth rates (Fig. 3.7 – 3.9, case [1]). This noisy pattern disappeared with increasing regularization (Fig. 3.7 – 3.9, case [2]–[4]). Small disturbances of the pixel velocities lead to high disturbances of the RGR, because it is the divergence of the velocity fields. A higher regularization of the velocity maps resulted in a smoother RGR map.

The patchiness obtained in image sequences that were evaluated with parameters [1] was independent of the object (synthetic or real leaf). However, patchiness of a real leaf (Fig. 3.9) was more pronounced than in case of the printouts (Fig. 3.7 or 3.8), independently of the regularization strength. This might be explained by the unevenness of a real leaf.

Single images are not suitable to test the spatial accuracy, as it is hard to measure the 'real' resolution. To achieve a higher significance of spatial patterns, several images or the whole sequence can be averaged. Small disturbances and noise are eliminated and real growth patterns get more pronounced, as long as they are long-living. Short-living patterns get lost in the average process. Here, we can see already a tradeoff between spatial and temporal resolution. The averaging is performed by means of RGRFlow (see p. 20).
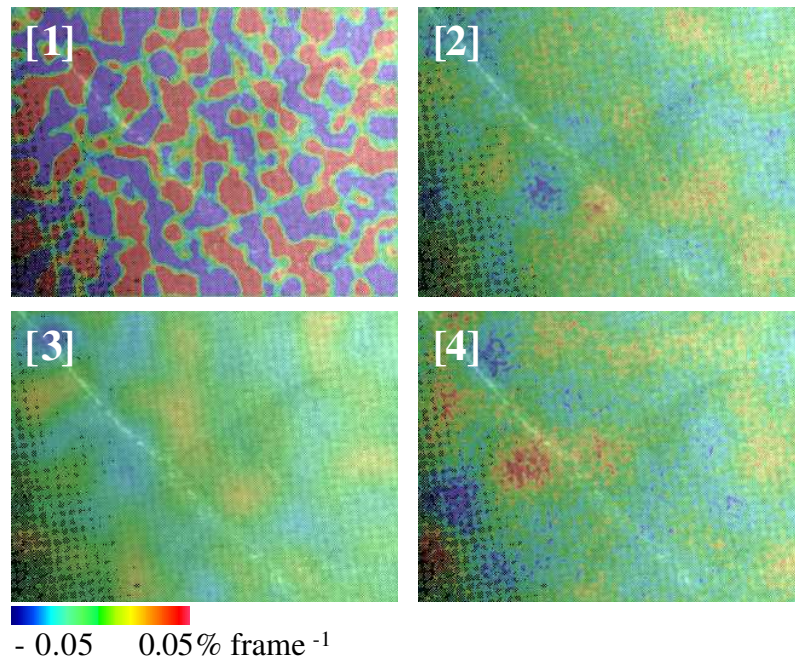
- 0.05   0.05 % frame $^{-1}$

Figure 3.7: Color-coded image of the relative growth rate (RGR) of a synthetic, non-growing leaf. The sequence was analyzed with four different parameter settings (see Tab. 3.1). Typical single image.
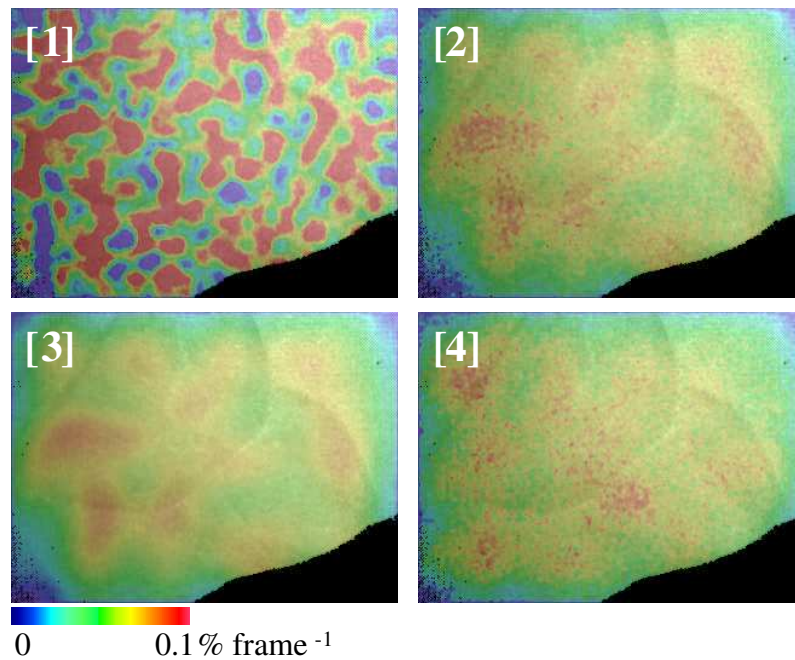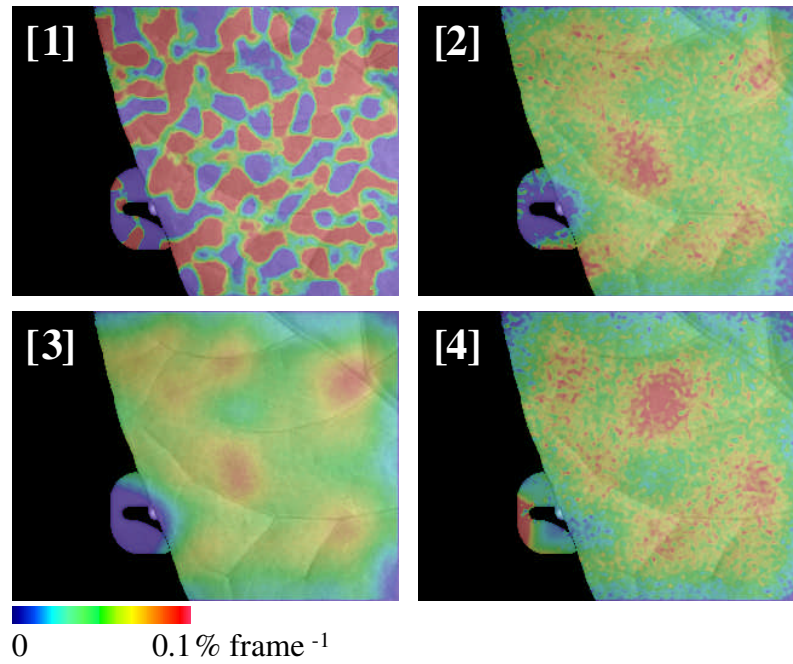

0   0.1 % frame $^{-1}$

Figure 3.8: Color-coded image of the relative growth rate (RGR) of a synthetic, growing leaf. The sequence was analyzed with four different parameter settings (Tab. 3.1). Typical single image.

Figure 3.9: Color-coded image of the relative growth rate (RGR) of a real leaf. The sequence was analyzed with four different parameter settings (Tab. 3.1). Typical single image.

RGRFlow: Average of Spatial Information

The more images were averaged with RGRFlow, the clearer appeared the overall growth pattern (Fig. 3.10). Averaging 360 images led to a relatively homogeneous RGR map of the synthetic as well as the real leaf. Additional regularization (parameter settings [2]) yielded an even smoother pattern (Fig. 3.10, left images).

It was tested how small an AOI could be defined depending on the number of averaged images. RGRFlow was used to average over different time ranges (2 – 360 images). The resulting RGR maps were split into 3x3 – 25x25 equally-sized AOIs (Fig. 3.11). This was done by the program *algotest*. In the next step, the standard deviation among the AOIs within an image was calculated, allowing a characterization of the error in dependence of the AOI size and averaging time space.

As mentioned before, the RGR map of the objects should expand homogeneously, but small disturbances led to noisy patterns. Small AOIs led to a higher SD in space and the effect was larger with less regularization strength (Fig. 3.12). This was valid until the AOIs were so small that neighboring fields were still in the same RGR patch. As before, the real leaf showed a higher SD because of the unevenness (Fig. 3.12, right graphs). The more images were averaged within a sequence, the smaller the AOI could be defined to achieve a similar SD.

Based on the achieved results, suggested combinations of AOI size and number of averaged images are outlined in Table 3.3. Combinations were chosen to attain a small standard deviation (Fig. 3.12). One has to keep in mind that these numbers were achieved with image sequences of tobacco leaves and can only be an advice, but should not be regarded as a general result applicable to leaves of different species. Furthermore, it has to be mentioned, that the suggested AOI pixel sizes are valid for pyramid level 1 (pyr 0 or Growflow: AOI size x 4).

A 0   0.025 %frame $^{-1}$

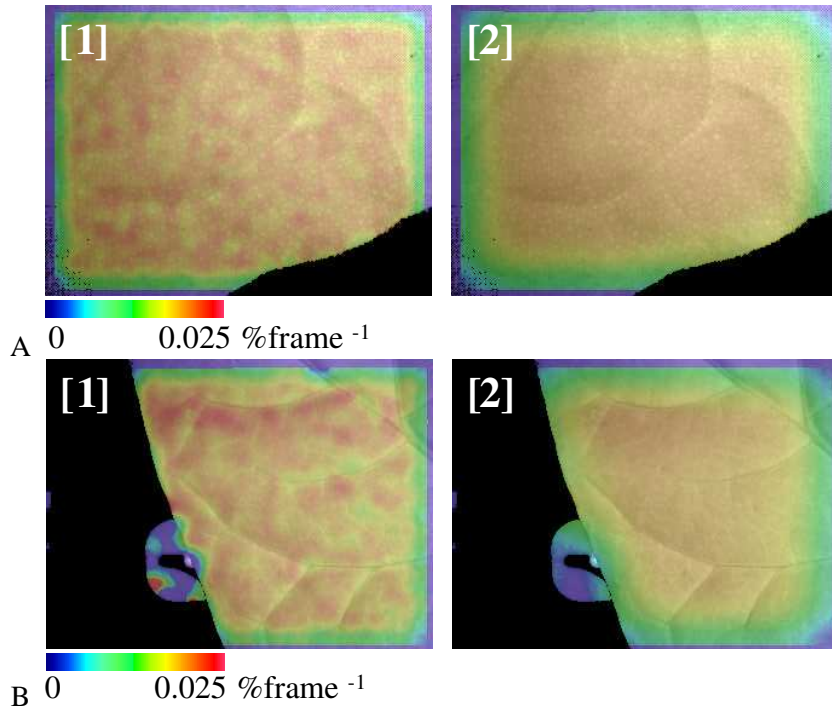B 0   0.025 %frame $^{-1}$

Figure 3.10: Mean color-coded image of the relative growth rate (RGR) of a synthetic and a real leaf. The RGR was averaged over the whole sequence (360 images) via RGRFlow: result of the synthetic (A) and the real leaf (B) analyzed with parameter settings [1] and [2], respectively (Tab. 3.1).

Figure 3.11:   Example of 5x5-AOI-grid to test the DISP method. 3x3 – 25x25 equally-sized 'areas of interest' (AOIs) were automatically generated and the standard deviation between these AOIs was calculated.
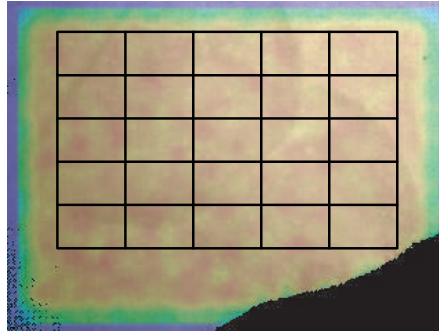
Table 3.3: Suggested combination of 'area of interest' (AOI) size and number of averaged images within a sequence and relative standard deviation (SD_{rel}) in % frame^{-1} with regularization parameters B_{rec} of 0.55-0.45 and 0.8-0.2. Values give only rough indications.

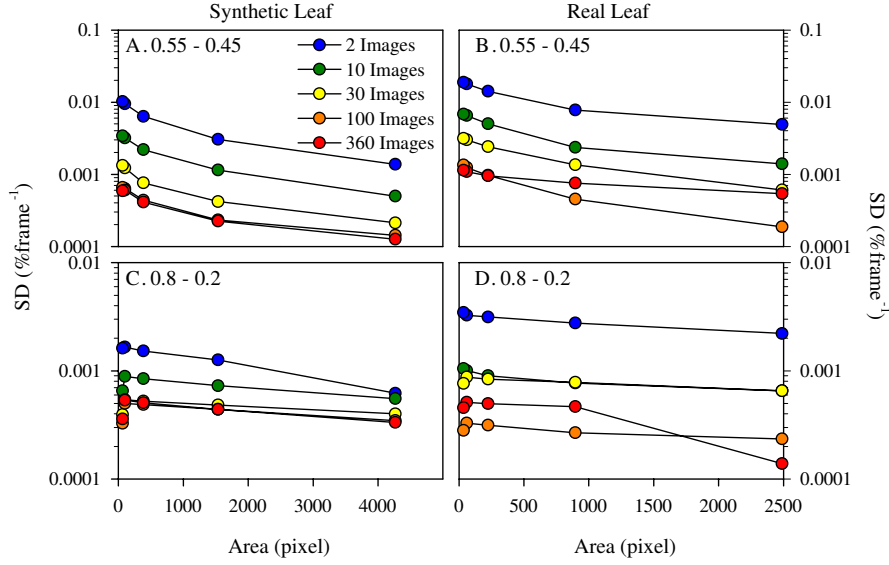| Averaged images	Minimal AOI size (pixel, pyr 1)	SD_{rel} B_{rec} 0.55-0.45	SD_{rel} B_{rec} 0.8-0.2
1 (single image)	50x50 – 100x100	0.2	0.01
2	30x30	0.7	0.25
10	30x30	0.2	0.07
30	15x15	0.3	0.09
>100	10x10	0.1	0.03

Figure 3.12: Standard deviation (SD) of the relative growth rate (RGR) of different equally-sized 'areas of interest' (AOIs) in RGR maps (representing the RGR of 2 – 360 averaged images). Two different regularization parameter settings ([1], A, B, and [2], C, D) for the synthetic (A, C) as well as the real (B, D) leaf were tested. The *y* axis is given as logarithmic scale.

We assumed that $SD_{rel} \sim \frac{1}{\sqrt{N}}$, with SD_{rel} being dependent on the mean RGR ($\overline{RGR}$). As the DISP method has a systematic error, this would result in

$$SD = \alpha \frac{\overline{RGR}}{\sqrt{N}} + SD^0 \qquad (3.1)$$

with a proportionality factor α and the systematic error SD^0. With $N = N_{frames} \cdot N_{pixel}$ and the results of this section, a reasonable value for N is between 6000 and 10000 pixel and can be obtained by e.g. either 1 image in time and 100x100 pixel in space or 100 images in time and 10x10 pixel in space (Tab. 3.3).

Example for typical leaf sequences: With a frame rate of 30 h^{-1} (every 120 sec) and pyr 1, 1-h-averages would have a suitable resolution of 15 x 15 pixel, i.e. 30 x 30 pixel in the original sequence. With a leaf with L = 6.4 cm taking 640 pixel this would result in approximately 3 mm length per AOI. An AOI size of 100 x 100 pixel (e.g. single image) would correspond to 1 cm^2, whereas 24-h-means (>360 images) would allow an AOI size of 1 mm^2.

Summary: Resolution of the DISP Method

For further analysis with the DISP method, the accuracy and resolution had to be estimated. This was achieved with a setup where a camera that was fixed on a moving stage was moved automatically towards a non-moving object. AOI size, regularization parameters and averaged image number in time determined how much fluctuations of the RGR were dampened.

In GrowFlow, the standard deviation of the RGR time course reached a minimum value at an AOI size of 100x100 pixel, independent from the regularization. It was 1.5 times higher when 5 images were averaged instead of 20 ("smoothing").

The more images were averaged with RGRFlow, the smaller an AOI could be determined. Experi-

ments with a homogeneously expanding tobacco leaf led to the conclusion that, with an acquisition rate of 30 h^{-1} and pyramid level 1, 1-h-averages (30 images) would allow AOI sizes of 15 x 15 pixel and 24-h-averages 10 x 10 pixel with an error of approximately 0.01 – 0.03 % h^{-1}.

For the analyses of the present study these results led to the conclusion that temporal courses of the leaf RGR could be analyzed with a resolution of at least 1-h-means. Furthermore, analyses where a very small spatial resolution was necessary, as it was the case for the heterogeneity determination, could be performed on 24-h-RGR maps.

3.2 Spatial and Temporal Growth Patterns

This section aims on outlining spatio-temporal growth patterns and their relationship with photosynthesis or assimilates. Temporal patterns as diel cycles were investigated to see if the different phasing of the diel growth rhythm of *P. deltoides* trees compared to tobacco or castor bean is caused by environmental or species-dependent, intrinsic factors. Spatial patterns like differences between veinal and interveinal leaf tissue or base-to-tip gradients were also examined. In the context of this work, interveinal tissue was defined as the tissue between first and second order veins, veins of higher orders were not considered. Veinal tissue included either only the midvein or involved both midvein and second order veins.

3.2.1 Effect of Cultivation Conditions on Leaf Growth of Cuttings of *Populus deltoides*: Growth Chamber and Intensive Forestry Biome (IFB)

The following experiments were performed to investigate the effect of growth chambers (artificial light, relatively constant light intensities and temperatures) in comparison to greenhouse conditions on spatio-temporal patterns of growth and photosynthetic assimilation of *P. deltoides*. Cuttings were grown either in a growth chamber or the IFB (400 ppm) in B2C (see Sect. 2.1.3). Growth parameters and the meteorological data of the IFB and growth chamber are given in Sect. 2.1.

Leaf Growth

Leaf growth of *P. deltoides* cuttings was followed from May to June 2003 by measuring the leaf areas A_L once a week. Leaf area of cuttings grown in the IFB was higher than that of cuttings grown in the growth chamber (Fig. 3.13) and the difference increased with time. IFB-grown cuttings had more branches per plant (4 instead of 2–3) and more leaves (1.3 times more per branch, 2 times more per plant) than cuttings grown in the growth chamber.
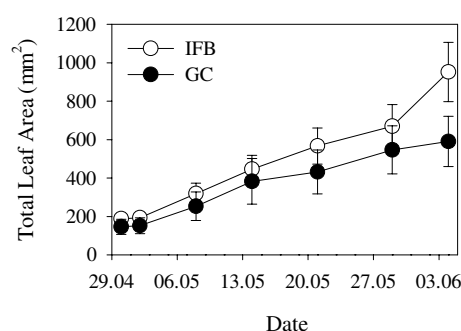

Figure 3.13: Leaf growth of *Populus deltoides* cuttings grown in the Intensive Forestry Biome (IFB) and the growth chamber (GC) at Biosphere 2 Center: Development of total leaf area from April to June 2003 (n = 6 or 7 ± SE).

Diel Leaf Growth

The diel leaf growth behavior of cuttings in the IFB and the growth chamber is shown in Fig. 3.14. In general, the RGR rose during the day, reaching the maximum at dusk and declined throughout the night. This pattern became more pronounced throughout the season.
In the growth chamber, the RGR did not rise continuously during day, but showed a slight decline in the afternoon (Fig. 3.14, B, D, F, G). At the day-night transition a sharp peak, followed by a decline, was observed (see also Fig. 3.15, D). After this decline the RGR began to rise again and started to decline after midnight.
In the IFB, the RGR also showed a decline, but earlier around midday (Fig. 3.14, A, C, E, G). In April,
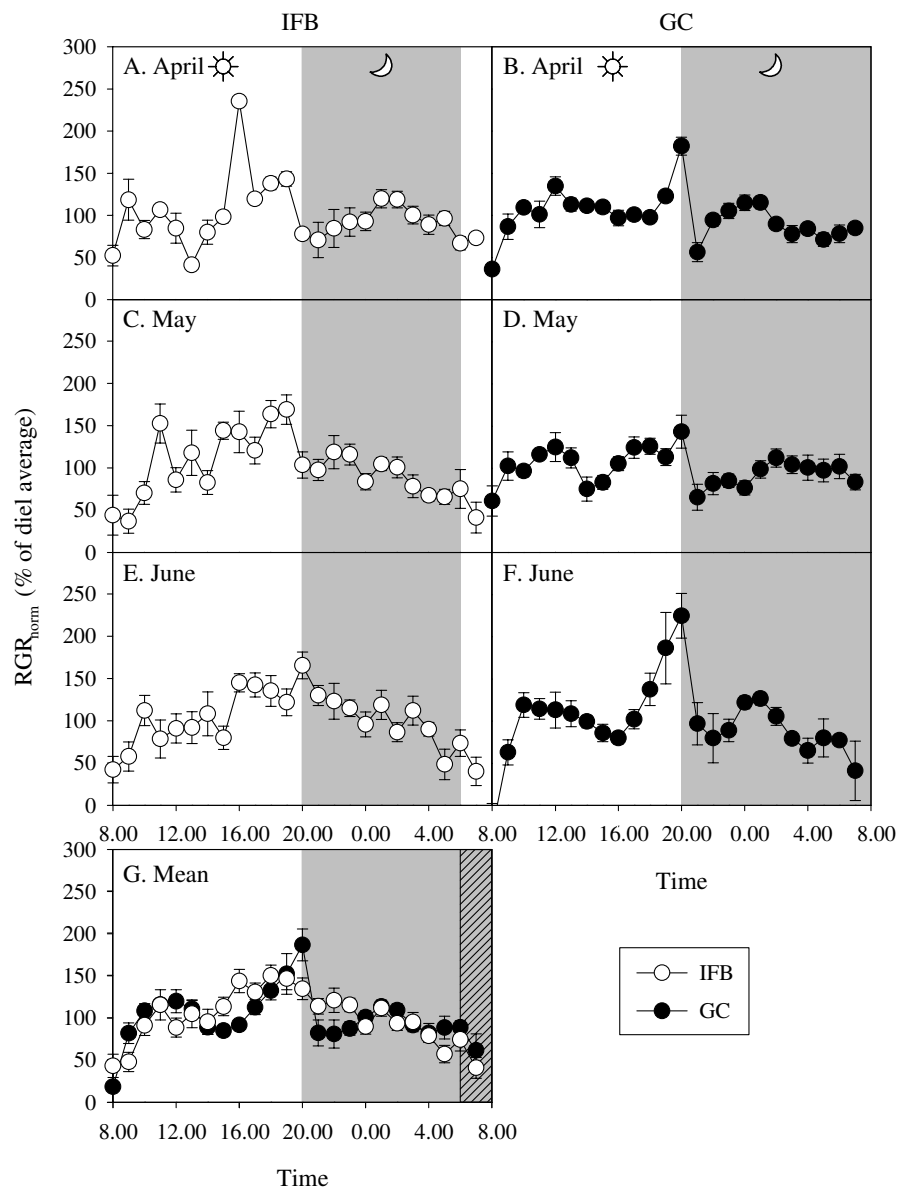
Figure 3.14: Diel time course of the relative growth rate (RGR) of *Populus del-toides* cuttings grown in the Intensive Forestry Biome (IFB) and in the growth chamber (GC) in Biosphere 2 Center in 2003. The RGR was determined by digital image sequence processing (DISP): Monthly mean of the normalized diel leaf growth rate (% of diel mean) in April (A, B), May (C, D) and June (E, F) in the IFB (left) and growth chamber (right), as well as the mean of May and June (G, n: A = 4; B = 6; C = 12; D = 10; E = 12; F = 11; G = 24 and 21 for the IFB and the GC, respectively ± SE).

the growth pattern of leaves in the IFB was still very similar to that of plants from the growth chamber, where the cuttings were let to root (see Sect. 2.1.3). The strong peak at midday was a result from the changed photoperiod (GC – IFB, see Sect. 2.1.3, p. 13). Thus, the diel growth course of April was excluded from the average (Fig. 3.14, G). Throughout May and June, the pattern changed slightly, in particular the RGR declined steadily in the night (Fig. 3.14, E). The averaged data show differences between the two treatments more clearly (Fig. 3.14, G). The overall pattern (time of RGR minimum and maximum) was not altered, but the nocturnal growth pattern differed.

The time course of the RGR of cuttings grown in the IFB and GC was tested with a Discrete Fast Fourier Transformation (FFT). For this purpose the RGR of five consecutive days in June 2003 was analyzed with the program *fft* (Fig. 3.15). Although the RGR course seemed to be more heterogeneous in the IFB compared to the growth chamber (Fig. 3.15, B, D), the FFT, that shows only periodic patterns, showed more small-wavelength patterns in the GC (Fig. 3.15, A, C, D). The most distinct wavelength in the IFB was approximately 6 h, other pronounced wavelengths occurred at approximately 70 and 40 min. In the growth chamber higher frequencies were more pronounced, in particular at approximately 15 min, 30–40 min and 90 min, but also a periodicity of approximately 8 h could be found.

Spatial Growth Patterns

Color-coded RGR maps, representing 1-h-averages of the RGR show the high patchiness of growth patterns of leaves in the IFB and GC (Fig. 3.16). The overall time course of the RGR can be seen clearly, with increasing growth rates during day and declining growth rates in the night, for both, the IFB (left graphs) and GC (right graphs). At 12:00, the RGR was highly patchy in the IFB, presumably due to fluctuations of the sun light.

Spatial RGR patterns were also studied by analyzing the spatial distribution of 24-h RGR mean (Fig. 3.17 and 3.19). As mentioned in section 3.1, short-living RGR patches were eliminated by averaging more time steps. The RGR of veins was clearly lower compared to that of interveinal tissue (Fig. 3.17 and 3.19).

Spatial patchiness was examined more closely (Fig. 3.18). For this purpose, 24-h RGR maps were analyzed with the program *energy*. The relative heterogeneity of the spatial distribution of the RGR of leaves was higher in the IFB than in the GC, approximately by a factor of 14.

Veinal versus Interveinal Tissue

The relationship of the RGR of the midvein and the interveinal tissue is illustrated in Fig. 3.19. In *P. deltoides* cuttings the midvein grew with 70.5 ± 2.2 % ($n = 15$) of the growth rate of interveinal tissue. However, this factor was not constant but depended on the developmental stage: leaves with high growth rates had also higher factors than slowly growing leaves (Fig. 3.19, B).

Base-to-Tip Gradient

Interestingly, *P. deltoides* did not show a distinct base-to-tip growth gradient (Fig. 3.17 and 3.20, B). Following data from literature, this result was not expected. The RGR, determined along the midvein, was approximately 10 % higher in the center of the leaves compared to the leaf base. At the leaf tip, the RGR was approximately 80 % of the mean RGR. There was no difference in the relative gradient between leaves of cuttings in the IFB or GC.
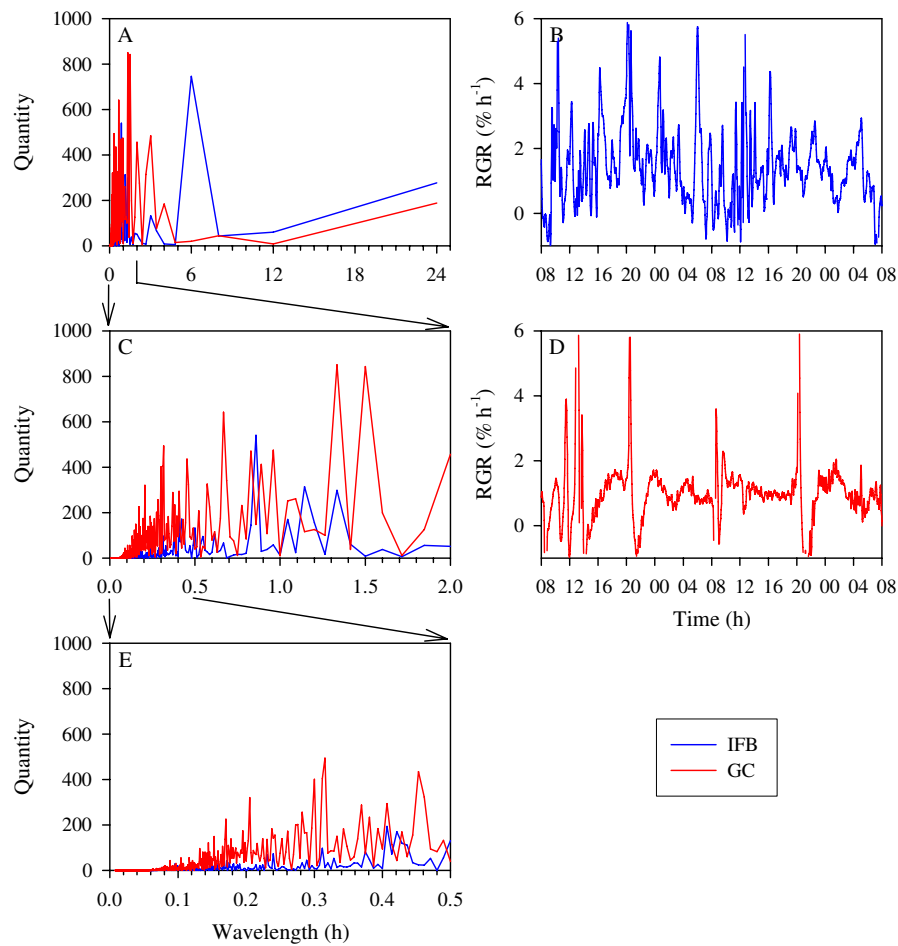
Figure 3.15: Analysis of the time course of the relative growth rate (RGR) of *Populus deltoides* cuttings: Discrete Fast Fourier Transformation (FFT) of the RGR time course over 5 consecutive days of cuttings in the Intensive Forestry Biome (IFB) and growth chamber (GC) at Biosphere 2 Center (A, C, E) with the RGR time course of two of these days of cuttings in the IFB (B) and GC (D).
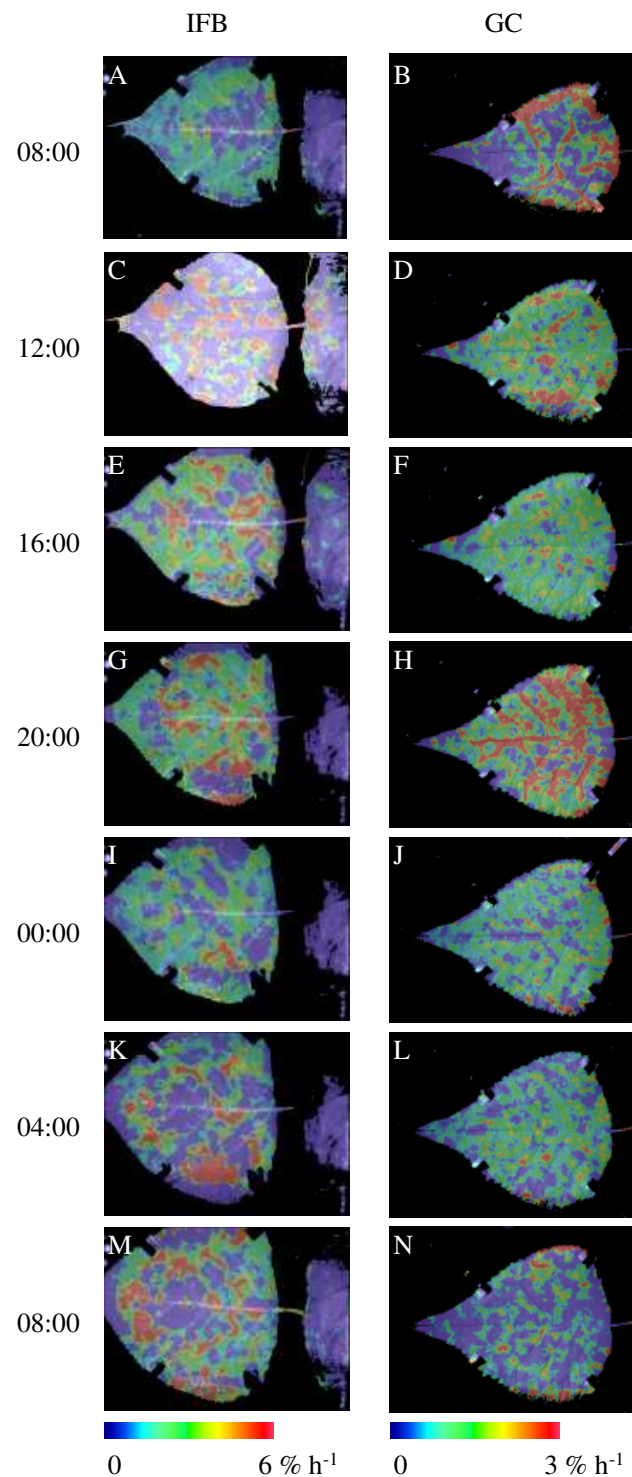
Figure 3.16: Spatio-temporal pattern of the relative growth rate (RGR, % h^{-1}) over 24 h of *Populus deltoides* cuttings grown in the Intensive Forestry Biome (IFB; A, C, E, G, I, K, M) and in the growth chamber (GC; B, D, F, H, J, L, N) in Biosphere 2 Center in 2003: color-coded RGR maps, representing 1-h-averages of the RGR (Blue color: 0 % h^{-1} or lower, red color: 6 and 3 % h^{-1} or higher in the IFB and GC, respectively).

IFB   GC

0   4 % h⁻¹   0   2 % h⁻¹
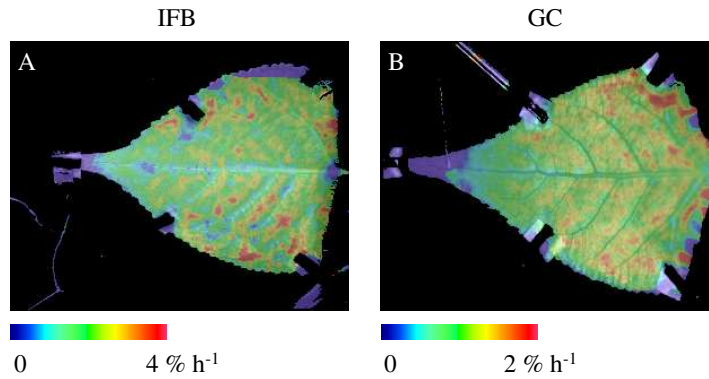
Figure 3.17: Color-coded 24-h-map of the relative growth rate (RGR) of a *Populus deltoides* leaf of cuttings that were either grown in the Intensive Forestry Biome (IFB; A) or in a growth chamber (GC; B): 24h-mean of the RGR (% h^{-1}), obtained with the program 'RGRFlow'. Blue color: 0 % h^{-1} or 'outflow' (the part of the leaf that grew out of the image during image acquisition), red color: 4 and 2 % h^{-1}, respectively.

Figure 3.18: Relative heterogeneity of 24-h-averages of the relative growth rate (RGR) pattern of *Populus deltoides* cuttings in the Intensive Forestry Biome (IFB) and growth chamber (GC) at Biosphere 2 Center (n = 12 ± SE).
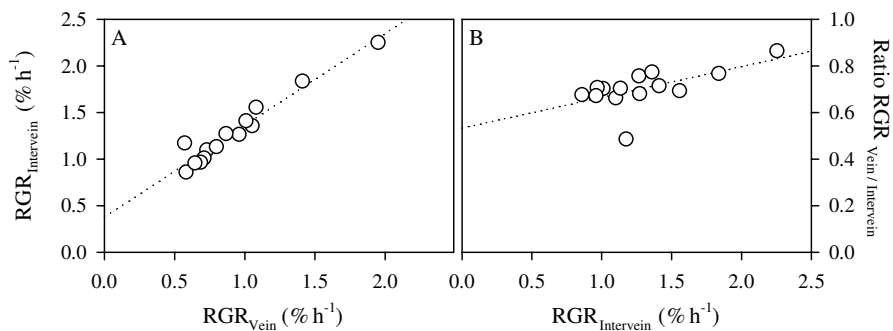
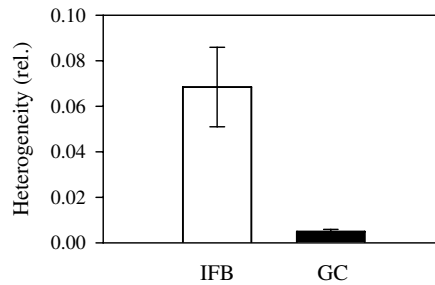
Figure 3.19: Relationship of the relative growth rate (RGR, % h^{-1}) between veinal and interveinal tissue of *Populus deltoides* leaves (A), and relationship between the RGR of veinal compared to interveinal tissue (%) and interveinal growth (B). Data points represent single values.
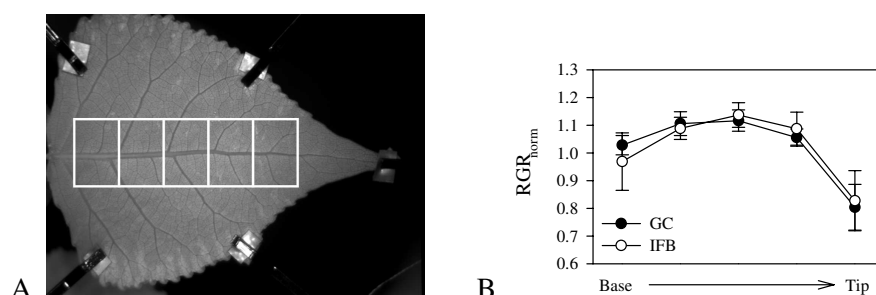
Figure 3.20: Base-tip gradient of the relative growth rate (RGR) in *Populus deltoides*: Illustration showing spatially averaged Areas of Interest (AOIs) along the midvein (A) and normalized RGR gradient (B, n = 8 and 13 ± SE, for the IFB and GC, respectively).

Diel Course of Carbohydrate Concentrations

Changes in the carbohydrate concentration (glucose, fructose, sucrose and starch) of growing and mature leaves of *P. deltoides* cuttings in the IFB and GC were followed over 24 hours in July 2003 (Fig. 3.21).

Leaf carbohydrate concentrations showed a diel rhythm and a tendency for lower concentrations in plants of the IFB, in particular in growing leaves (Fig. 3.21, A, C, E, G). Hexose and starch concentrations increased during daytime and decreased at night.

In growing leaves, glucose (A) was 1.8 times higher in the GC, fructose (C) 3.4, sucrose (E) 1.6, and starch (G) nearly 4 times. In mature leaves, hexose concentrations did not differ much between the IFB and the GC (Fig. 3.21, B, D). Sucrose concentrations (F) were 1.6 times higher in plants that were grown in the GC, starch (H) was also higher by a factor of 2.6.

Glucose:fructose (Glc:Fru) ratio was higher in growing than in mature leaves and higher in the IFB compared to the GC (mean IFB: growing: 2.8 ± 0.4, mature: 1.2 ± 0.1; mean GC: growing: 1.3 ± 0.1, mature: 1.1 ± 0.1).

Relationship Between Diel Leaf Growth and Carbohydrate Concentrations

The diel changes in carbohydrate concentrations (24 h measurement, Fig. 3.21) was plotted against the RGR of leaves at the respective point in time (Fig. 3.14). Although leaves in the GC had higher carbohydrate concentrations and lower growth rates than in the IFB, the overall patterns were similar (Fig. 3.22). No clear relation between soluble sugar concentrations and RGR could be found (Fig. 3.22, A–C). However, starch concentrations correlated positively with RGR (Fig. 3.22, D).

Carbohydrate Concentration of Veinal and Interveinal Tissue

Carbohydrate concentrations of growing and mature leaves of the *P. deltoides* cuttings in the IFB and GC were measured in July 2003. Samples were taken in the afternoon, between 3 and 5 pm and numerated as outlined in Fig. 2.18 (p. 26). As leaf carbohydrates had no significant spatial differences (shown for glucose in Fig. 3.23), the samples of veinal and interveinal tissue were averaged as subreplicates.

Carbohydrate concentrations were mainly elevated in leaves of cuttings grown in the GC, apart from hexoses in interveinal tissue (Fig. 3.24 and 3.25). Hexose concentrations showed no significant differences between the two cultivation conditions, but concentrations in the GC were slightly higher in veinal than in interveinal tissue (Fig. 3.24 and 3.25, A, B).

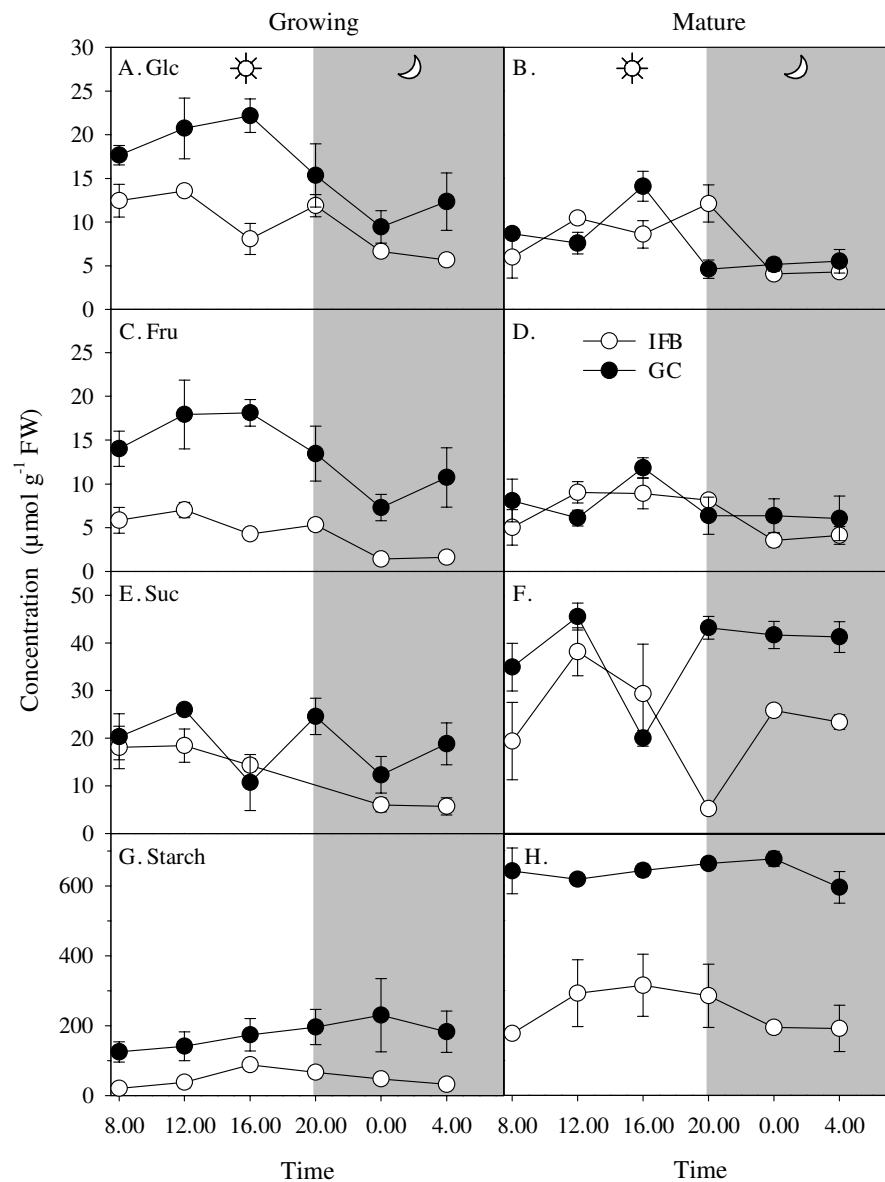Glucose concentrations of veins were twice as high in growing than in mature leaves, independent

Figure 3.21: Diel carbohydrate concentrations of growing and mature leaves of *Populus deltoides* cuttings in the Intensive Forestry Biome (IFB) and the growth chamber (GC): concentration of glucose (A, B), fructose (C, D), sucrose (E, F) and starch (G, H) of growing (left) and mature (right) leaves (n = 3± SE).
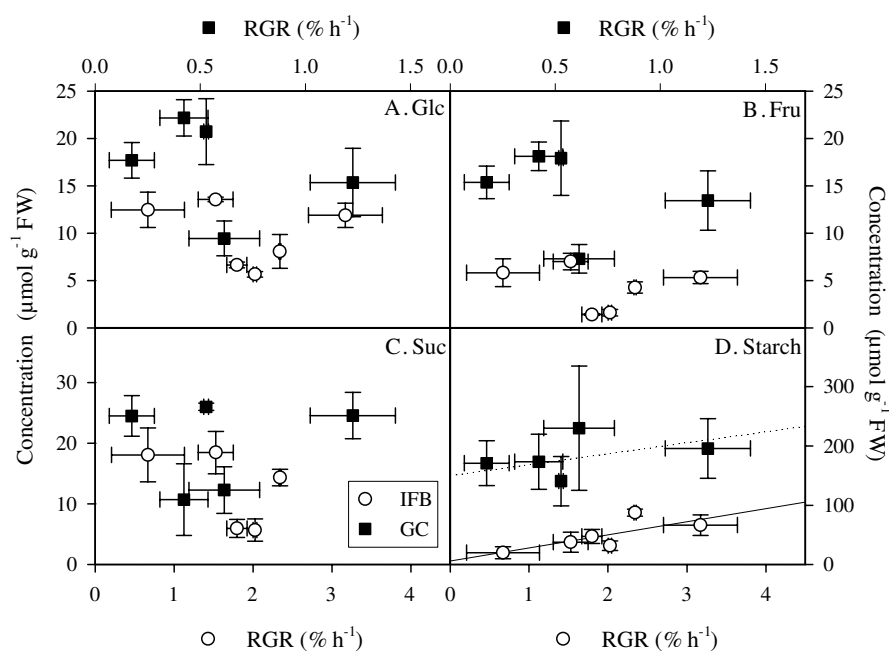
Figure 3.22: Relationship between diel carbohydrate concentration and relative diel growth rate (RGR) of *Populus deltoides* cuttings in the Intensive Forestry Biome (IFB) and the growth chamber (GC) at Biosphere 2 Center: glucose (A), fructose (B), sucrose (C) and starch (D, n = 3 ± SE). Note different scales for RGR for IFB and GC.

from the cultivation conditions (Fig. 3.24, A). Fructose concentrations did not differ between the two developmental stages (Fig. 3.24 and 3.25, B). Sucrose concentrations were similar in veinal and interveinal tissue and 1.4 times higher in growing than in mature leaves (Fig. 3.24 and 3.25, C). In the GC leaves had slightly higher concentrations of sucrose than in the IFB (between 20 and 40 %).

Notably, leaf starch strongly accumulated in both interveinal and veinal tissue in cuttings of the GC compared to plants in the IFB (Fig. 3.24 and 3.25, D). This was true for both, mature and growing leaves, but concentrations were 3 times higher in growing than in mature leaves. Veinal tissue had only half of the starch concentration of interveinal tissue in the GC, and 3–4 times less in the IFB.
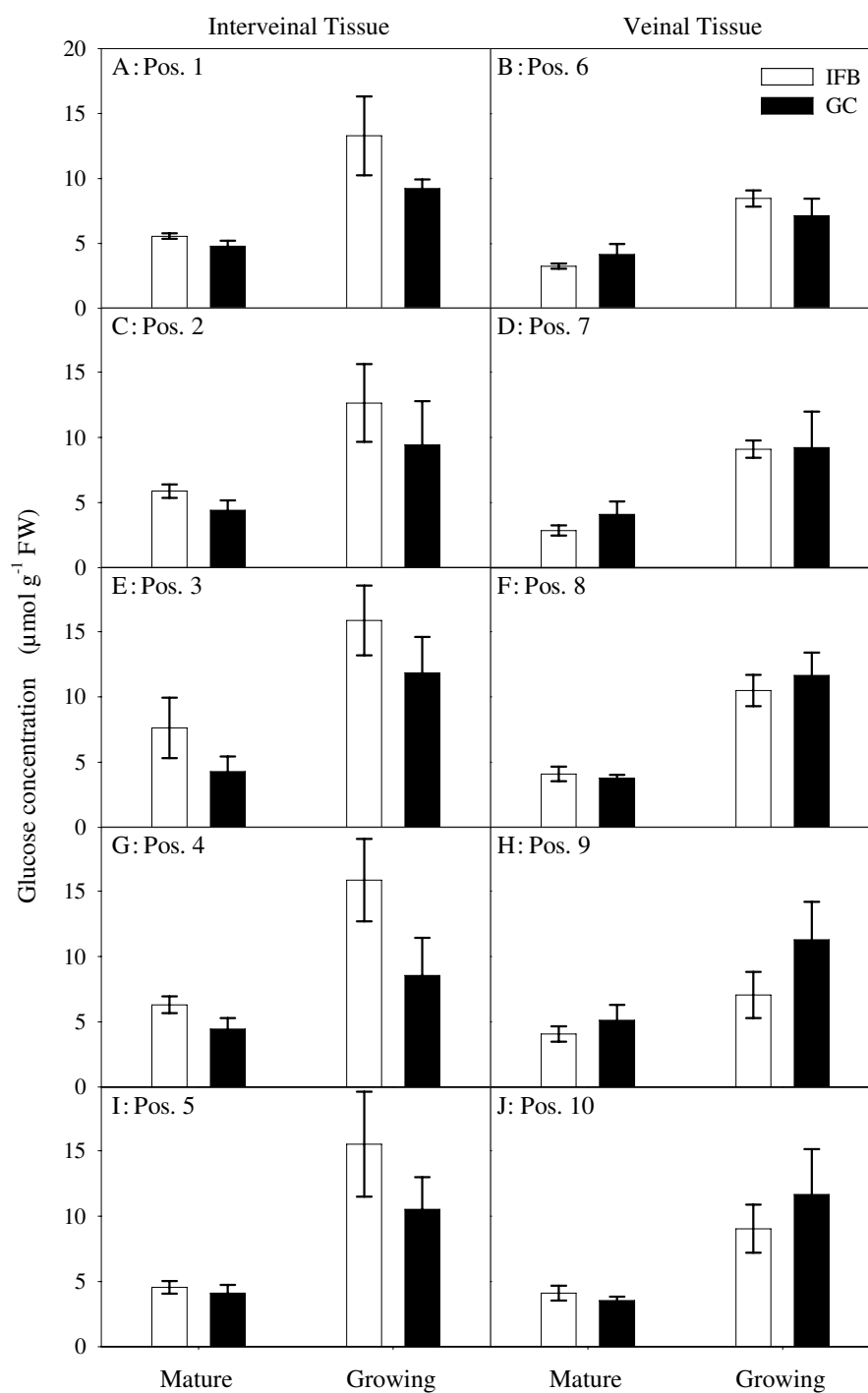
Figure 3.23: Spatial distribution of leaf glucose concentration of *Populus deltoides* cuttings: glucose concentration in μmol g^{-1} FW of interveinal (A, C, E, G, I) and veinal (B, D, F, H, J) tissue of growing and mature leaves in the afternoon. Cuttings were grown either in the Intensive Forestry Biome (IFB) or a growth chamber (GC) at Biosphere 2 Center (n = 3 $\pm$ SE). Position numbers are defined as described in Fig. 2.18.
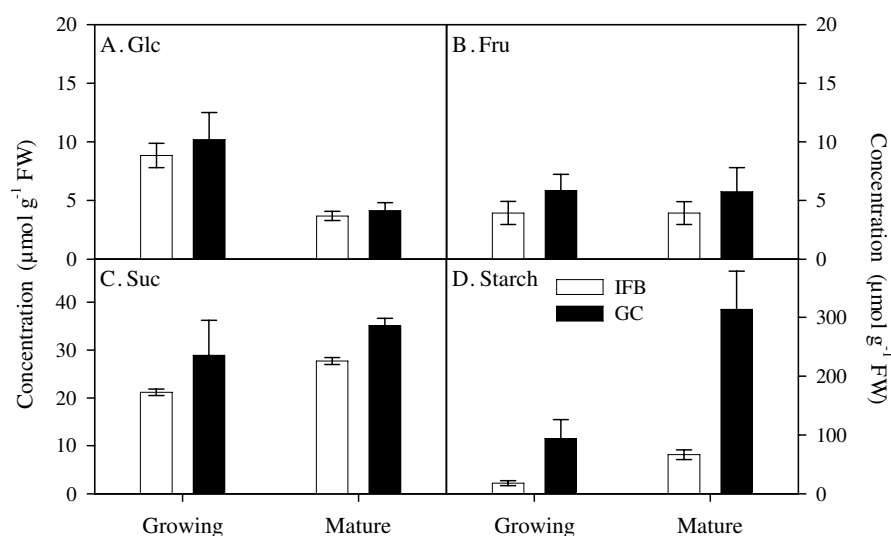
Figure 3.24: Carbohydrate concentrations in veinal tissue of leaves of *Populus deltoides* cuttings: glucose (A), fructose (B), sucrose (C) and starch (D) concentrations in μmol g^{-1} FW of growing and mature leaves in the afternoon. Cuttings were grown either in the Intensive Forestry Biome (IFB) or a growth chamber (GC) at Biosphere 2 Center (n = 3 $\pm$ SE).
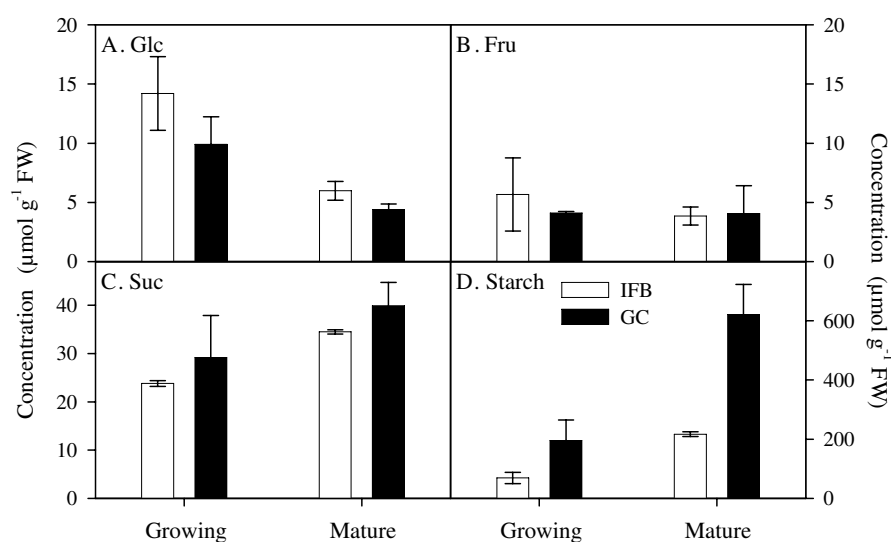

Figure 3.25: Carbohydrate concentrations in interveinal tissue of leaves of *Populus deltoides* cuttings: glucose (A), fructose (B), sucrose (C) and starch (D) concentrations in μmol g^{-1} FW of growing and mature leaves in the afternoon. Cuttings were grown either in the Intensive Forestry Biome (IFB) or a growth chamber (GC) at Biosphere 2 Center (n = 3 $\pm$ SE).

3.2.2 Diel Growth Dynamics in Different Species

As mentioned at the beginning of this section, leaves of different plant species can have diverse patterns of the diel RGR. Here, some diel RGR rhythms of herbaceous plants and trees in different cultivation places (controlled conditions and field) are presented (Fig. 3.26).
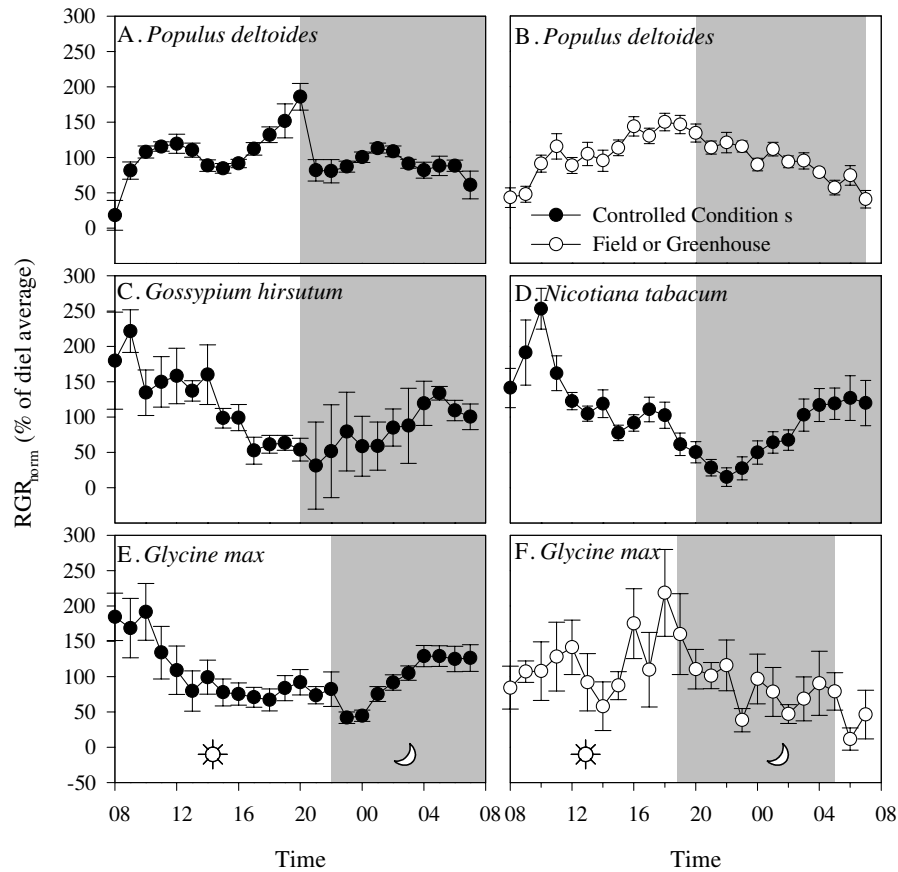

Figure 3.26: Diel course of the relative growth rate (RGR) of several plant species in different cultivation places obtained by digital image sequence processing (DISP): *Populus deltoides* cuttings in the growth chamber (A, n = 24) and Intensive Forestry Biome at Biosphere 2, AZ, USA (B, n = 21), *Gossypium hirsutum* (C, n = 2) and *Nicotiana tabacum* (D, n = 3) in the growth chamber, and *Glycine max* in the growth chamber (E, n = 14) and the field at SoyFACE, IL, USA (F, n = 6 ± SE, respectively).

The diel course of *P. deltoides* under two different cultivation conditions (Fig. 3.26, A, B) was already presented in the last section. A complete inverse pattern could be found for herbaceous plants like cotton (*Gossypium hirsutum*, Fig. 3.26, C), *Nicotiana tabacum* (Fig. 3.26, D) or soybean (Fig. 3.26, E) under controlled conditions. Interestingly, first investigations of the diel course of soybean under full field conditions (Fig. 3.26, F) indicated a reverse trend of diel RGR. Unfortunately, the measurements were not replicated on a high number of plants in the field and showed high disturbances.

3.2.3 Tissue Specific Growth Patterns: Veinal and Interveinal Tissue

Veinal and interveinal tissues have to grow in a precisely coordinated manner. An important question is how this balance occurs, in particular if one keeps in mind that after leaf emergence, interveinal tissue grows mainly two-dimensionally by increasing leaf area and not much thickness during the period of

rapid expansion, while veins still expand in diameter and in length. In an attempt to compare the 2D-growth in interveinal tissue and 3D-growth in veinal tissue, the weight of veinal and interveinal tissue was analyzed in relation to the leaf expansion (monitored via the DISP method, Sect. 3.2.1).

Relationship Between the Weight of Veinal and Interveinal Tissue in *P. deltoides*

Leaves of different developmental stages of *P. deltoides* were sampled. Plants were grown in the greenhouse (PhyTec) for one year. Immediately after cutting off the leaf, its fresh weight was determined. The midvein was excised and also weighed. The ratio between the weight of interveinal tissue (whole leaf – midvein) and the midvein was nearly constant, but depended to some extent on the leaf weight (Fig. 3.27, A). The ratio of veinal to interveinal tissue ranged from 10 – 40 % and could be fitted with a hyperbolic function (Fig. 3.27, B). It was shown that young leaves had more veinal tissue for a unit of leaf weight than large, older leaves.
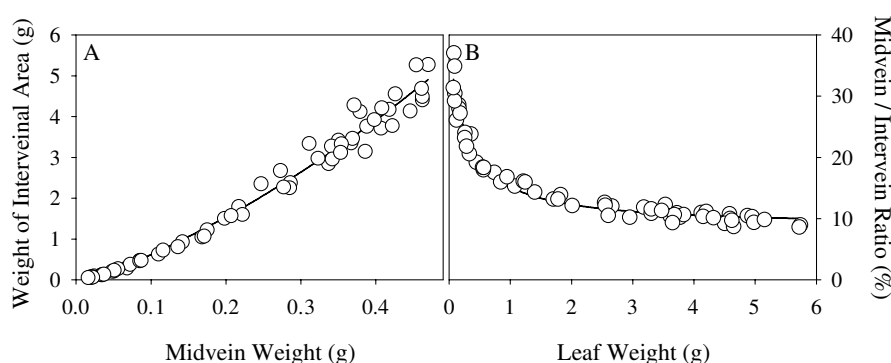

Figure 3.27: Relationship of the fresh weight (g) between midvein and interveinal tissue of *Populus deltoides* leaves (A) and relationship between the ratio of the midvein to interveinal (remaining leaf) tissue (%) and whole leaf fresh weight (g, B). Data points represent single leaves at a range of developmental stages.

Photosynthesis of Veinal and Interveinal Tissue

The potential quantum yield of PS II (F_v/F_m) was measured on dark-adapted *Populus deltoides* leaves in May 2003. Fluorescence induction kinetics were also analyzed in May and June 2003. Leaves of different developmental stages of trees in the IFB were detached and measured with the FluorCam in the laboratory of B2C. The spatial distribution of F_v/F_m was determined for leaves at different developmental stages (Fig. 3.28). F_v/F_m was dependent on the developmental stage of the leaf and differed between midvein and interveinal tissue (Fig. 3.29). In young, fast growing leaves F_v/F_m did not differ significantly between the two tissue types and was slightly higher in the midvein. With progressive developmental stages of the leaves, F_v/F_m of the interveinal tissue increased.

Fluorescence induction kinetics show how fast the photosynthetic apparatus reacts when leaves are exposed to light. Midveins and interveinal tissue reacted differently at the tested developmental stages (Fig. 3.30). In young, growing leaves effective quantum yield ($\Delta F/F_m\prime$) of the midvein increased faster than in the interveinal tissue and reached slightly higher values (Fig. 3.30, A). In slightly older, growing leaves veinal tissue still showed a slightly greater initial slope but there was no difference between the two tissues at saturation (Fig. 3.30, B). In mature leaves the photosynthetic apparatus in the interveinal tissue reacted faster upon illumination than in the midvein (Fig. 3.30, E). In contrast to $\Delta F/F_m\prime$, non-photochemical quenching (NPQ) was always higher in the interveinal tissue, independent of the developmental stage (Fig. 3.30, B, D, F).
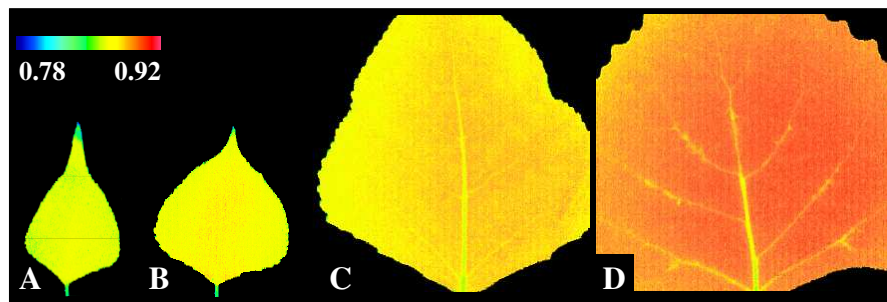
Figure 3.28: Color-coded potential quantum yield of PS II (F_v/F_m) of dark-adapted *Populus deltoides* leaves at different developmental stages with a relative growth rate (RGR) of 35 (A), 10 (B), 6 (C) and 0 (D) % d^{-1} (colors as indicated by color bar).

Figure 3.29: Potential quantum yield of PS II (F_v/F_m) of veinal and interveinal tissue of dark-adapted *Populus deltoides* leaves at different developmental stages.
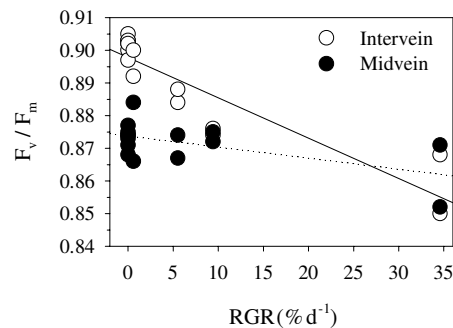
3.2.4   Summary of Spatio-Temporal Patterns

Cuttings of *P. deltoides* were grown either in controlled conditions in a growth chamber (GC) or in the IFB in semi-controlled conditions at Biosphere 2 Center. In the IFB, cuttings had more branches and 2 times more leaves per plant than in the GC. The diel leaf growth pattern differed between the two cultivation conditions, but the general diel course was not altered and completely inverse to the diel course of tobacco, cotton or soybean, cultivated in the GC. The temporal RGR pattern of *P. deltoides* cuttings showed less fluctuations in the GC than in the IFB with sharp peaks at day-night-transitions. Nevertheless, periodic oscillations were more pronounced in the absence of fluctuating conditions. The spatial RGR pattern was more heterogenous in the IFB, where light and temperature fluctuations were present. Carbohydrates in *P. deltoides* leaves showed a diel rhythm. In the GC, starch was accumulated.

A growth-base-tip-gradient was only slightly present with less growth at the base and the tip. Carbohydrate concentrations did not show pronounced spatial variations, beside differences between veinal and interveinal tissue. Whereas in the GC veinal tissue had less concentrations of carbohydrates, in the IFB it showed higher values than in interveinal tissue. A difference between veinal and interveinal tissue in *P. deltoides* could also be found for 2D-growth, with veinal tissue growing approximately $\frac{3}{4}$ of interveinal tissue. The ratio of midvein weight and the weight of interveinal tissue was approximately 10 % for larger leaves but could reach values up to 40 % for very small leaves. Beside growth, also the potential quantum yield differed development-dependent between veinal and interveinal tissue. In young leaves, midvein-surrounding tissue had a similar quantum yield as interveinal tissue, while in mature leaves, yield of vein-surrounding tissue was much smaller.
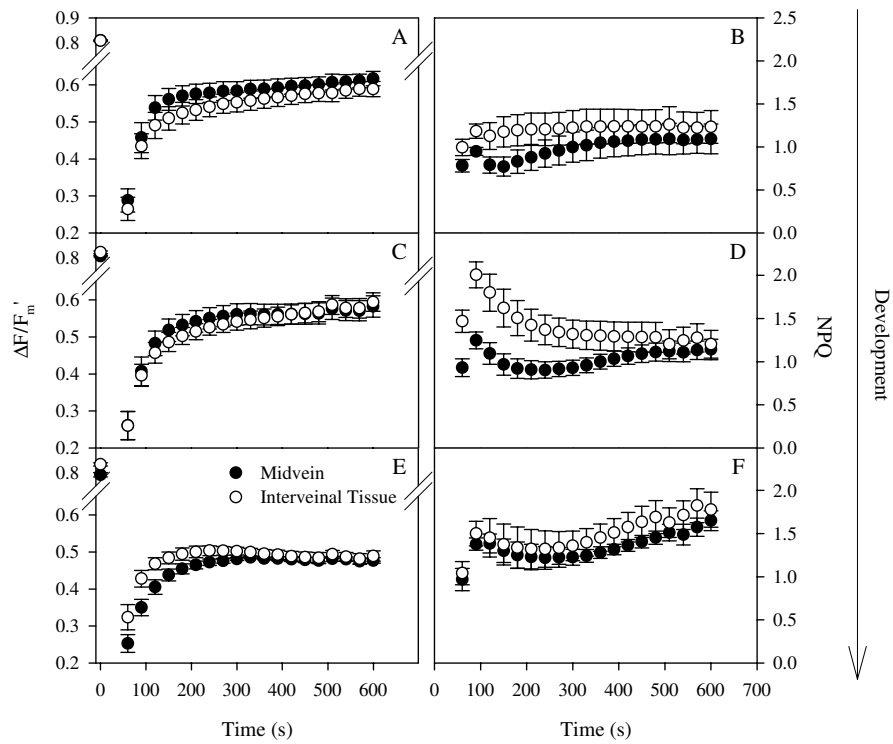
Figure 3.30: Fluorescence induction kinetic of veinal and interveinal tissue of dark-adapted *Populus deltoides* leaves at three different developmental stages. Potential quantum yield (F_v/F_m) for dark-adapted and effective quantum yield ($\Delta F/F_m\prime$) for light-saturated leaves (A, C, D) and NPQ (B, D, F) of growing (unrolling: A, B; fully unrolled: C, D) and mature (E, F) leaves (n = 6 ± SE).

3.3   Effect of Long-Term Elevated CO_2 on Growth and Photosynthesis of *Populus deltoides*

The aim of the following experiments was to investigate the effect of long-term elevation of CO_2 on leaf growth and photosynthesis of *P. deltoides*. Leaf growth was followed manually as well as with DISP. Photosynthesis was investigated on the level of electron transport (chlorophyll fluorescence), assimilation rate (gas exchange) and assimilate pools (carbohydrate concentration). Experiments were performed in the Intensive Forestry Biome (IFB) of Biosphere 2 Center (B2C), AZ, USA.

3.3.1   Effect of Elevated CO_2 on Growth of *Populus deltoides*

Leaf Size

Leaf growth of *P. deltoides* trees in the IFB was followed over three weeks in September 2002. In each bay (400, 800 and 1200 ppm) three trees were chosen, and at each tree leaf areas of the following branches were measured thrice a week: side branches in three height levels on the southern and the northern side, respectively, as well as the shoot tip. Furthermore, the branch volume was estimated. At this time, trees had reached a height of approximately 5 m.

A profile of the distribution of leaf area and RGR of the first 30 leaves of the tree tip showed that leaf area was positively correlated with $[CO_2]$ (Fig. 3.31), beside younger leaves in 800 ppm, whose RGR was reduced, which led to smaller leaves.
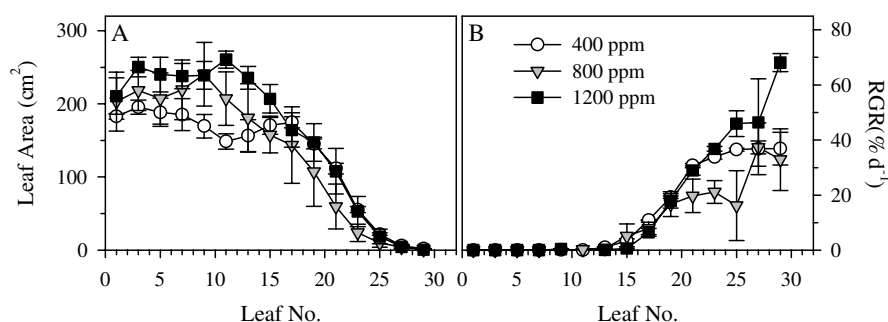

Figure 3.31: Leaf area (cm^2; A) and relative growth rate (RGR, % d^{-1}; B) of *Populus deltoides* in ambient and elevated $[CO_2]$ in September 2002: First 30 leaves of the tree tip of trees that were grown in 400, 800 and 1200 ppm (n = 3 $\pm$ SE).

The development of leaf area and RGR of leaves that were just unrolling (defined as emerging) at the end of August 2002 (the beginning of the measurements) is depicted in Fig. 3.32. At that time, leaves of trees that were grown in 800 ppm still had a leaf area that was between the area of leaves of trees grown in 400 and 1200 ppm, respectively.

Leaf area at emergence was dependent on branch height and $[CO_2]$ and showed a high variability (Fig. 3.33). Leaf area of the first unrolling leaf at the tree tip declined with rising $[CO_2]$, whereas the CO_2 response was absent or inverse at the measured side branches. Furthermore, with approximately 6–10 cm^2, leaf area at emergence did not differ significantly between tree tip and the uppermost measured side branches.
Final leaf area (FLA, measured in mid September) of the tree tip rose slightly with $[CO_2]$ (13 % higher in 800 ppm and 27 % higher in 1200 ppm, compared to ambient $[CO_2]$, Fig. 3.34, A). Side branches
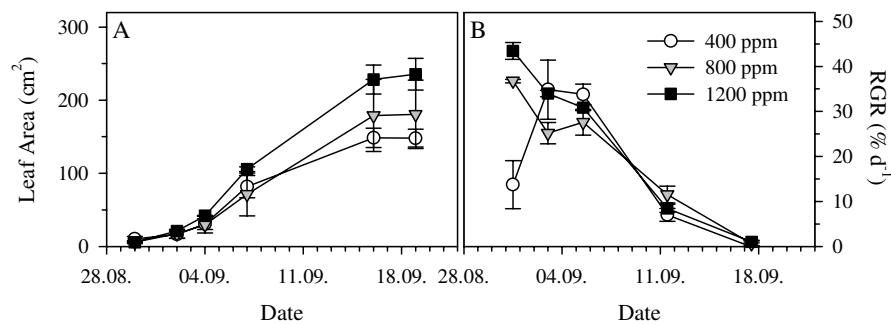
Figure 3.32: Development of leaf area (cm^2; A) and relative growth rate (RGR, % d^{-1}; B) of *P. deltoides* in ambient and elevated [CO$_2$] in September 2002: Leaves at the tree tip, which were emerging at the beginning of the measurements. Trees were grown in 400, 800 and 1200 ppm (n = 3 $\pm$ SE).

showed either similar leaf areas (E, G) or rising values in elevated [CO$_2$] (B–D, F). When all measured data was averaged, this resulted in a leaf area increase of 13 % in 800 and 22 % in 1200 ppm. Like the leaf area at emergence, higher branches reached higher final leaf areas, and the tree tip obtained 50 – 80 % higher values as the uppermost measured side branches.

The relative leaf area (RLA) of leaves at the tree tip and southern lower side branch was plotted against the RGR of the specific point in time (Fig. 3.35). Leaves did not grow for a long time with high growth rates but gained most increase in leaf area during growth rates of approximately 20 – 40 % d^{-1} and matured slowly (Fig. 3.35, A, B). The overall pattern did not depend significantly on the CO$_2$ treatment or the type of branch, but leaves grew faster at the main stem (tree tip, Fig. 3.35, A).

The response of branch parameters like length, volume and mean internode length to elevated [CO$_2$] showed a similar tendency as the final leaf area with longer and thicker branches in elevated [CO$_2$] and higher positions at the tree (Tab. 3.4). Measured parameters were variable; in average, branch length was increased by 15 % in 800 and 44 % in 1200 ppm. Volume was increased by 43 and 100 %, respectively, internode length by 5 and 24 %.

Diel Leaf Growth

Diel leaf growth was followed with the DISP method. Because of the height of the trees, leaves of lower side branches were used for analysis. The overall growth course was similar in all three treatments: the RGR increased during the day with intense fluctuations, reached its maximum at dawn, and declined throughout the night with a smoother RGR course (Fig. 3.36).

The averaged data (Fig. 3.36, G) illustrate homologies and slight differences between the two treatments. At the beginning of the night, the RGR declined only slightly and after midnight more rapidly in both treatments. In the afternoon, a decline in the RGR at approximately 4 pm was present in elevated [CO$_2$]. In April 2003, the RGR was unusual high in the afternoon, but this pattern could not be found in the other months. But also without this peak, the normalized RGR was lower in 1200 ppm at that time.
The growth decline in the afternoon could also be found by A. Walter (Walter et al., 2005), and was analyzed in more detail in terms of assimilation rate and carbohydrate concentration.
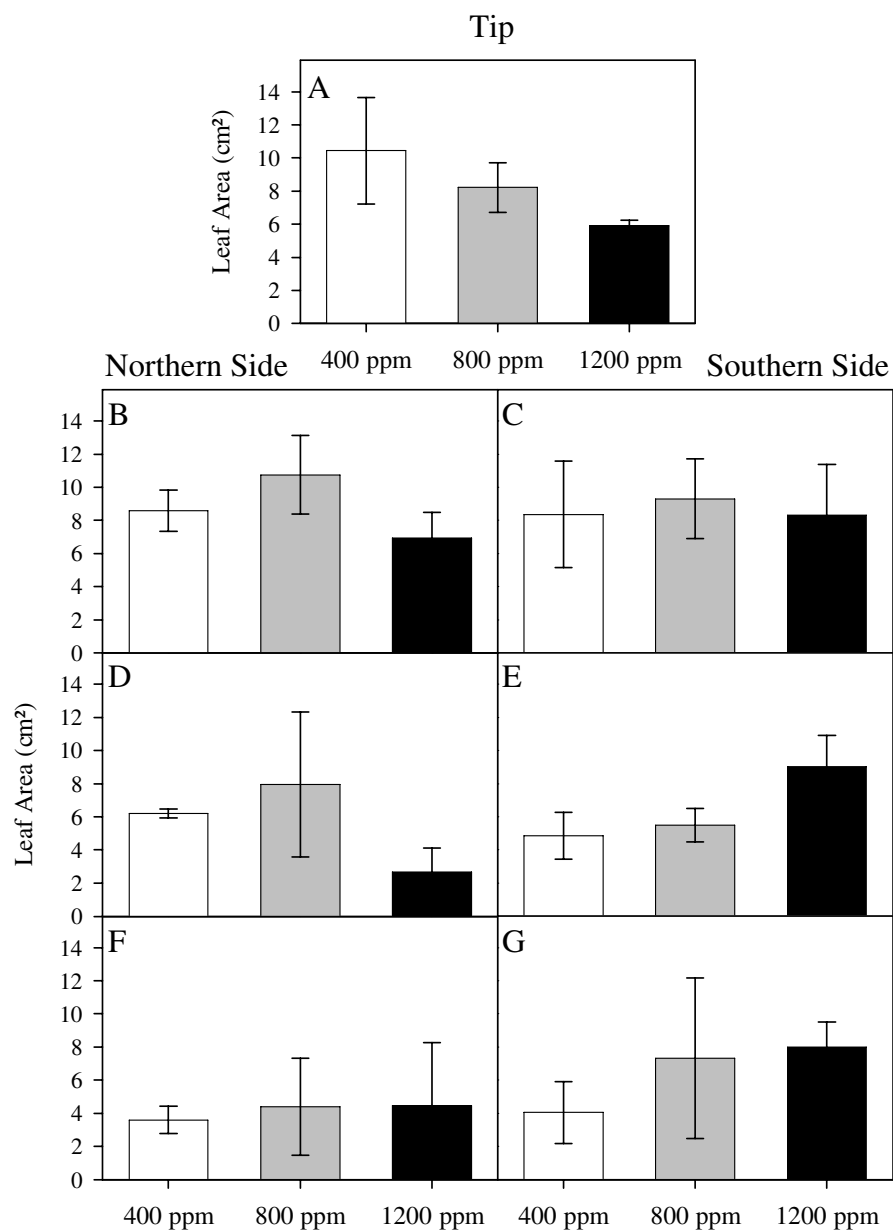
Figure 3.33: Leaf area (cm^2) of unrolling leaves of *Populus deltoides* in ambient and elevated [CO_2] in September 2002: Latest unrolling leaf of the tree tip (A) and of side branches in three different heights on the northern (B, D, F) and southern side (C, E, G) of trees grown in 400, 800 and 1200 ppm (n = 3 $\pm$ SE).

Figure 3.34: Final leaf area (cm^2) of *Populus deltoides* in ambient and elevated [CO$_2$] in September 2002: Fully expanded leaves of the tree tip (A) and of side branches in three different heights on the northern (B, D, F) and southern side (C, E, G) of trees grown in 400, 800 and 1200 ppm (n = 13 $\pm$ SE).

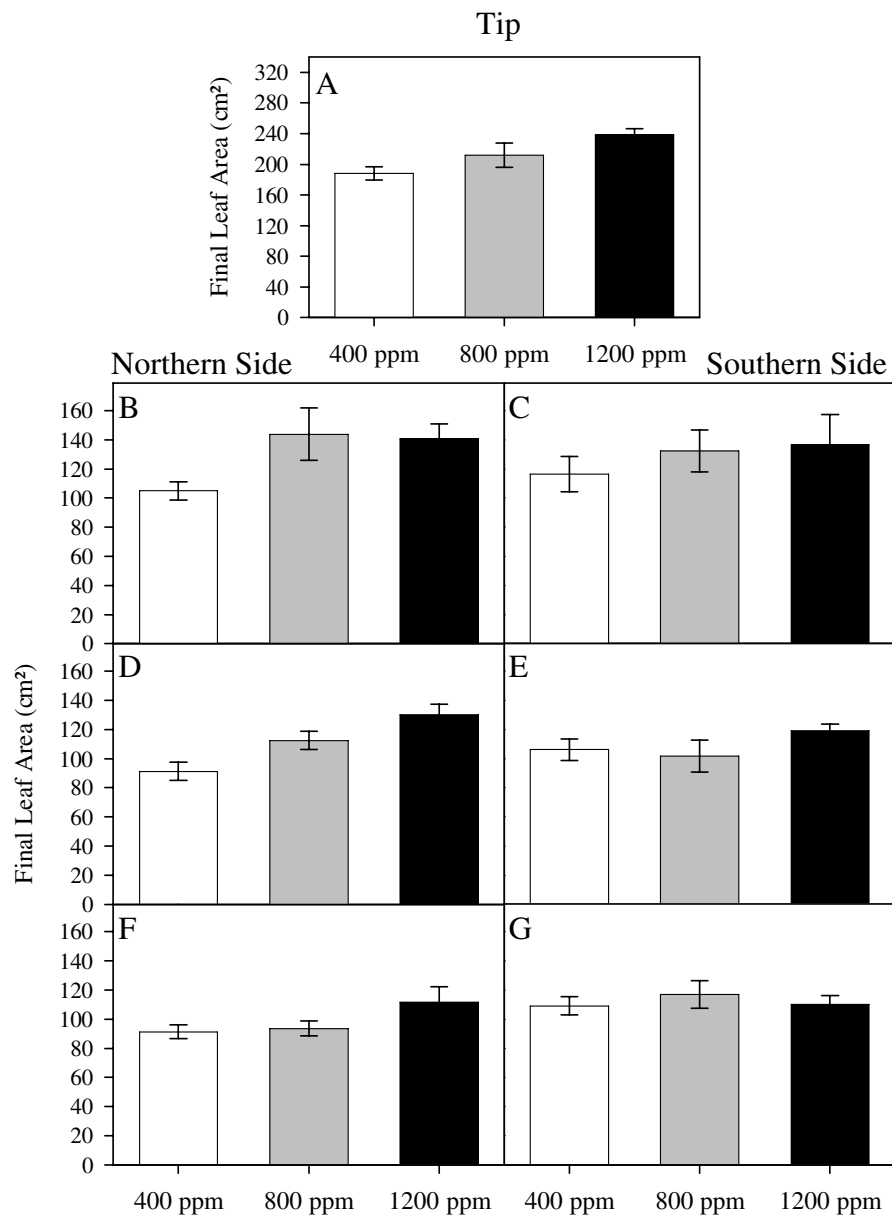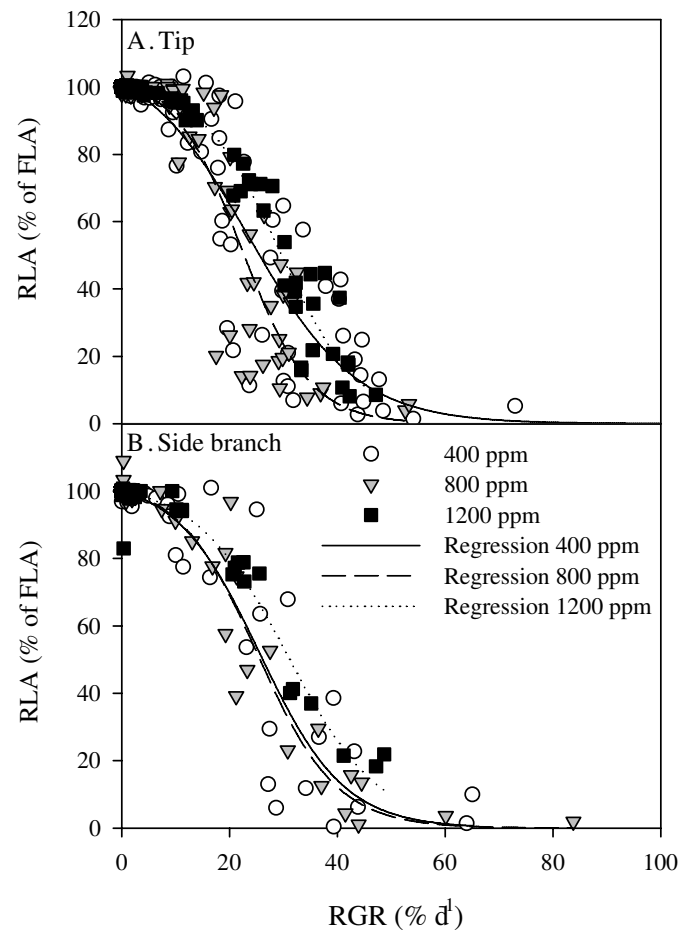Figure 3.35: Relative leaf area (RLA, %) in relation to the relative growth rate (RGR, % d^{-1}) of *Populus deltoides* in ambient and elevated [CO_2] in September 2002: Tree tip (A) and lower side branch (B) of trees grown in 400, 800 and 1200 ppm (single values and regression).

Table 3.4: Effect of elevated [CO$_2$] on branch parameters of *Populus deltoides*:
Branch length, volume, and averaged internode length of different branches (tree tip
and side branches in three different heights on the northern and southern side of the
tree, n = 3 $\pm$ SE).

| [CO$_2$]	Branch		Length (cm)	Volume (cm^3)	Internode length (cm)
400 ppm	Tip		58.0 $\pm$ 1.2	1000.7 $\pm$ 167.7	2.9 $\pm$ 0.1
	South	top	27.8 $\pm$ 8.1	211.0 $\pm$ 66.5	1.9 $\pm$ 0.3
		middle	22.8 $\pm$ 2.4	177.0 $\pm$ 47.4	1.7 $\pm$ 0.1
		bottom	37.0 $\pm$ 8.0	343.2 $\pm$ 95.7	2.0 $\pm$ 0.2
	North	top	27.4 $\pm$ 10.3	320.3 $\pm$ 193.5	1.6 $\pm$ 0.3
		middle	17.0 $\pm$ 2.3	111.5 $\pm$ 23.3	1.2 $\pm$ 0.1
		bottom	25.7 $\pm$ 5.6	187.7 $\pm$ 54.8	1.7 $\pm$ 0.3
800 ppm	Tip		60.8 $\pm$ 6.6	1375.2 $\pm$ 337.1	2.7 $\pm$ 0.2
	South	top	21.7 $\pm$ 2.4	174.2 $\pm$ 42.7	1.5 $\pm$ 0.1
		middle	23.0 $\pm$ 3.1	184.0 $\pm$ 58.0	1.5 $\pm$ 0.1
		bottom	46.8 $\pm$ 2.4	517.0 $\pm$ 127.9	2.5 $\pm$ 0.1
	North	top	15.4 $\pm$ 1.2	85.7 $\pm$ 13.3	1.2 $\pm$ 0.1
		middle	23.8 $\pm$ 2.6	185.1 $\pm$ 52.9	1.6 $\pm$ 0.1
		bottom	51.0 $\pm$ 3.5	632.3 $\pm$ 174.8	2.4 $\pm$ 0.1
1200 ppm	Tip		68.7 $\pm$ 3.9	1462.3 $\pm$ 469.2	3.3 $\pm$ 0.1
	South	top	34.2 $\pm$ 9.2	349.7 $\pm$ 174.5	1.9 $\pm$ 0.3
		middle	29.7 $\pm$ 2.5	244.1 $\pm$ 29.8	1.8 $\pm$ 0.1
		bottom	56.5 $\pm$ 12.1	786.8 $\pm$ 257.4	2.7 $\pm$ 0.5
	North	top	37.5 $\pm$ 15.4	628.5 $\pm$ 444.9	2.0 $\pm$ 0.6
		middle	26.8 $\pm$ 3.1	291.0 $\pm$ 88.8	1.6 $\pm$ 0.0
		bottom	48.8 $\pm$ 11.6	552.8 $\pm$ 183.0	2.6 $\pm$ 0.5
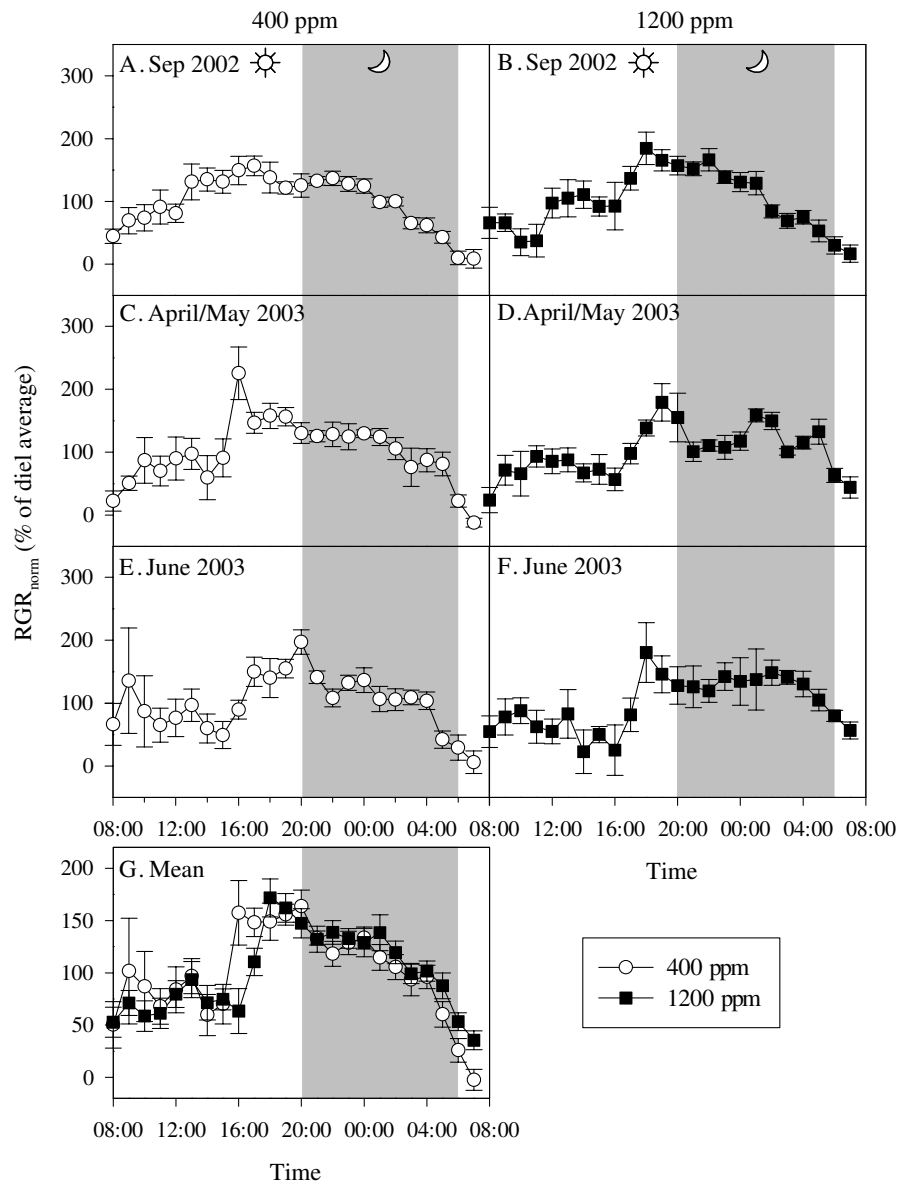
Figure 3.36: Diel growth of *Populus deltoides* leaves in ambient (400 ppm, left) and elevated (1200 ppm, right) [CO_2] in September 2002 (A, B), April/May 2003 (C, D), June 2003 (E, F) and the mean of all measurements (G). The hourly averaged relative growth rate (RGR) was normalized (% of diel average, n: A = 10, B = 9, C = 6, D = 5, E = 7, F = 7, G = 23 and 21, respectively $\pm$ SE).

Color-coded RGR maps, representing 1-h-averages of the RGR, show the high patchiness of growth patterns (Fig. 3.37). The overall time course of the RGR can be seen, with increasing growth rates during day and declining growth rates in the night, for both, leaves in 400 ppm (left graphs) and 1200 ppm (right graphs). The average RGR maps over 24 h of a leaf in 400 and 1200 ppm, respectively, show less patchiness, and differences between veins and interveinal tissue can be seen (Fig. 3.38).
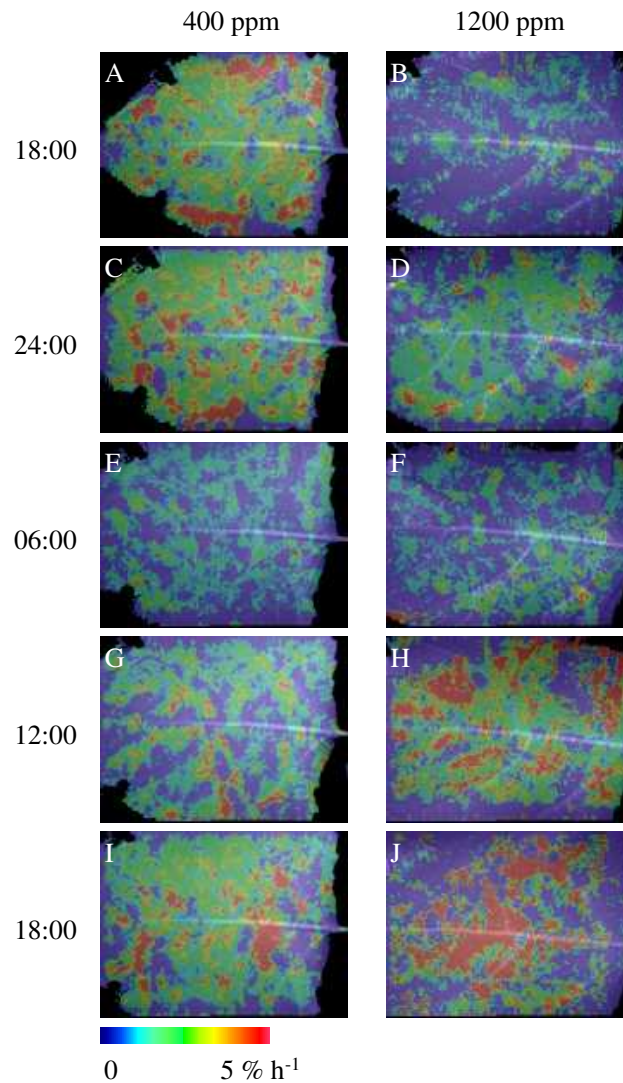

Figure 3.37: Spatio-temporal pattern of the relative growth rate (RGR, % h^{-1}) over 24 h of *Populus deltoides* leaves grown in 400 ppm (A, C, E, G, I) and 1200 ppm (B, D, F, H, J) in the Intensive Forestry Biome of Biosphere 2 Center in September 2002: Color-coded RGR maps, representing 1-h-averages of the RGR (Blue color: 0 % h^{-1} or lower, red color: 5 % h^{-1} or higher).

Spatial patchiness was estimated for 24-h RGR maps of sequences in September 2002. The relative heterogeneity of the 24-h-averaged RGR of leaves in elevated [CO$_2$] was approximately 1.7 times higher compared to ambient conditions (Fig. 3.39).
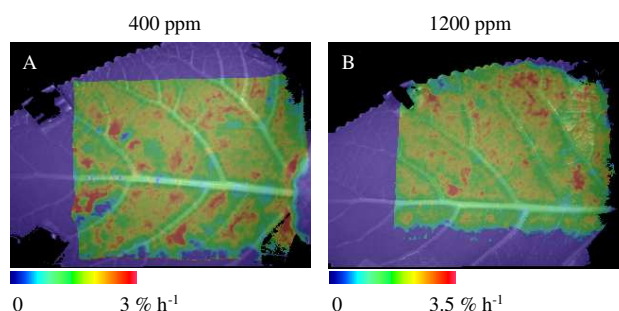
400 ppm   1200 ppm

A   B

0   3 % h^{-1} 0   3.5 % h^{-1}

Figure 3.38: 24-h-average of the relative growth rate (RGR, % h^{-1}) of *Populus deltoides* leaves grown in 400 ppm (A) and 1200 ppm (B) the Intensive Forestry Biome of Biosphere 2 Center in September 2002: Color-coded RGR map, representing 24-h-averages of the RGR (Blue color: 0 % h^{-1} or 'outflow', red color: 3 and 3.5 % h^{-1}, respectively, or higher).

Figure 3.39: Relative heterogeneity of 24-h-averages of the relative growth rate (RGR) pattern of *Populus deltoides* trees grown in 400 and 1200 ppm at Biosphere 2. DISP sequences were achieved in September 2002 (n = 7 and 9 $\pm$ SE for 400 and 1200 ppm, respectively).
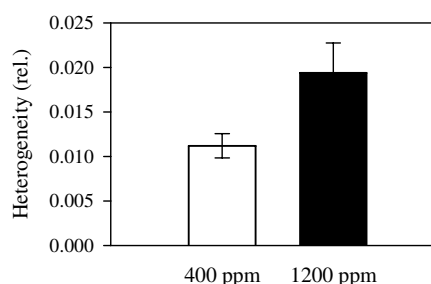
3.3.2   Effect of Elevated CO_2 on Photosynthesis of *Populus deltoides*

Potential Quantum Yield and Induction Kinetics

The potential quantum yield of Photosystem (PS) II (F_v/F_m) was determined on leaves with different developmental stages (Fig. 3.40). Mature leaves reached higher yields (0.85 – 0.875) than growing leaves (0.81 – 0.84). F_v/F_m declined slightly with increasing RGR. In this experiment, F_v/F_m was measured *in situ* on attached leaves and showed no significant difference between the CO_2 treatments.

In a second experiment, a fluorescence induction kinetic was accomplished on detached leaves at three different developmental stages (Tab. 3.5). As shown in the last experiment, F_v/F_m showed a clear dependence on the developmental stage with lower F_v/F_m values in growing leaves. The initial slope $\Delta F/F_m\prime_{ini}$ (a measure for fast processes like formation of a proton concentration gradient across the thylakoid membrane) declined with leaf age and took values between 0.004 and 0.002. No effect of [CO_2] on the measured parameters could be found. Neither the initial slope nor the value at 150 μmol m^{-2}s^{-1} of NPQ indicate a correlation with developmental stage or with CO_2 concentration.

In a third experiment, effective quantum yield ($\Delta F/F_m\prime$) was quantified under ambient conditions over a range of light intensities. $\Delta F/F_m\prime$ is controlled by light intensity primarily, however, if plotted against light intensity, $\Delta F/F_m\prime$ and electron transport rate (ETR) showed a dependency on development (Fig. 3.41). Mature leaves in 1200 ppm had slightly, but not significantly higher values for $\Delta F/F_m\prime$ and ETR than leaves in 400 ppm (Fig. 3.41, B). Growing leaves did not clearly exhibit this tendency, as not enough growing leaves in 1200 ppm were exposed to high light intensities during the time of the
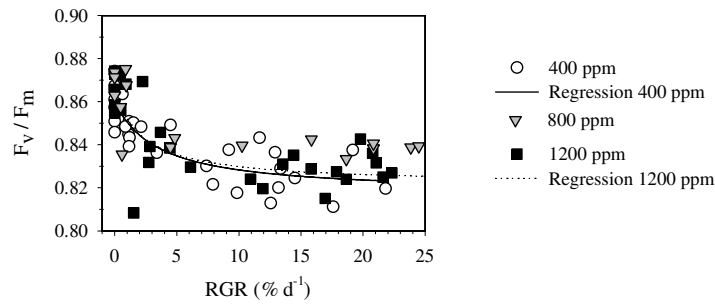
Figure 3.40: Potential quantum yield of PS II (F$_v$/F$_m$) of dark-adapted *Populus deltoides* leaves in different developmental stages in ambient and elevated [CO$_2$]. Trees were grown in 400, 800 and 1200 ppm for four years at Biosphere 2 Center. Data points represent single values, measurements were performed on attached leaves.

Table 3.5: Parameters of chlorophyll fluorescence induction kinetic of detached leaves of *Populus deltoides* grown in three different CO$_2$ concentrations: F$_v$/F$_m$, ΔF/F$_m$$\prime$ $_{ini}$, ΔF/F$_m$$\prime_{150}$, NPQ$_{ini}$ and NPQ$_{150}$. Index $_{ini}$ stands for the initial slope, $_{150}$ for maximal values at 150 μmol m^{-2}s^{-1}. Parameters were gained of mean values of three replicates per leaf age and CO$_2$ concentration.

Leaf Age	Parameter	400 ppm	800 ppm	1200 ppm
	F$_v$/F$_m$	0.805	0.794	0.797
	ΔF/F$_m$$\prime$ $_{ini}$	0.004	0.004	0.004
Growing	ΔF/F$_m$$\prime_{150}$	0.606	0.541	0.576
unrolling	NPQ$_{ini}$	0.010	0.014	0.013
	NPQ$_{150}$	1.006	1.228	1.020
	F$_v$/F$_m$	0.813	0.805	0.808
	ΔF/F$_m$$\prime$ $_{ini}$	0.003	0.004	0.004
Growing	ΔF/F$_m$$\prime_{150}$	0.633	0.613	0.614
fully unrolled	NPQ$_{ini}$	0.021	0.021	0.020
	NPQ$_{150}$	0.947	1.228	1.020
	F$_v$/F$_m$	0.825	0.839	0.835
	ΔF/F$_m$$\prime$ $_{ini}$	0.002	0.003	0.003
Mature	ΔF/F$_m$$\prime_{150}$	0.512	0.528	0.558
	NPQ$_{ini}$	0.000	0.013	0.007
	NPQ$_{150}$	1.390	1.442	1.141

experiment (Fig. 3.41, A). $\Delta F/F_m\prime$ of mature leaves in 400 ppm saturated at high light intensities, in contrast to 1200 ppm.
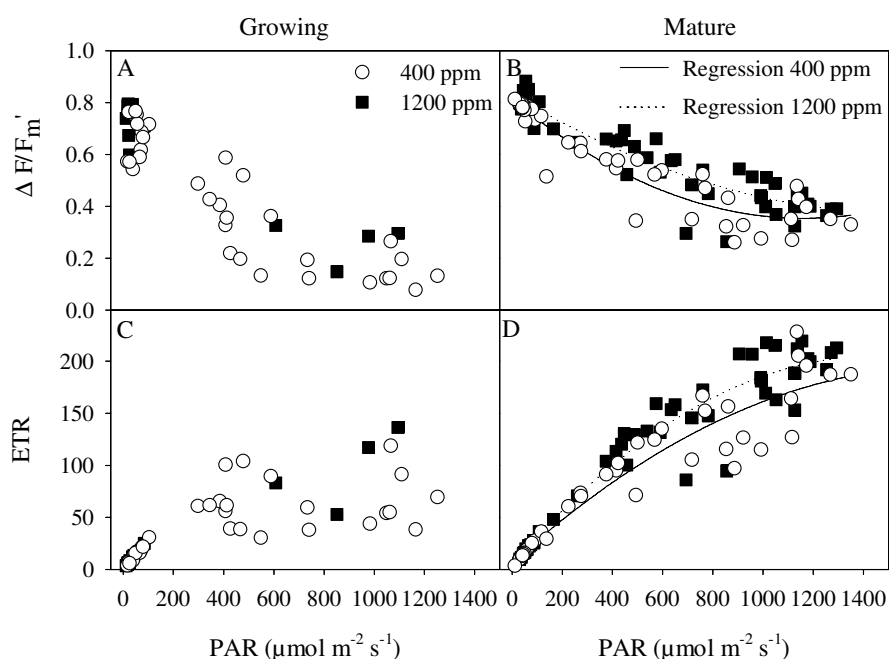

Figure 3.41: Effective quantum yield ($\Delta F/F_m\prime$; A, B) and electron transport rate (ETR; C, D) light curves of growing (A, C) and mature leaves (B, D) of *Populus deltoides* in ambient (400 ppm) and elevated (1200 ppm) [CO_2]. Data points were collected under ambient light intensities and were fitted using single exponential functions.

Net CO_2 exchange rate and stomatal conductance – Gas exchange

In contrast to the response of the quantum yield, net CO_2 exchange rate (A) was significantly higher in elevated [CO_2] (Fig. 3.42, top). The assimilation rate of leaves in 1200 ppm compared to 400 ppm was increased by a factor of approximately 2.4 in growing and by a factor of 1.6 in mature leaves. Stomatal conductance (g_S) of growing leaves was comparable in all three [CO_2] treatments and only slightly elevated in 1200 ppm. In mature leaves, g_S was decreased in both elevated [CO_2] treatments (Fig. 3.42, bottom).

The relationship between net CO_2 exchange rate and stomatal conductance showed a dependency on [CO_2] (Fig. 3.43). In elevated [CO_2] leaves could achieve higher net CO_2 exchange rates with lower g_S. This effect was even more distinct in mature leaves (Fig. 3.43, B).

Average water-use efficiency (WUE, A/E, calculated from data of Fig. 3.42) was dependent on [CO_2] and development (Tab. 3.6). In growing leaves WUE was 1.6 and 2 times higher in 800 and 1200 ppm, respectively, compared to ambient conditions. In mature leaves WUE was increased to a similar extent, by a factor of 1.3 and 2 in 800 ppm and 1200 ppm, respectively.
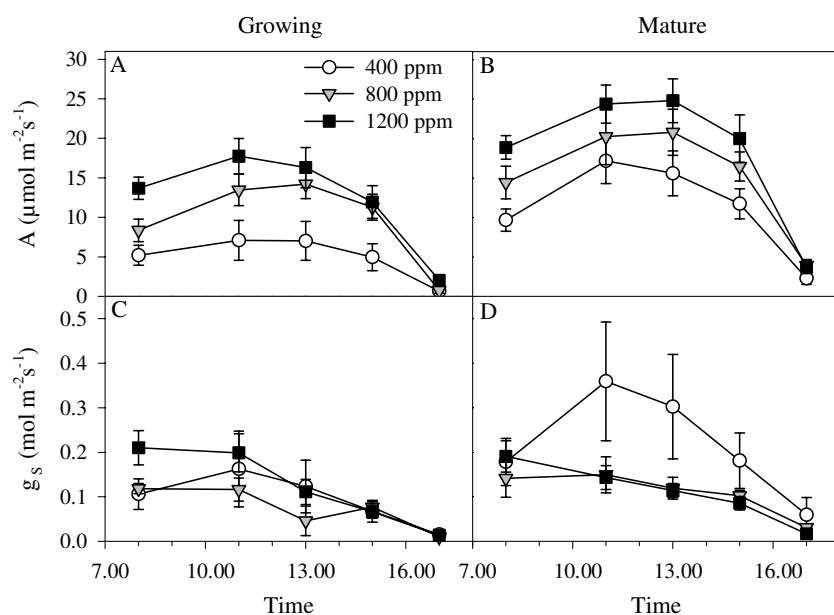
Figure 3.42: Diurnal net CO$_2$ exchange rate A (μmol m^{-2} s^{-1}, A, B) and stomatal conductance g$_S$ (mol m^{-2} s^{-1}, C, D) of growing (A, C) and mature (B, D) leaves of *Populus deltoides* in ambient and elevated CO$_2$. Light intensities were set to mean values of the respective point in time: 400, 1200, 1100, 675 and 100 μmol m^{-2} s^{-1} at 8:00, 11:00, 13:00, 15:00 and 17:00 (n = 5 $\pm$ SE).
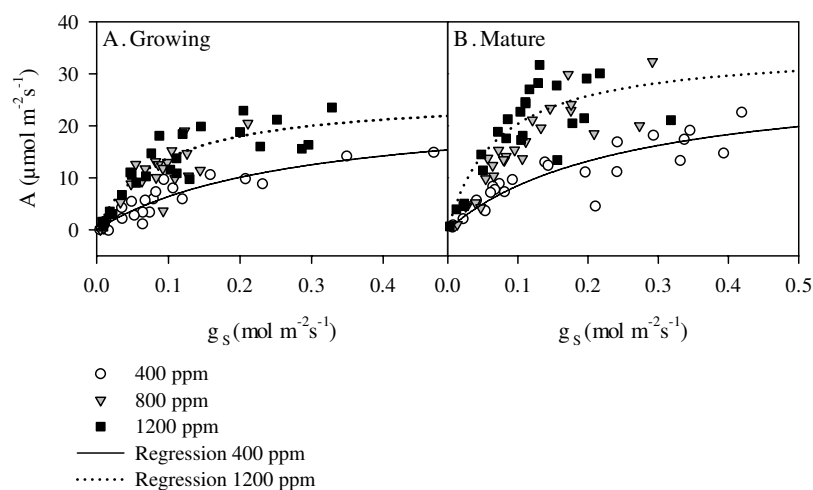

Figure 3.43: Relationship between net CO$_2$ exchange rate A and stomatal conductance g$_S$ in growing (A) and mature (B) leaves of *Populus deltoides* in ambient and elevated [CO$_2$]. Data were fitted using a Michaelis-Menten kinetic.

Table 3.6: Average water-use efficiency (WUE) of growing and mature leaves of *Populus deltoides* trees grown in 400, 800 and 1200 ppm in October 2003 at Biosphere 2 Center (n = 25 ± SE).

	WUE (mmol^{-1} mol^{-1})		
	400 ppm	800 ppm	1200 ppm
Growing	6.5 ± 2.2	10.6 ± 1.6	12.9 ± 1.8
Mature	10.6 ± 2.0	13.9 ± 1.6	20.8 ± 3.5

Photosynthesis under Fluctuating Light Conditions

In the next step, assimilation in fluctuating conditions was investigated (Fig. 3.44 – 3.47). Experiments were performed in April/May (growing leaves) and June/July (growing and mature leaves) in 400 and 1200 ppm. An original data set of a growing leaf in 400 and 1200 ppm, respectively, is shown in Fig. 3.44. Although light intensities in 1200 ppm were lower at midday, in April as well as in June, net CO_2 exchange rates of growing leaves were approximately 3 times higher (mean) in elevated [CO_2]. In April, they reached maximum values of 3 – 3.5 μmol m^{-2}s^{-1} in ambient [CO_2] and 7 – 9 μmol m^{-2}s^{-1} in 1200 ppm (data not shown). Dark respiration rate of growing leaves, measured in April 2003 in combination with the diel photosynthesis, was elevated in 1200 ppm, compared to 400 ppm (Tab. 3.7).

Table 3.7: Mean dark respiration of growing leaves of *Populus deltoides* trees grown in 400 and 1200 ppm in April 2003 at Biosphere 2 Center (n = 4 ± SE).

	Dark respiration (μmol m^{-2}s^{-1})	
	400 ppm	1200 ppm
Growing	1.06 ± 0.07	1.56 ± 0.12

In June, net CO_2 exchange rate reached higher maximum values than at the beginning of the growing season. In ambient conditions, growing leaves showed maximal rates of 3.5 – 3.7 μmol m^{-2}s^{-1}, mature leaves up to 12.3 μmol m^{-2}s^{-1}. In elevated [CO_2], growing leaves reached nearly the same photosynthetic rates as mature leaves with 18 – 20 compared to 25 μmol m^{-2}s^{-1}.

The 1-h-averages for growing and mature leaves show lower values (Fig. 3.45 and 3.46), due to the fact that high light intensities did not persist for a long time, and were lowered frequently by shading due to the building structure and other leaves. This resulted in reduced mean PAR and thus reduced photosynthesis. However, the averaged net CO_2 exchange rate was also three times higher in 1200 ppm in growing leaves (Fig. 3.45, B). Stomatal conductance, g$_S$, as well as transpiration, E, were decreased in elevated [CO_2] (Fig. 3.45, C, D), but E showed a high variability among the plants in 400 ppm (Fig. 3.45, D).
In mature leaves, only a single experiment could be done in June 2003 (Fig. 3.46, SD bars indicate variation of 1-h means). The effect of elevated [CO_2] on mature leaves was similar to that on growing leaves.

The net CO_2 exchange rate in June was plotted against the respective light intensity, PAR (Fig. 3.47). Although this light response curve was not achieved with steady state values, the effect of elevated [CO_2] on the photosynthetic rates can be seen clearly. Net CO_2 exchange rate of growing and mature leaves in 400 ppm saturated at approximately 400 μmol m^{-2}s^{-1}, whereas leaves in 1200 ppm, growing as well as mature, could still increase their assimilation and were not CO_2 limited in the covered range
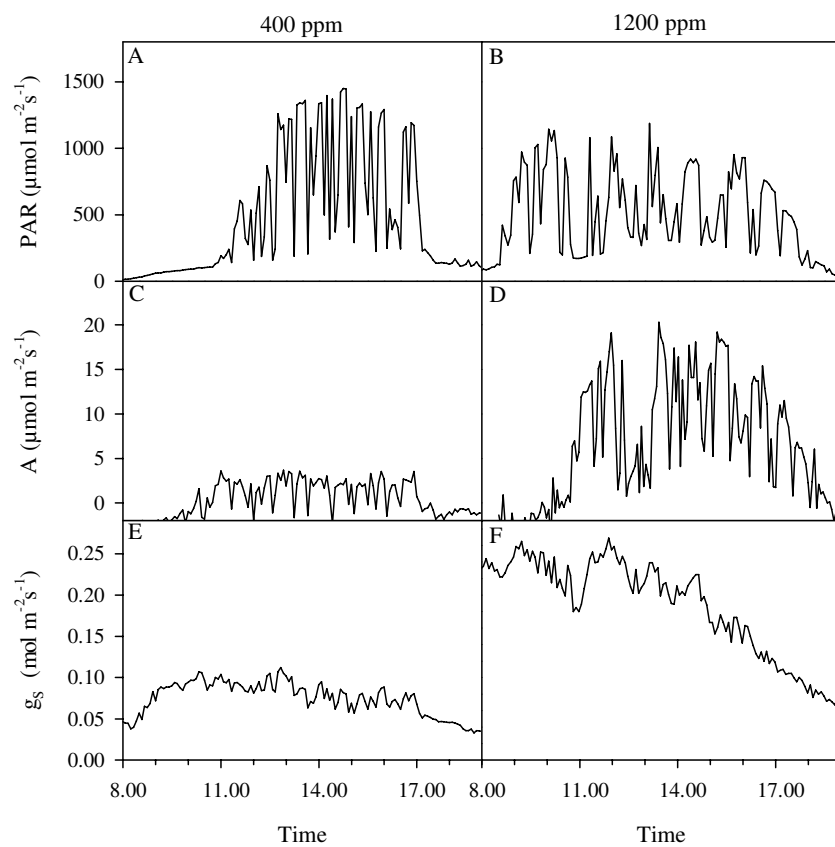
Figure 3.44: Diurnal course of the light intensity (PAR; A, B), photosynthetic CO$_2$ exchange rate (A; B, C) and stomatal conductance (g$_S$; D, E) of growing leaves of *Populus deltoides* in ambient and elevated [CO$_2$] under fluctuating light conditions in June in 400 and 1200 ppm, respectively (n = 1).
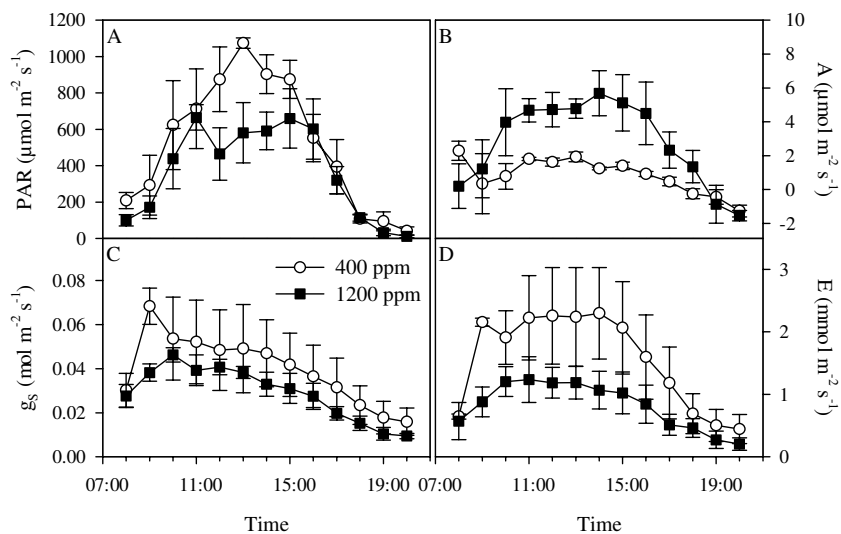
Figure 3.45: Diurnal photosynthesis of growing leaves of *Populus deltoides* in ambient and elevated [CO_2] under fluctuating light conditions: Hourly mean of the diurnal course of the light intensity PAR (μmol m^{-2} s^{-1}, A), net CO_2 exchange rate A (μmol m^{-2} s^{-1}, B), stomatal conductance g$_S$ (mol m^{-2} s^{-1}, C) and transpiration rate E (mmol m^{-2} s^{-1}, D) in 400 and 1200 ppm, respectively (n = 4 $\pm$ SE).
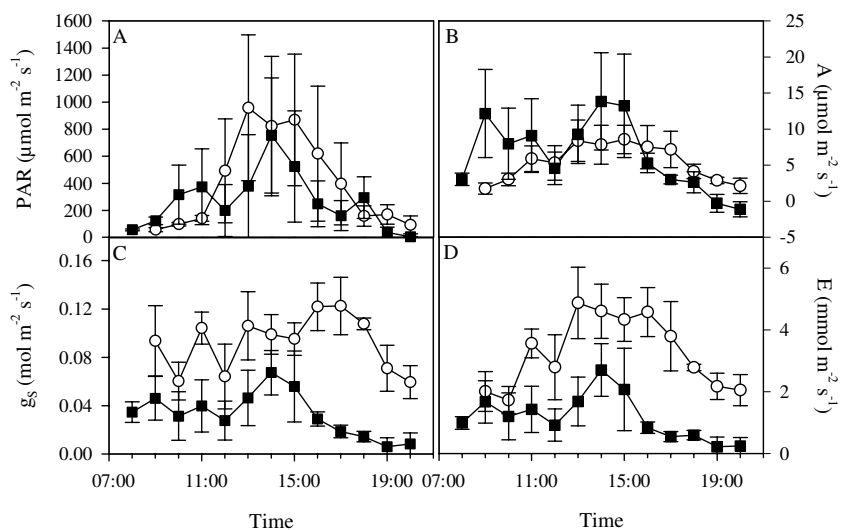

Figure 3.46: Diurnal photosynthesis of mature leaves of *Populus deltoides* in ambient and elevated [CO_2] under fluctuating light conditions in June: Diurnal course of the light intensity PAR (μmol m^{-2} s^{-1}, A), net CO_2 exchange rate A (μmol m^{-2} s^{-1}, B), stomatal conductance g$_S$ (mol m^{-2} s^{-1}, C) and transpiration rate E (mmol m^{-2} s^{-1}, D) in 400 and 1200 ppm, respectively (single leaf $\pm$ SD of the hourly mean).

of light intensity. Apparent quantum yield was estimated by the slope between 50 and 150 μmol m^{-2} s^{-1}, according to Ehleringer and Björkman (1977), (Fig. 3.47, C, D). For growing leaves, a quantum yield of 0.019 and 0.029 was found in 400 and 1200 ppm, respectively (accounting for 52 and 35 Photons per assimilated CO$_2$, respectively). In mature leaves, values of 0.018 and 0.068 were determined for 400 and 1200 ppm, respectively (54 and 15 Photons per CO$_2$).
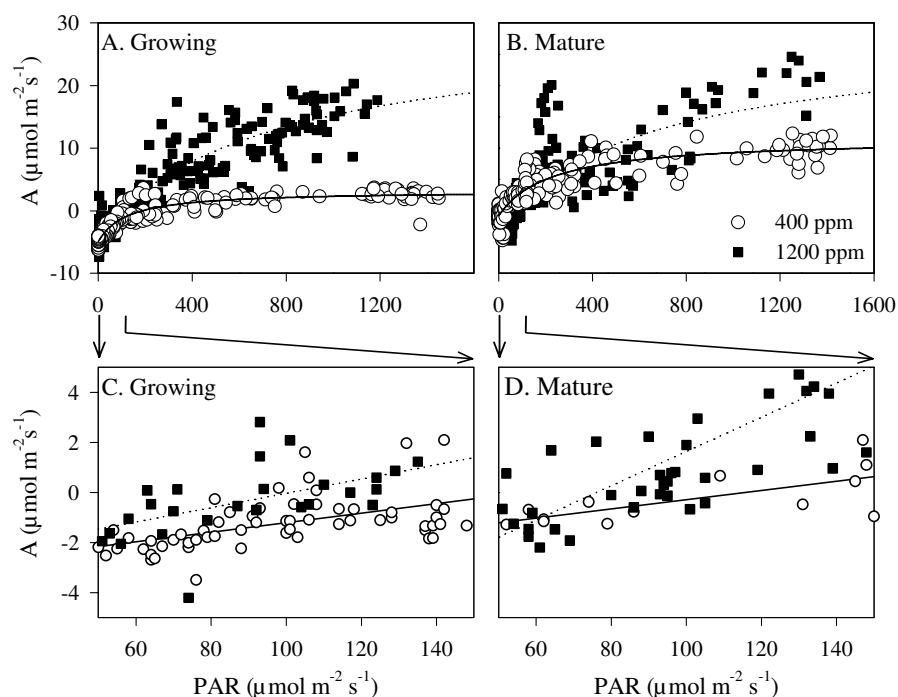

Figure 3.47: Light response curve of net [CO$_2$] exchange rate A in μmol m^{-2} s^{-1} of growing (A) and mature (B) leaves of *Populus deltoides* in ambient (400 ppm) and elevated (1200 ppm) [CO$_2$] under fluctuating light conditions. Data were fitting using a Michaelis-Menten kinetic. The initial slope of the light response curve for light intensities between 50 and 150 μmol m^{-2} s^{-1} is shown for growing (C) and mature (D) leaves (regression: 400 ppm solid line, 1200 ppm dotted line).

The ETR (Fig. 3.41), plotted against the net CO$_2$ exchange rate (Fig. 3.47) of the respective PAR reveals information about how many electrons are needed per fixed CO$_2$ (Fig. 3.48). In 400 ppm, A was already saturated at high light intensities (CO$_2$-limited), resulting in increased photorespiration, while the ETR still rose (Fig. 3.48, A). In 1200 ppm, leaves were not CO$_2$-limited in the covered range of light. In light-limiting situations (low ETR, Fig. 3.48, B), photosynthesis should not have been CO$_2$-limited in both treatments. For mature leaves in 1200 ppm an increased initial slope was found (0.135 compared to 0.105, accounting for ca. 8.4 electrons per assimilated CO$_2$ in 1200 ppm instead of ca. 7.1 in 400ppm).
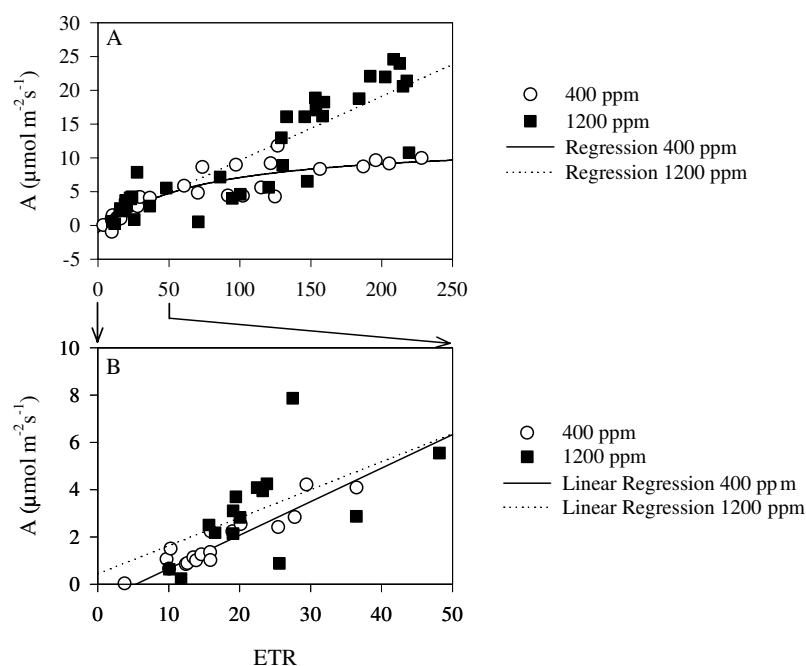
Figure 3.48: Relationship between net CO_2 exchange rate, A (μmol m^{-2} s^{-1}) and electron transport rate (ETR) of *Populus deltoides* in ambient (400 ppm) and elevated (1200 ppm) [CO_2] (A) and closer look at the ETR between 0 and 50 with linear regression (B).

3.3.3 Effect of Elevated CO_2 on Carbohydrate Concentration of Growing and Mature Leaves of *Populus deltoides*

Carbohydrate concentrations of growing and mature leaves of *P. deltoides* were measured throughout the growing season in 2003. Measurements for carbohydrate turnover were performed at sunset (7 pm) and sunrise (7 am). The diel course of carbohydrate concentration was measured in June, spatial distribution of leaf carbohydrates in the afternoon was investigated in July. Measurements were performed to correlate carbohydrate concentrations with growth and photosynthesis processes.

General Carbohydrate Concentrations

Samples for soluble sugar and starch concentrations were taken at 7 pm ('sunset') and 7 am ('sunrise') in 400, 800 and 1200 ppm from growing and mature leaves (Tab. 3.8).

In the first measurements, no significant differences could be found for glucose and fructose, but sucrose was increased at sunset (Tab. 3.8). Leaf starch concentration was increased in elevated [CO_2] in both, growing and mature leaves and nearly completely consumed at sunrise in growing leaves.

The turnover of carbohydrates was estimated from the concentrations of Table 3.8 (Tab. 3.9). It reveals information about how much carbohydrate was used relatively overnight (Eq. 2.14). Hexoses were produced overnight (negative turnover) and showed high variations. Sucrose turnover was dependent on the developmental stage and CO_2 treatment with lower values in mature than in growing leaves and in elevated [CO_2]. In mature leaves, starch turnover was also higher in ambient [CO_2] than in elevated, but in growing leaves, that showed a higher turnover than mature leaves, there was no effect of [CO_2]. Taking all measured carbohydrates into account (total non-structural carbohydrates, TNC), growing leaves showed an inverse response to [CO_2] than mature leaves with higher turnover at elevated [CO_2].

Table 3.8: Carbohydrate concentrations in June and July 2003 of growing and mature leaves of *Populus deltoides* trees that were grown in 400, 800 and 1200 ppm at Biosphere 2 Center at sunset and sunrise (n = 6 ± SE).

[CO$_2$]	Leaf Age	Time	Glc (μmol g^{-1} FW)	Fru (μmol g^{-1} FW)	Suc (μmol g^{-1} FW)	Starch (μmol g^{-1} FW)
400 ppm	Growing	sunrise	14.3 ± 2.9	10.0 ± 2.9	18.4 ± 3.5	9.4 ± 6.1
		sunset	12.3 ± 2.2	8.3 ± 2.1	27.3 ± 2.9	43.3 ± 17.8
	Mature	sunrise	8.9 ± 0.6	7.4 ± 0.7	54.7 ± 2.2	45.2 ± 8.5
		sunset	8.6 ± 0.5	7.7 ± 0.7	66.7 ± 2.0	99.4 ± 8.6
800 ppm	Growing	sunrise	11.6 ± 2.4	7.9 ± 2.8	14.2 ± 5.3	18.3 ± 8.6
		sunset	9.4 ± 1.9	6.0 ± 2.1	27.6 ± 4.1	95.9 ± 23.8
	Mature	sunrise	7.9 ± 0.4	8.3 ± 1.1	58.3 ± 2.3	78.6 ± 14.4
		sunset	7.0 ± 0.6	6.8 ± 1.1	75.0 ± 4.0	140.3 ± 20.6
1200 ppm	Growing	sunrise	12.8 ± 2.0	9.5 ± 2.1	9.5 ± 3.1	21.4 ± 8.9
		sunset	12.3 ± 1.0	8.0 ± 1.4	28.4 ± 1.5	85.6 ± 19.4
	Mature	sunrise	10.5 ± 0.9	13.5 ± 2.6	55.0 ± 2.1	244.4 ± 60.3
		sunset	8.7 ± 1.1	9.4 ± 1.1	76.8 ± 3.3	267.2 ± 64.7

The measurements of leaf gas exchange in April resulted in a mean dark respiration of growing leaves of approximately 1.06 ± 0.07 and 1.56 ± 0.12 μmol m^{-2} s^{-1} in 400 ppm and 1200 ppm, respectively (Tab. 3.7). The sum over the night (7 pm–7 am) was 4.6 and 6.7 μmol cm^2 /12 h in 400 ppm and 1200 ppm, respectively. Similar leaves used 10.0 and 20.3 μmol cm^2 /12 h starch over night. This would result in 5.5 μmol cm^2 in 400 ppm and 13.5 μmol cm^2 in 1200 ppm, i.e. 2.5 times more, that would remain directly for growth and other processes.

Table 3.9: Carbohydrate turnover (%) in June and July 2003 of growing and mature leaves of *Populus deltoides* trees that were grown in 400, 800 and 1200 ppm at Biosphere 2 Center: glucose, fructose, sucrose, starch and sum (total non-structural carbohydrates, TNC) (n = 6 ± SE).

[CO$_2$]	Leaf	Glc	Fru	Suc	Starch	TNC
400 ppm	Growing	-15 ± 6	-15 ± 7	35 ± 5	82 ± 5	41 ± 8
	Mature	-3 ± 4	2 ± 7	18 ± 3	55 ± 7	36 ± 3
800 ppm	Growing	-30 ± 23	-42 ± 38	38 ± 30	79 ± 10	58 ± 14
	Mature	-18 ± 15	-67 ± 59	21 ± 5	37 ± 16	30 ± 10
1200 ppm	Growing	-3 ± 13	-25 ± 25	66 ± 11	80 ± 5	11 ± 2
	Mature	-25 ± 14	-44 ± 25	28 ± 3	8 ± 4	11 ± 2

Specific leaf area (SLA, Tab. 3.10) decreased in mature leaves in elevated [CO$_2$], mainly due to an accumulation of starch (Tab. 3.8, Fig. 3.54 – 3.49). Glucose:fructose ratio (Glc:Fru) decreased slightly in mature leaves in elevated [CO$_2$] (Tab. 3.10).

Table 3.10: Specific leaf area (SLA) and leaf Glc:Fru ratio of *Populus deltoides* in ambient and elevated CO_2 in $cm^2 \ g^{-1}$ (n = 12 $\pm$ SE).

[CO_2]	Leaf Age	SLA ($cm^2 \ g^{-1}$)	Glc:Fru
400 ppm	Growing	63.8 ± 1.3	1.4 ± 0.1
	Mature	48.1 ± 3.1	1.4 ± 0.1
800 ppm	Growing	64.0 ± 1.2	1.8 ± 0.2
	Mature	40.9 ± 1.2	1.2 ± 0.1
1200 ppm	Growing	62.8 ± 2.0	1.4 ± 0.1
	Mature	38.6 ± 0.9	1.1 ± 0.1

Temporal Distribution of Assimilates in Elevated CO_2

Leaf carbohydrate concentrations of *P. deltoides* were measured over 24 h in 400, 800 and 1200 ppm in June 2003. Carbohydrate concentrations showed a diel rhythm in growing and mature leaves (Fig. 3.49). In growing leaves, glucose was increased in 800 ppm (in average by 36 %), but decreased in 1200 ppm, at least during the day (on average 30 % less than in 400 ppm, Fig. 3.49, A). In mature leaves, this was inverse with 30 % higher values in 1200 ppm than in 400 ppm (Fig. 3.49, B). Fructose concentrations showed a similar response to [CO_2] (Fig. 3.49, C, D). Sucrose was only increased in growing leaves in 800 ppm by 90 %, but not altered significantly between 400 and 1200 ppm or in mature leaves, that had much higher values than growing leaves (Fig. 3.49, E, F). At the time of the experiment, starch was significantly increased in growing leaves, at 800 ppm (by a factor of 3.6) and in mature leaves, at 1200 ppm (by a factor of 2.7, Fig. 3.49, G, H).

At the same time, leaf water potential (LWP) of growing and mature leaves was measured in all three bays over 24 h (Fig. 3.50). LWP was lower at day than at night. In growing leaves, no significant difference between the CO_2 treatments could be found (Fig. 3.50, A), but mature leaves in 400 ppm were highly water-stressed, as the LWP went down to -2 MPa at day. This could explain why hexose concentrations in June were lower in 400 ppm than expected from other samplings (Fig. 3.49).

The diel leaf carbohydrate concentrations and LWP of growing leaves were correlated with typical diel RGRs (Fig. 3.51). Variations were high, but glucose, fructose and sucrose concentrations were higher at times of low growth in 400 ppm (Fig. 3.51, A – C). In 1200 ppm, the relationship was nearly constant or rather highly variable. Starch concentration was higher in times of high growth in both [CO_2] treatments (Fig. 3.51, D). The LWP of growing leaves did not show a clear correlation with the RGR (Fig. 3.52).

Spatial Distribution of Assimilates in Elevated [CO_2]

Carbohydrate concentrations of growing and mature leaves of *P. deltoides* trees of 400, 800 and 1200 ppm were measured in July 2003. Samples were taken in the afternoon, between 3 and 5 pm and numerated as outlined in Fig. 2.18, p. 26. This sampling time was selected, as this was the time at which RGR differed significantly between leaves from ambient and elevated [CO_2] (lower RGR in 1200 ppm, see p. 60). In 400 ppm, leaf carbohydrates had no significant spatial differences (shown for glucose in Fig. 3.53). In 1200 ppm however, spatial distribution of glucose showed higher heterogeneity. This was also found for fructose, but not for sucrose or starch (data not shown). To compare the heterogeneity of the spatial carbohydrate distribution, the standard deviation of the measured leaf positions, relative to the mean concentration was estimated. For glucose, growing leaves showed 4 and 7 times higher relative SD values in interveinal and veinal tissue, respectively, in 1200 ppm compared to 400
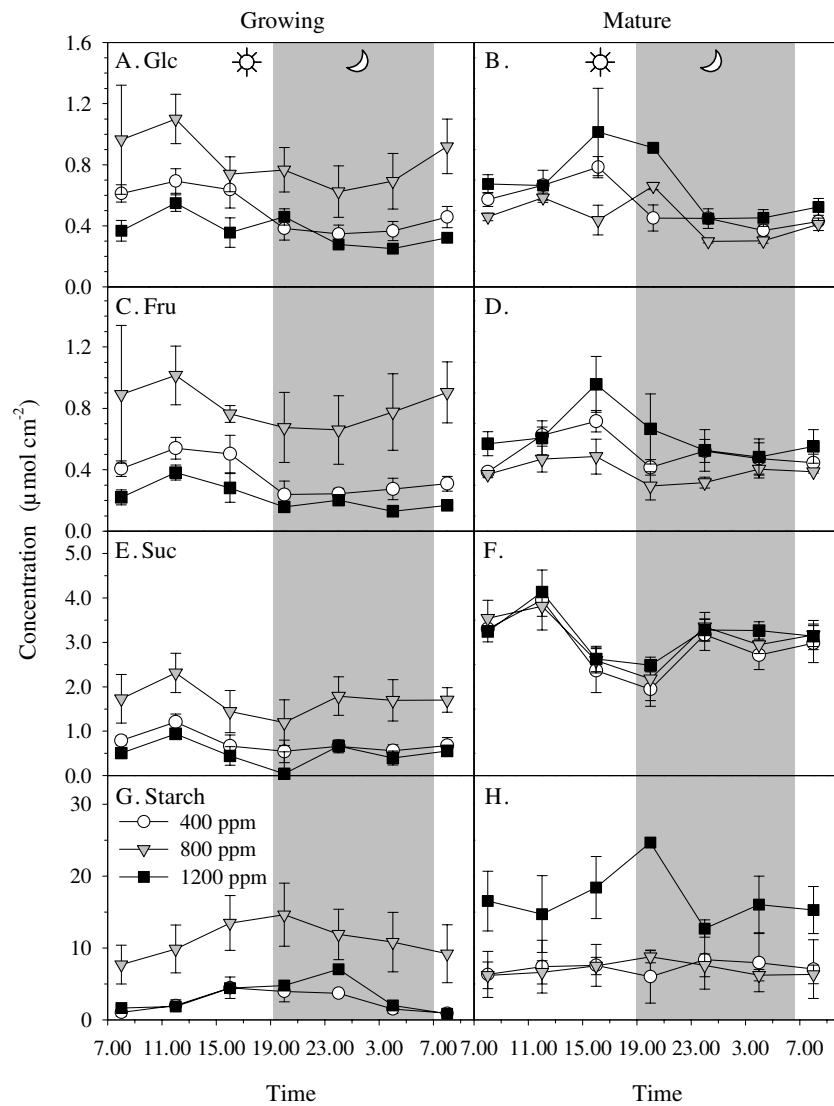
Figure 3.49: Diel pattern of the carbohydrate concentration of leaves of *Populus deltoides* in ambient and elevated [CO$_2$]: Concentrations of glucose (A, B), fructose (C, D), sucrose (E, F) and starch (G, H) of growing (left) and mature (right) leaves in μmol cm^{-2}. Trees were grown in 400, 800 and 1200 ppm CO$_2$ for four years (n = 3 $\pm$ SE).
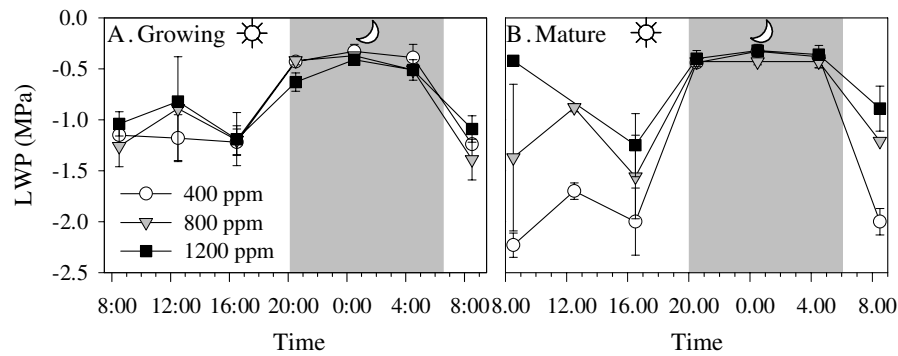
Figure 3.50: Diel leaf water potential (LWP) of growing (A) and mature (B) leaves of *Populus deltoides* in ambient and elevated CO_2. Trees were grown in 400, 800 and 1200 ppm CO_2 for four years (n = 3 ± SE).
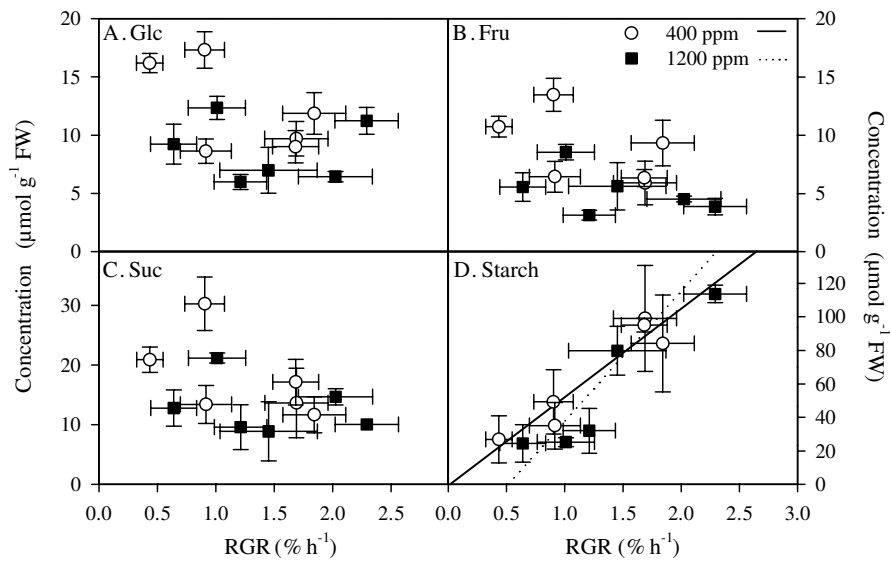

Figure 3.51: Relationship between diel carbohydrate concentration (μmol g^{-1} FW) and relative diel growth rate (RGR, % h^{-1}) of *Populus deltoides* in 400 ppm and 1200 ppm at Biosphere 2 Center: glucose (A), fructose (B), sucrose (C) and starch (D, n = 3 and 10 ± SE, for carbohydrate concentration and RGR, respectively).
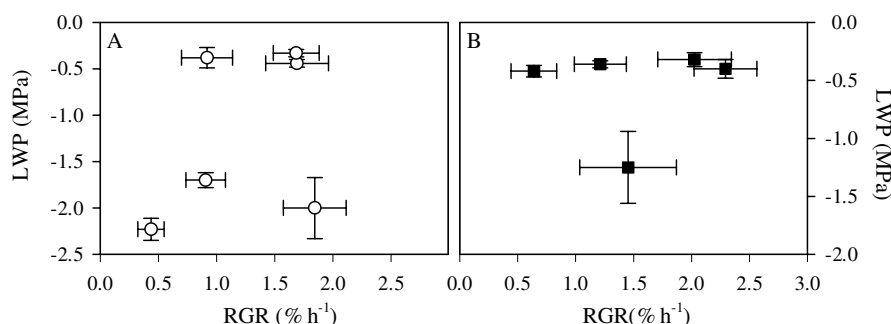
Figure 3.52: Relationship between diel leaf water potential (LWP, MPa) and relative diel growth rate (RGR, % h^{-1}) of *Populus deltoides* in 400 ppm (A) and 1200 ppm (B) at Biosphere 2 Center (n = 3 and 10 $\pm$ SE, for carbohydrate concentration and RGR, respectively).

ppm. For fructose, this value was 4 and 3 times higher in interveinal and veinal tissue, respectively. Samples of veinal and interveinal tissue were averaged as sub-replicates. In general, leaf glucose concentration was decreased in elevated [CO$_2$] in both, growing and mature leaves and veinal as well as interveinal tissue (Fig. 3.54 and 3.55 A). Glucose was decreased in 800 ppm by 20 % and 55 % in growing and mature leaves, respectively and 70 % in 1200 ppm in both developmental stages. Fructose was decreased mainly in mature leaves in elevated [CO$_2$] (Fig. 3.54 and 3.55 B), and only half as high in growing leaves in 400 ppm compared to mature leaves. Glucose and fructose concentrations did not differ between veinal and interveinal tissue.

Sucrose was not altered significantly by [CO$_2$] but increased more than twice in mature compared to growing leaves (Fig. 3.54 and 3.55 C). As before, starch was increased in elevated [CO$_2$], in growing leaves by 2.8 and 4.2 in interveinal and veinal tissue, respectively (1200 compared to 400 ppm), in mature leaves by a factor of 6.6 and 6.8 (Fig. 3.54 and 3.55 D). Veinal starch concentration was around half of the concentration of interveinal tissue.

Different from the measurements at sunrise and sunset, the Glc:Fru ratio of growing leaves declined with increasing [CO$_2$] from 3 in 400 ppm to 1.1 in 1200 ppm in interveinal and from 2.5 to 0.6 in veinal tissue (data not shown). In mature leaves, the Glc:Fru ratio was much smaller and showed a weaker reduction with increasing [CO$_2$]. It declined from 1.1 in interveinal tissue from leaves of the 400 ppm treatment to 0.7 in 1200 ppm and from 0.9 to 0.5 in veinal tissue, respectively.
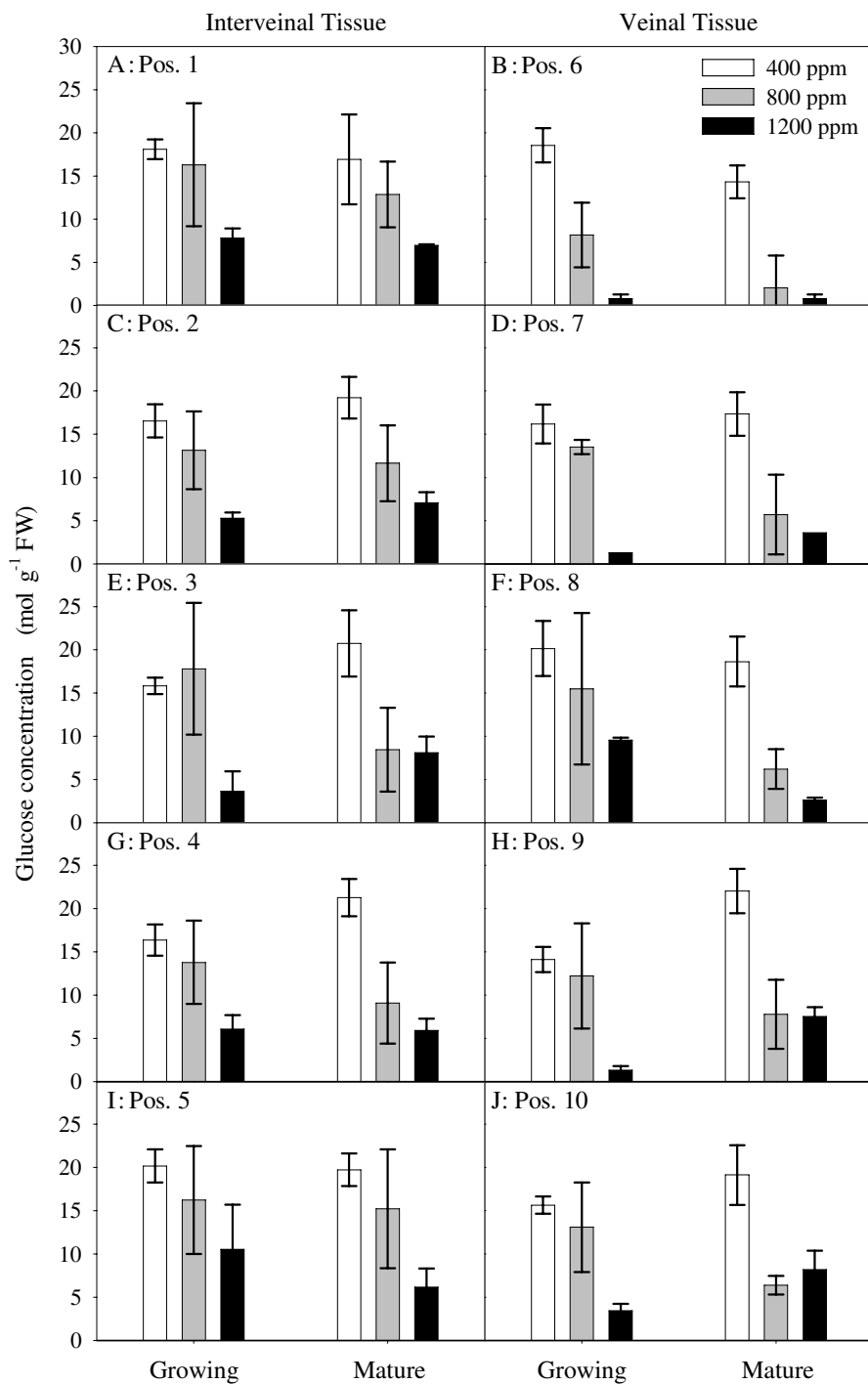
Figure 3.53: Spatial distribution of leaf glucose concentration of *Populus deltoides* in ambient and elevated [CO_2]: Glucose concentration in μmol g^{-1} FW of inter-veinal (A, C, E, G, I) and veinal (B, D, F, H, J) tissue in growing and mature leaves in the afternoon. Trees were grown in 400, 800 and 1200 ppm CO_2 for four years (n = 3 $\pm$ SE).
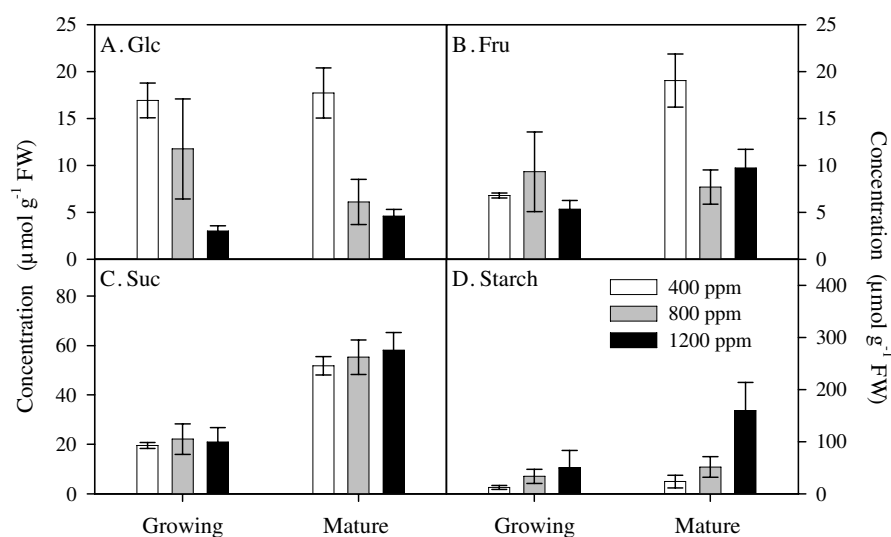
Figure 3.54: Carbohydrate concentration in veinal tissue of *Populus deltoides* leaves in ambient and elevated [CO$_2$]: Concentrations of glucose (A), fructose (B), sucrose (C) and starch (D) of growing and mature leaves in μmol g^{-1} FW in the afternoon. Trees were grown in 400, 800 and 1200 ppm CO$_2$ for four years (n = 3 ± SE).
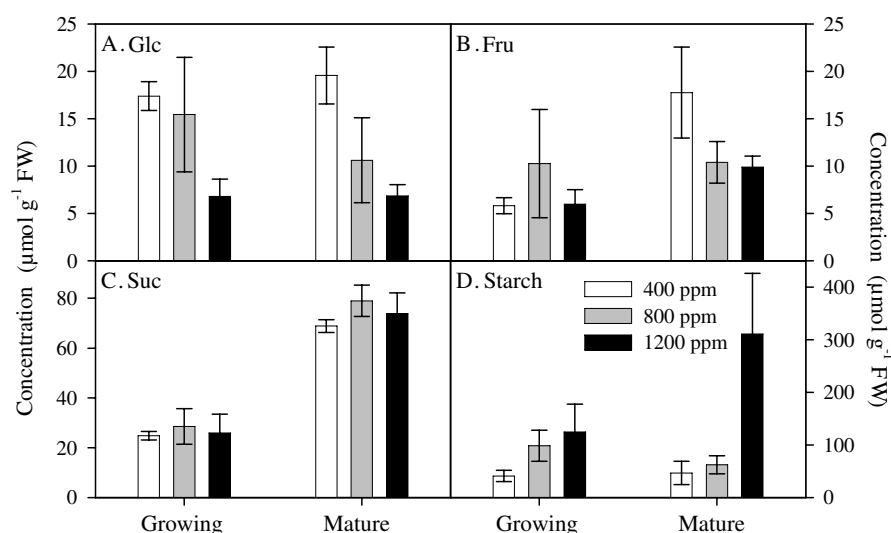

Figure 3.55: Carbohydrate concentration in interveinal tissue of *Populus deltoides* leaves in ambient and elevated [CO$_2$]: Concentrations of glucose (A), fructose (B), sucrose (C) and starch (D) of growing and mature leaves in μmol g^{-1} FW in the afternoon. Trees were grown in 400, 800 and 1200 ppm CO$_2$ for four years (n = 3 ± SE).

3.3.4 Short-term Elevation of CO_2

To examine the effect of short-term [CO_2] elevation on photosynthetic yield in different developmental stages, [CO_2] in the East Bay was raised from 400 to 1600 ppm for one day. Chlorophyll fluorescence was measured on leaves at three different developmental stages at midday at two successive days with 400 and 1600 ppm and plotted against the light intensity. Light intensities at the respective leaf and point in time were measured with a separate light sensor as the internal light sensor of the Minipam was inactive. They were highly variable but did not differ between the two days (Fig. 3.56). It was assumed that the fluorescence parameters $\Delta F/F_m\prime$ and NPQ correlate with the light intensity (Schreiber and Bilger, 1993; Demmig-Adams et al., 1996) and they were arranged in ascending order, high values of $\Delta F/F_m\prime$ and low values of NPQ referring to low light intensities.
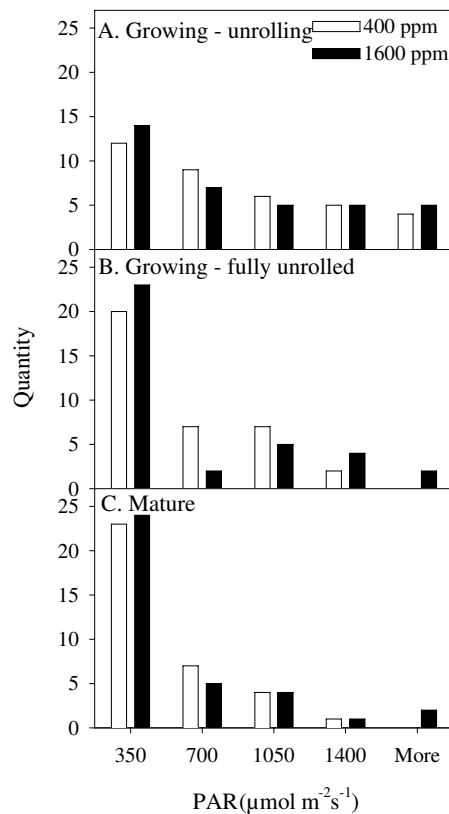

Figure 3.56: Histogram of the light intensity distribution at leaves that were used for chlorophyll fluorescence measurements during a short-term elevation of [CO_2] from 400 to 1600 ppm for one day.

Effective quantum yield ($\Delta F/F_m\prime$) of young, still unrolling leaves was higher in middle light intensities in elevated [CO_2] (Fig. 3.57, A), and non-photochemical quenching (NPQ) was lowered (Fig. 3.57, B). Both parameters were not altered significantly in fully unrolled, growing (Fig. 3.57, C, D) and mature (Fig. 3.57, E, F) leaves. Thus, sensitivity to an elevation of [CO_2] was much stronger in very young leaves.
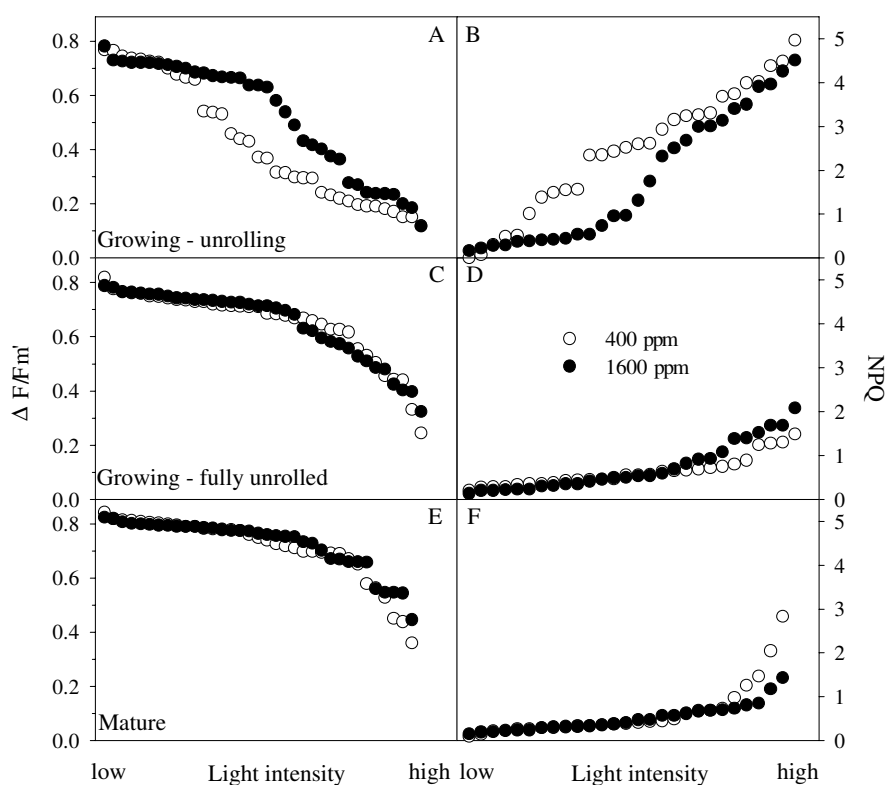
Figure 3.57: Chlorophyll fluorescence of leaves of *Populus deltoides* during a short-term [CO$_2$] elevation: Single values of effective quantum yield (ΔF/F$_m$') and non-photochemical quenching (NPQ) of leaves in ambient [CO$_2$] (400 ppm) and during a one-day elevation of [CO$_2$] (1600 ppm) versus light intensity of leaves of three different developmental stages: Growing (still unrolling and already fully unrolled) and mature leaves.

3.3.5   Summary of Effects of Elevated [CO_2] on *Populus deltoides*

A long-term elevation of [CO_2] led to increased leaf growth and assimilation of *P. deltoides*. Trees were cultivated for four years in 400, 800 and 1200 ppm at Biosphere 2 Center. Single leaf growth was stimulated by approximately 1.13 and 1.2 in 800 and 1200 ppm, respectively. The relationship between relative leaf area (RLA) and RGR was not significantly altered by elevated [CO_2]. Leaf growth showed a clear diel rhythm and was altered by elevated [CO_2] (1200 ppm) by a transient decline in the afternoon. Spatial heterogeneity of the RGR pattern was increased in elevated [CO_2].

Potential quantum yield of PS II was age- but not [CO_2]-dependent. However, effective quantum yield and ETR of mature leaves were slightly increased in high light intensities by elevated [CO_2] (1200 ppm).
In 1200 ppm, net CO_2 exchange rate was increased by a factor of 2.4 and 1.6 in growing and mature leaves, respectively. Stomatal conductance was decreased in mature leaves. WUE was age- and CO_2-dependent and 2 times higher in 1200 ppm. In fluctuating light conditions, results were similar, although light intensities were reduced in the 1200 ppm. In contrast to trees in 400 ppm, photosynthesis of trees in 1200 ppm did not reach saturation in the existing light intensities.

Carbohydrate concentrations varied throughout the season. In elevated [CO_2], leaves accumulated starch, in particular in 1200 ppm. This resulted also in decreased SLA. Carbohydrates showed a diel course. While diel starch concentrations correlated positively with the diel RGR, hexose concentrations correlated only slightly and negatively. Sampling in the afternoon, at time of the growth decline, resulted in reduced glucose in elevated [CO_2] in both, growing and mature leaves, indicating a role of glucose in controlling the response of growth to elevated [CO_2].
Diel LWP did not correlate with diel RGR, but showed that trees in 400 ppm were water-stressed in June at the time of sampling, in contrast to trees in 1200 ppm.

A short-term elevation of [CO_2] from 400 to 1600 ppm for one day showed no effect in mature and fully unrolled, growing leaves in terms of effective quantum yield and NPQ but very young leaves were sensitive to the elevation with reduced NPQ in middle light intensities.

3.4 Effects of Elevated O$_3$ on Leaf Growth and Photosynthesis of *Glycine max*

Experiments with elevated [O$_3$] were performed on *Glycine max* L. Merr. cv. Spencer (soybean) at the SoyFACE facility in Illinois, USA in August 2004 (see Sect. 2.1). Leaf growth in ambient conditions and elevated [O$_3$] (ambient x 1.2) was analyzed throughout the month. Leaf gas exchange (net CO$_2$ exchange rate and stomatal conductance), stomatal density and concentrations of carbohydrates and chlorophyll were measured during reproductive growth and pod-filling.
A second experiment was done under controlled conditions in two growth chambers. Soybeans were analyzed during early vegetative growth. [O$_3$] was elevated to approximately 70 ppb for 6 hours a day. In this experiment, diel leaf growth was monitored over two weeks.

3.4.1 Effects of Elevated O$_3$ on Leaf Growth of *Glycine max* in the Field

Leaf growth was measured three times a week under ambient and elevated [O$_3$]. Measurements were performed in three plots with four sub-replicates per ring. In the elevated [O$_3$] treatment, leaves did not show apparent ozone damage. Necroses or chlorosis effects were observed in both treatments at the end of August 2004, presumably due to other pathogenic factors that occurred in the field (Fig. 3.58).
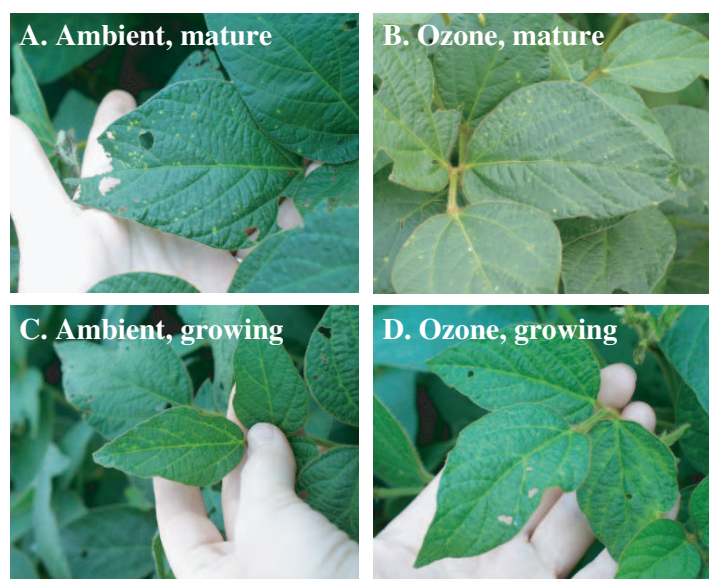

Figure 3.58: Mature (A, B) and growing (C, D) leaves of *Glycine max* in ambient (A, C) and elevated [O$_3$] (B, D) at the end of August 2004. Necroses were observed in mature leaves in both treatments.

The effect of elevated [O$_3$] on leaf growth was cumulative (Fig. 3.59 and 3.60). At the beginning of August, there was no significant difference in leaf growth, with a difference in total leaf area of approximately 3%. At the end of the month total leaf area in elevated [O$_3$] was 10% lower than in ambient conditions.
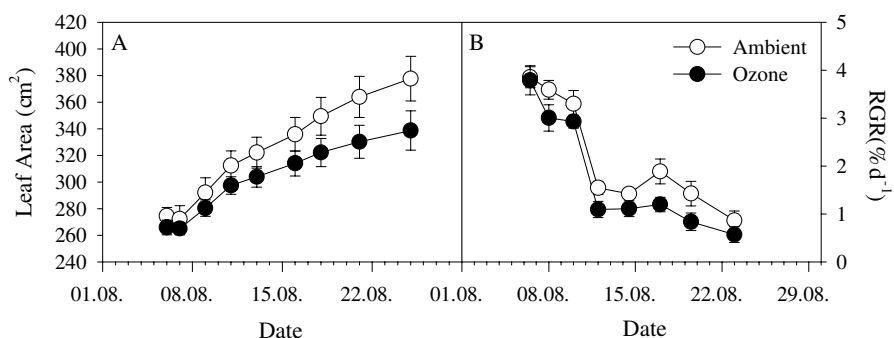The reduction of total leaf area in elevated [O$_3$] was mainly caused by growth reduction in newly

Figure 3.59: Development of total leaf area of soybean in ambient and elevated (ambient x 1.2) [O_3] in August 2004 at SoyFACE. Total leaf area (cm^2; A) and mean relative growth rate (RGR, % d^{-1}; B) of leaves $0 - 7$ (n = $3 \pm$ SE).
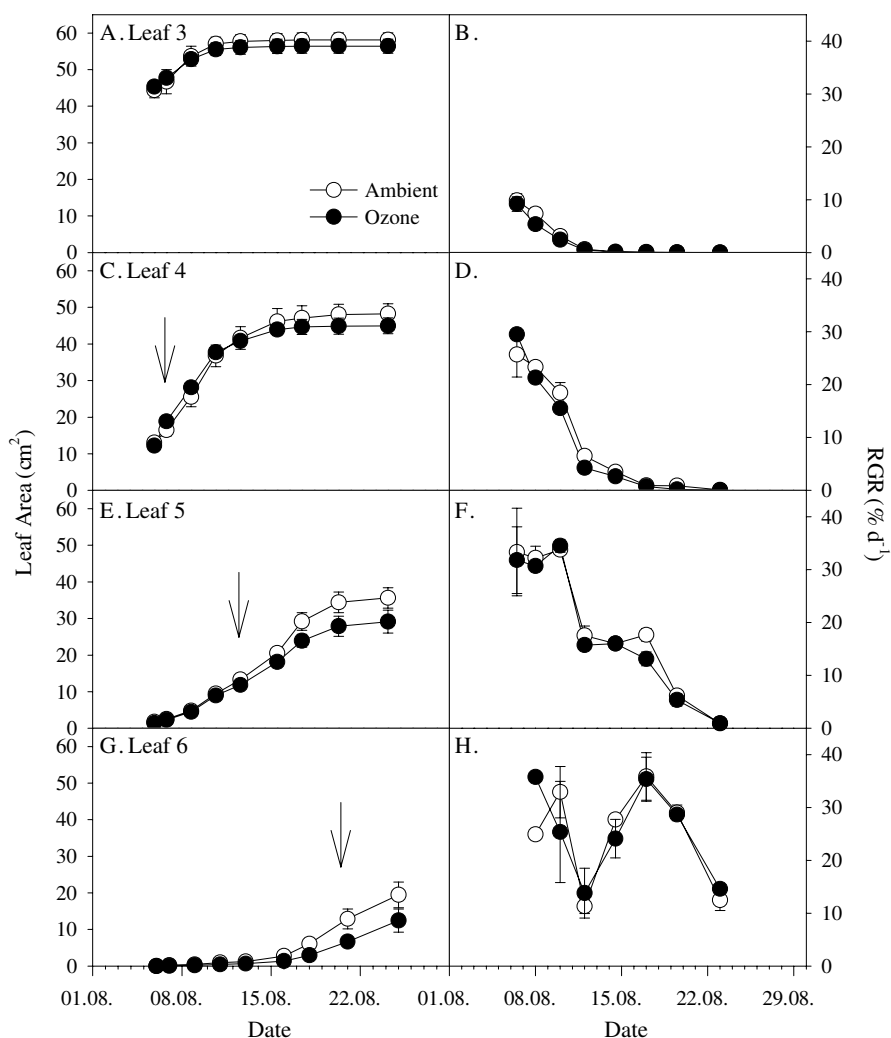

Figure 3.60: Effect of elevated [O_3] on growth and development of leaves of *Glycine max*. Development of leaf area (cm^2; A, C, E, G) and relative growth rate (RGR, % d^{-1}; B, D, F, H) of leaf 3 to leaf 6 in August 2004 at SoyFACE in ambient and elevated (1.2 x ambient) [O_3]. Arrows indicate the point in time when leaves were fully unfolded (n = $3 \pm$ SE).

emerged leaves (Fig. 3.60). On August 25th, leaf area of leaf 3 – 6 was reduced by 3, 7, 18 and 36 %, respectively. The growth reduction could also be seen very clearly in the comparison of leaf area distribution along the shoot at the beginning and end of August (Fig. 3.61).
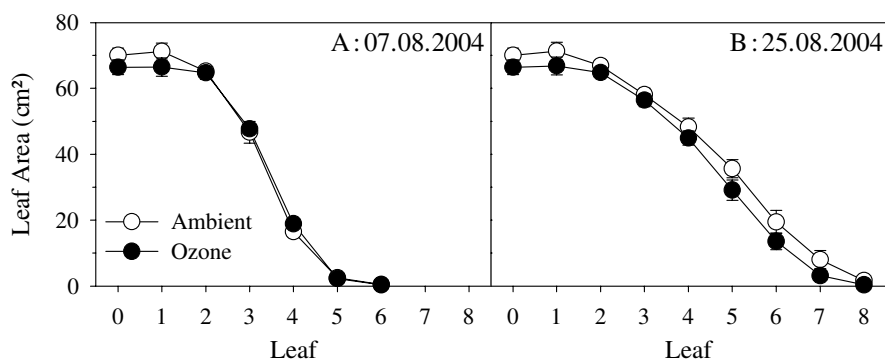

Figure 3.61: Effect of elevated [O$_3$] on leaf area distribution along the shoot of *Glycine max*. Leaf area (cm^2) of leaves 0 – 7 on August 7th (A) and 25th (B) 2004 at SoyFACE in ambient and elevated (1.2 x ambient) [O$_3$] (n = 3 $\pm$ SE).

In both treatments, leaves 0 – 2 reached final leaf areas of approximately 70 cm^2 (data not shown), while leaves 3 and 4 did not exceed an average of 60 and 45 cm^2, respectively. This decrease in final leaf area at higher leaf positions could be due to the transition from a vegetative to a reproductive phase or the cold temperatures in August.

Specific leaf area (SLA, cm^2 g^{-1}), based on leaf fresh weight, was not affected significantly by elevated [O$_3$] (Tab. 3.11), except for leaf 1, which showed a slight increase. Relative leaf area (RLA) at a respective RGR was not affected by elevation of [O$_3$] (Fig. 3.62).

Table 3.11: Effect of elevated [O$_3$] on specific leaf area (SLA, cm^2 g^{-1}) of different developmental stages of leaves of *Glycine max*. SLA of leaves 1 – 5 with the respective relative growth rate (RGR) in ambient and elevated (1.2 x ambient) [O$_3$] (n = 3 $\pm$ SE).

Leaf	Ambient		Ozone	
	SLA (cm^2 g^{-1})	RGR (% d^{-1})	SLA (cm^2 g^{-1})	RGR (% d^{-1})
Leaf 1	67.0 $\pm$ 1.0	0 $\pm$ 0	75.6 $\pm$ 1.9	0 $\pm$ 0
Leaf 2	66.9 $\pm$ 2.5	0 $\pm$ 0	70.0 $\pm$ 2.5	0 $\pm$ 0
Leaf 3	71.5 $\pm$ 1.4	0.7 $\pm$ 0.2	72.9 $\pm$ 3.2	0.5 $\pm$ 0.1
Leaf 4	67.9 $\pm$ 0.5	6.5 $\pm$ 0.6	70.6 $\pm$ 3.9	4.3 $\pm$ 0.8
Leaf 5	47.9 $\pm$ 2.7	17.5 $\pm$ 1.8	45.9 $\pm$ 2.6	15.7 $\pm$ 0.8

3.4.2 Effects of Elevated O$_3$ on Photosynthesis of *G. max* in the Field

Leaf gas exchange was measured twice in August 2004 with two sub-replicates per ring (see Sect. 2.3.2). Measurements were performed on leaves 2 – 5 on August 15th, and leaves 2 – 6 on August 31st. At the latter measurements, all leaves were fully expanded.

Net CO$_2$ exchange rate at saturating light conditions, A$_{sat}$ (1500 and 1800 μmol m^{-2} s^{-1}), was reduced in elevated [O$_3$] by 10 – 34 %, depending on the developmental stage and time of measurement
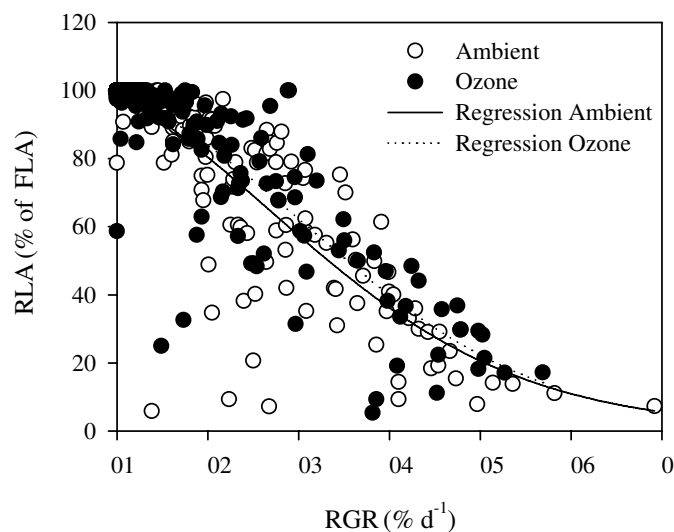
Figure 3.62: Relative leaf area (RLA, %) in relation to the relative growth rate (RGR, % d^{-1}) of *Glycine max* in ambient and elevated (1.2 x ambient) [O_3] at SoyFACE (single values and regression).

(Fig. 3.63). A_{sat} was dependent on the developmental stage with rates in young, growing leaves approximately half of the rates in mature leaves (Fig. 3.63, B). The stomatal conductance, g_S, showed the same pattern and was reduced in young leaves by $30 - 50$ % on August 15th (Fig. 3.63, D). On Aug 15th, the photosynthetic rate per leaf (taking the leaf area into account) was reduced by 36, 30, 25 and 38 % in leaves 2–5 in elevated [O_3], respectively. When averaged, for all measured leaves reduction was estimated to be 33 % (0.43 μmol s^{-1} in ambient versus 0.29 μmol s^{-1} in elevated conditions).

At the end of the month, when leaves were fully expanded, A_{sat} was approximately 30 μmol m^2 s^{-1} in leaves growing under ambient conditions, whereas it was 25 μmol m^2 s^{-1} in the elevated [O_3] treatment. The decrease in photosynthetic capacity in elevated [O_3] was greater in older than in young leaves (on Aug 31st e.g. 24 versus 10 %). Despite a comparable A_{sat}, g_S was approximately 25 % lower in younger leaves at the stage of final leaf size (Fig. 3.63, E).

The lower stomatal conductance was not a result of a reduced number of stomata but probably due to stomatal closure, as the stomatal density showed no significant difference between the two treatments (Tab. 3.12). Stomata were counted on leaves with RGRs from 0 to 4–6 % d^{-1}. For leaf 4 only fully developed stomata were taken into account. The number of stomata was 2.8 times lower on the adaxial (upper) than on the abaxial (lower) side of the leaf.
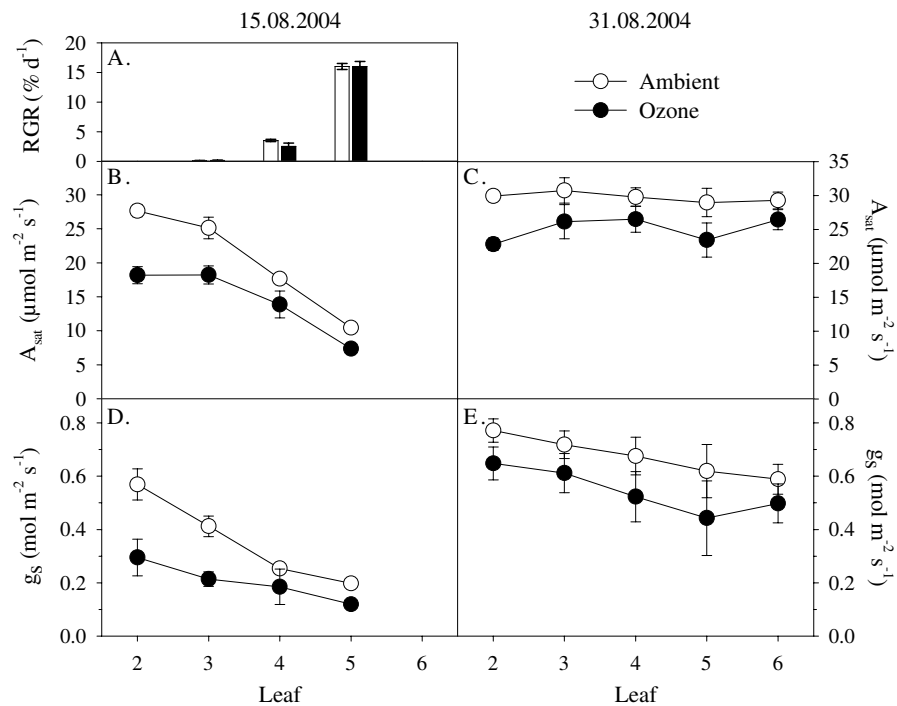
Figure 3.63: Effect of elevated [O_3] on photosynthesis of *Glycine max*. Relative growth rate (RGR, % d^{-1}, A), net CO_2 exchange rate (A_{sat}, μmol m^{-2}s^{-1}, B, C) and stomatal conductance (g_S, mol m^{-2}s^{-1}, D, E) at saturating light intensity (1500 and 1800 μmol m^{-2} s^{-1}) of leaves at different developmental stages (leaves 2 – 5) on August 15th (A, B, D) and 31st (C, E) 2004 at SoyFACE in ambient and elevated (1.2 x ambient) [O_3] (n = 3 $\pm$ SE).

Table 3.12: Effect of elevated [O_3] on stomatal density (mm^{-1}) at different developmental stages in leaves of *Glycine max*. The stomatal density on the abaxial and adaxial side of leaves 1 – 4 are given with the respective relative growth rates (RGR, % d^{-1}) in ambient and elevated (1.2 x ambient) [O_3] (n = 3 $\pm$ SE).

Leaf	Ambient			Ozone		
	adaxial	abaxial	RGR	adaxial	abaxial	RGR
Leaf 1	144 ± 12	361 ± 11	0 ± 0	148 ± 3	387 ± 13	0 ± 0
Leaf 2	127 ± 12	371 ± 10	0 ± 0	133 ± 11	390 ± 20	0 ± 0
Leaf 3	139 ± 4	429 ± 21	0.7 ± 0.2	141 ± 12	408 ± 2	0.5 ± 0.1
Leaf 4	123 ± 9	330 ± 27	6.5 ± 0.6	114 ± 22	371 ± 25	4.3 ± 0.8
Mean	133 ± 5	373 ± 13		134 ± 7	389 ± 8	

3.4.3   Effects of Elevated O_3 on Carbohydrate Concentrations in Leaves of *G. max* in the Field

At the beginning of August (Aug 5th), carbohydrate and chlorophyll concentrations were measured over 24 hours on mature (leaf 1) and growing (30 % d^{-1}, leaf 4) leaves. Elevated [O_3] had no effect on the chlorophyll concentration, mature leaves contained nearly three times more chlorophyll than growing leaves in both treatments (Fig. 3.64, A). Soluble sugars (glucose, fructose and sucrose) and starch showed clear diel variations (Fig. 3.64, B–E). Growing leaves had lower concentrations of fructose, sucrose and in particular starch, while there was no difference in glucose concentration between growing and mature leaves. Mean values over 24 h are outlined in Tab. 3.13.
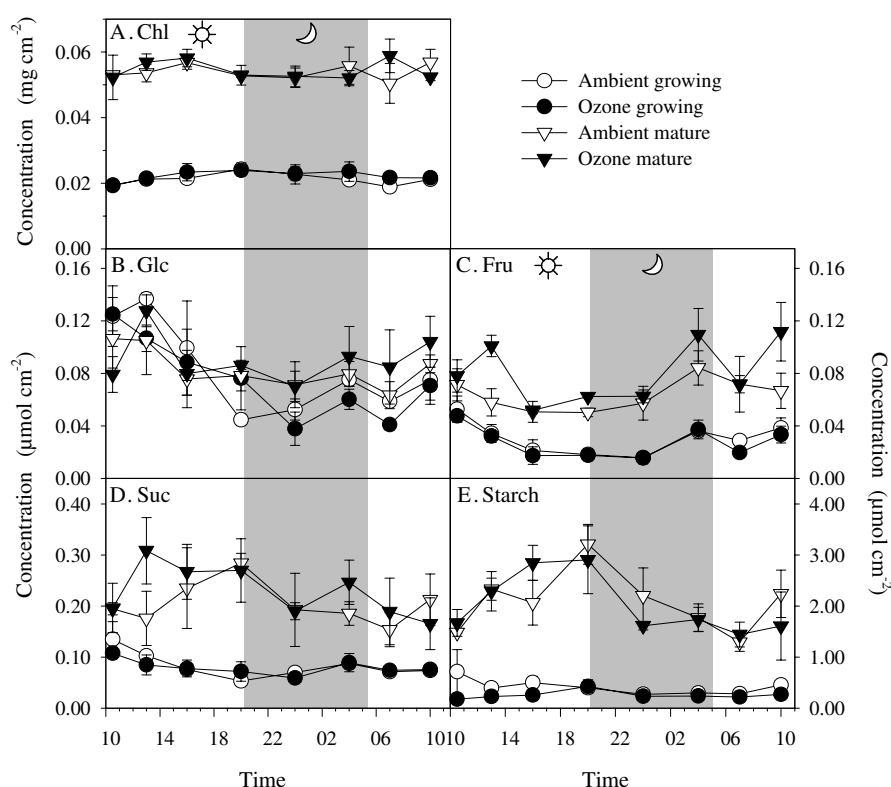

Figure 3.64: Effect of elevated [O_3] on diel chlorophyll and carbohydrate concentrations in leaves of *Glycine max*. Shown is the concentration of chlorophyll (A) in mg cm^{-2}, and of glucose (B), fructose (C), sucrose (D) and starch (E) in μmol cm^{-2} of growing and mature leaves on August 5th 2004 at SoyFACE in ambient and elevated (1.2 x ambient) ozone (n = 3 $\pm$ SE).

At the end of August, samples were collected from leaves covering a range of developmental stages (leaf 4, mature, to leaf 7, 30–45 % d^{-1}) in the afternoon (4 – 5 pm). At that time, elevated [O_3] affected the leaf carbohydrate concentration (Fig. 3.65). The concentration of glucose, fructose and sucrose was reduced in elevated [O_3] (Fig. 3.65, C–E). Beside leaf 7, chlorophyll concentrations were slightly lower in ambient conditions although differences were not significant (Fig. 3.65, B). In contrast to soluble sugars, starch accumulated in mature leaves in elevated [O_3] (Fig. 3.65, F). Leaf 6, which was approaching its final size, had the highest hexose concentrations (glucose and fructose).
The distribution of carbohydrates in the measured leaves at the second sampling is illustrated in Fig. 3.66. When averaged for all leaves, glucose, fructose and sucrose were decreased by 20, 36 and 16 % in elevated [O_3], respectively. In mature leaves, starch was increased by 46 % on average.

Table 3.13: Effect of elevated [O_3] on chlorophyll and carbohydrate concentration in soybean leaves (mean of 24 h). Concentrations of chlorophyll (mg cm^{-2}), glucose, fructose, sucrose and starch (μmol cm^{-2}) in growing and mature leaves on August 5th 2004 at SoyFACE in ambient and elevated (1.2 x ambient) ozone (n = 3 $\pm$ SE, 8 time points).

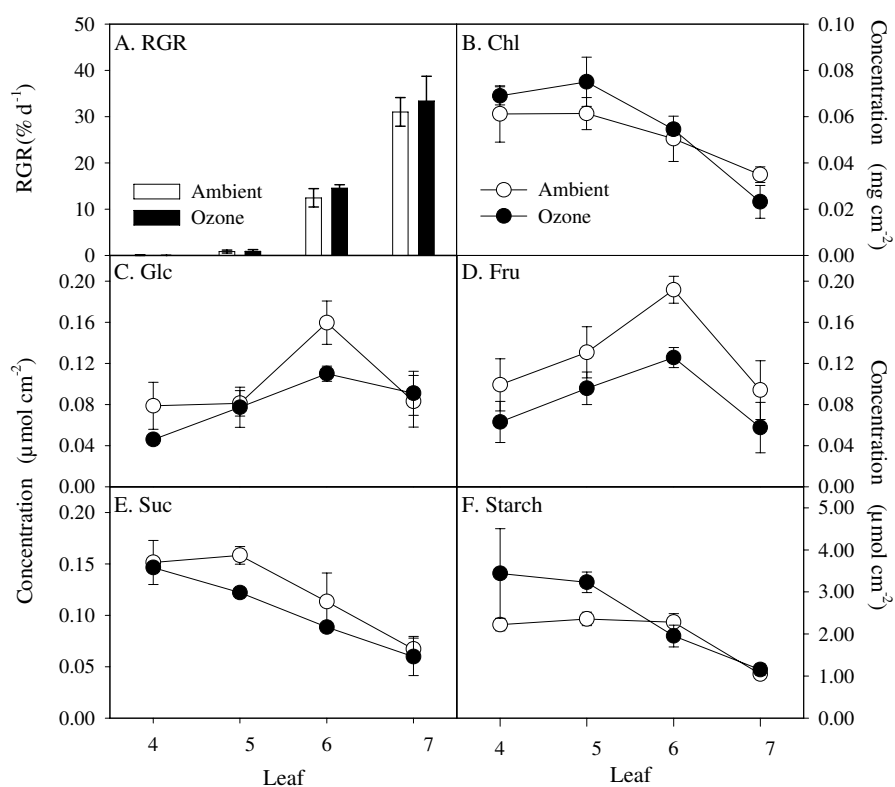| Substance	Growing leaves		Mature leaves	
(μmol or mg cm^{-2})	Ambient	Ozone	Ambient	Ozone
Chlorophyll	0.021 $\pm$ 0.001	0.022 $\pm$ 0.001	0.054 $\pm$ 0.001	0.055 $\pm$ 0.001
Glucose	0.083 $\pm$ 0.008	0.076 $\pm$ 0.007	0.084 $\pm$ 0.006	0.091 $\pm$ 0.006
Fructose	0.031 $\pm$ 0.003	0.028 $\pm$ 0.003	0.064 $\pm$ 0.004	0.081 $\pm$ 0.006
Sucrose	0.084 $\pm$ 0.006	0.080 $\pm$ 0.005	0.205 $\pm$ 0.016	0.230 $\pm$ 0.018
Starch	0.041 $\pm$ 0.006	0.026 $\pm$ 0.002	0.208 $\pm$ 0.016	0.202 $\pm$ 0.017

Figure 3.65: Effect of elevated [O_3] on chlorophyll and carbohydrate concentrations in leaves of *Glycine max* at different developmental stages. Relative growth rate (RGR, % d^{-1}, A) and concentrations of chlorophyll (mg cm^{-2}, B), glucose (C), fructose (D), sucrose (E) and starch (F) in μmol cm^{-2} in leaves at different developmental stages on August 25th 2004 (n = 3 $\pm$ SE).
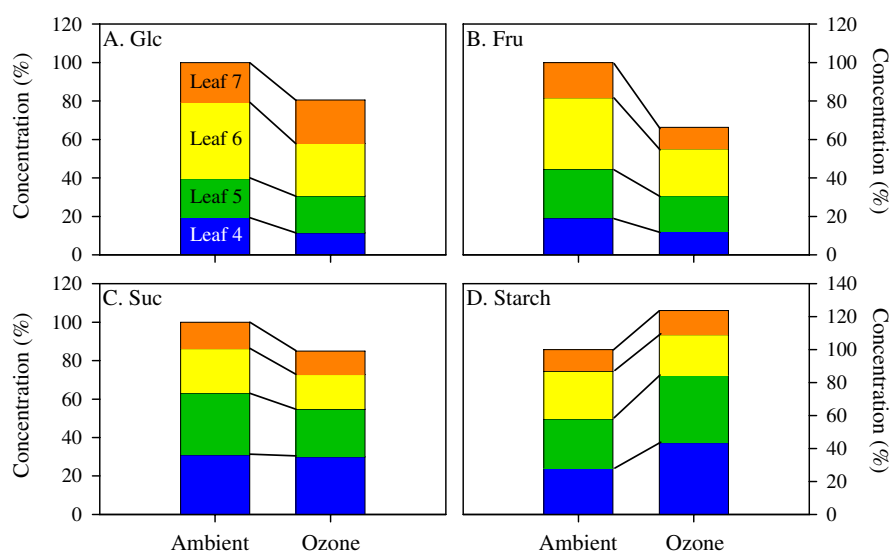
Figure 3.66: Effect of elevated [O_3] on the distribution of carbohydrate concentrations in leaves of *Glycine max* at different developmental stages: Glucose (A), fructose (B), sucrose (C) and starch (D) in %. Data from Fig. 3.65 (n = 3).

Trends of the developmental stage were consistent with the results from the first experiment at the beginning of August 2004 (Fig. 3.64 and Tab. 3.13).

3.4.4   Effect of Short-Term Elevation of O_3 on Spatio-Temporal Leaf Growth Patterns

In August 2004, soybean (*G. max* L. Merr. cv. Spencer) was cultivated in two growth chambers in Illinois, USA (see Sect. 2.1.3). One chamber was kept at ambient conditions, in the other chamber, [O_3] was elevated to 70 ppb for 6 h per day.

Leaf growth was measured over a period of two weeks on two plants per treatment. During this time, no difference in leaf RGR between plants in ambient and elevated [O_3] could be found (Fig. 3.67). At the same time, DISP measurements were performed on leaves in the two treatments (Fig. 3.68). After two weeks, photosynthesis was measured under lab conditions. A$_{sat}$ and g$_S$ were increased under elevated [O_3] (data not shown).

Effect of Elevated O_3 on Diel RGR Course and Heterogeneity

Diel leaf growth rate pattern was not affected by elevated [O_3] (Fig. 3.68). In the growth chamber, the RGR showed a maximum in the morning, declined until early afternoon and stayed constant until lights were switched off (Fig. 3.68, A). At night, after a short decrease, the RGR rose continuously until one hour before light were switched on. In the field, acquisitions could only be made two nights in ambient and four nights in elevated [O_3]. The RGR was highly noisy and no differences in the two treatments were found, but the time course seemed to differ from the one in the growth chamber, i.e. RGR did not increase at night.

The RGR of leaves in the growth chamber, averaged over 24 h, was investigated also in terms of spatial patterns. In the color-coded RGR maps, the different high RGR of veinal and interveinal tissue can be seen (Fig. 3.69), but differences between the two treatments appear more clearly, when the heterogeneity of the RGR maps is calculated (Fig. 3.70).
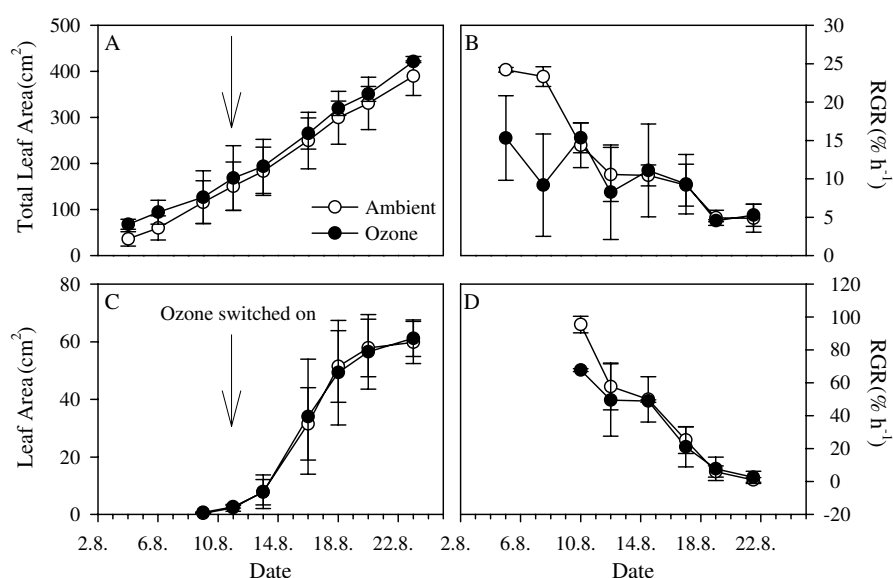
Figure 3.67: Effect of short-term elevation of [O$_3$] on leaf growth of *Glycine max* in the growth chamber (GC): Development of whole plant leaf area (cm^2, A) and relative growth rate (RGR, % d^1, B) , and single leaf area (C) and RGR (D) of a trifolium with the central leaflet being 20–30 cm long when ozone was switched on (n = 2 ± SE).
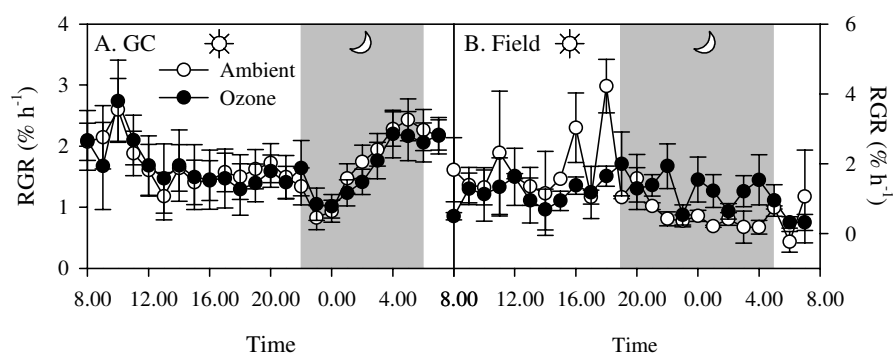

Figure 3.68: Diel course of the relative growth rate (RGR) of *Glycine max* in the growth chamber (GC, A) and in the field at SoyFACE, IL, USA (B) in August 2004 (A: n = 14 and 7 ± SE; B: n = 2 and 4 ± SE, for ambient and elevated ozone, respectively).
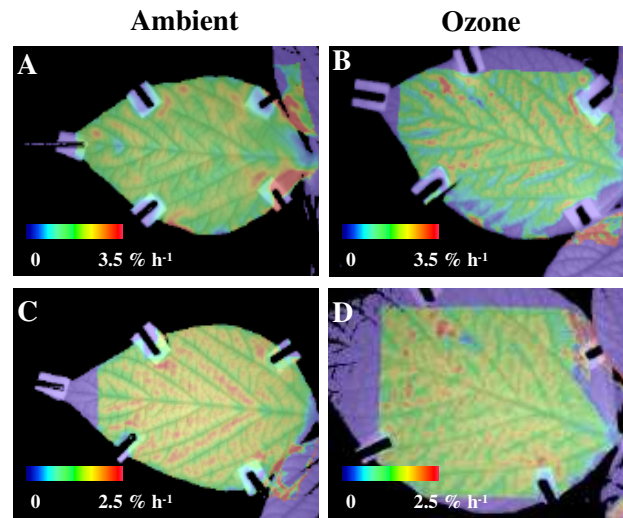
Ambient   **Ozone**

Figure 3.69: Color-coded 24-h-average of the spatial distribution of the relative growth rate (RGR) of *Glycine max* in ambient conditions (A, C) and elevated ozone (70 ppb, B, D) in the growth chamber.

Relative heterogeneity of 24-h means of the RGR increased in leaves of plants that were exposed to elevated $[O_3]$ by a factor of approximately 2 (Fig. 3.70).

Figure 3.70: Relative heterogeneity of 24-h-averages of the relative growth rate (RGR) pattern of *Glycine max* in ambient conditions and elevated ozone (70 ppb) in the growth chamber ($n = 7 \pm$ SE).
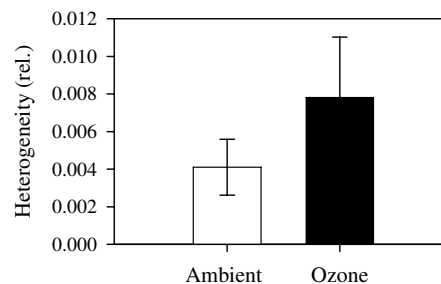
3.4.5   Summary of Effects of Elevated $[O_3]$ on *Glycine max*

A season-long elevation of $[O_3]$ by a factor of 1.2 led to a reduced photosynthesis rate by 10 – 34 % in mature and growing leaves of soybean in the field as a result of stomata closure without any change in stomatal density. Depending on time and leaf age, g_S was reduced by 15 – 50 %.

Soluble carbohydrates like glucose, fructose and sucrose were reduced in elevated $[O_3]$ late in the growing season when pod-filling started. Furthermore, increased accumulation of starch was observed in mature leaves under elevated $[O_3]$.

Leaf growth was affected late in the growing season, but the relationship between RLA and RGR did not change.

Short-term elevation of $[O_3]$ for two weeks in the growth chamber had no significant effect on leaf growth, neither on leaf area nor on the diel growth pattern. However, the spatial RGR pattern showed increased heterogeneity in elevated $[O_3]$.

Chapter 4

Discussion

The aim of this thesis was to investigate effects of the atmospheric gases [CO_2] and [O_3] on spatio-temporal patterns of leaf growth and photosynthesis in dicotyledonous plants.

Long-term elevation of [CO_2] led to increased leaf growth and assimilation in *Populus deltoides*. Trees were cultivated for four years in 400, 800 and 1200 ppm at Biosphere 2 Center. Whereas leaf net CO_2 exchange rate was increased by a factor of 2.4 in growing leaves, single leaf growth was stimulated by a factor of approximately 1.2 in 1200 ppm compared to 400 ppm. Leaf growth showed a clear diel rhythm with a transient decline in the afternoon in elevated [CO_2] that was accompanied by reduced glucose concentration, while starch accumulated.

Season-long elevation of [O_3] by 20 % above ambient [O_3] led to a reduced photosynthesis rate by 10–34 % in leaves of *Glycine max* in the field and was accompanied by a reduction in soluble carbohydrates in growing leaves that might have caused a reduction of leaf growth late in the growing season.

Experiments on cuttings of *Populus deltoides* showed that fluctuating environmental conditions can alter the diel course of the leaf RGR, as well as spatial growth patterns. It could further be shown that veinal and vein-surrounding tissue develops faster than interveinal tissue in *Populus deltoides*.

The results clearly show different mechanisms of response to elevated [CO_2] and [O_3] at the whole plant and the single leaf level. Therefore, these aspects will be treated separately in this discussion.

4.1   Elevated CO_2: Large-Scale Leaf Growth and Development

By the end of the four-year experiment at Biosphere 2 Center, the 800 and 1200 ppm [CO_2] treatments produced nearly 1.3 times the foliar and total aboveground biomass than in 400 ppm (Barron-Gafford et al., 2005). Cumulative root biomass was increased by a factor of approximately 1.3 and 1.4 in 800 and 1200 ppm, respectively, after 3 years of experiment (Barron-Gafford et al., 2005).

Leaf growth of *Populus deltoides* continued to be stimulated after three years in elevated [CO_2] (e.g. Fig. 3.32). The stimulation of final leaf area (FLA) was dependent on the position of the branch on the tree and was increased on average by 13 % and 22 % in 800 and 1200 ppm compared to ambient conditions (400 ppm), respectively (Fig. 3.34). Stimulation of leaf growth is a common response to elevated [CO_2] (Bosac, 1995; Ceulemans, 1996; Ainsworth et al., 2003a,b; Calfapietra et al., 2003) but varies enormously, even for similar species grown under the same basic experimental conditions (such as nutrient supply and light conditions, Kerstiens, 2001; Ainsworth et al., 2002).

Leaves from different canopy positions showed slightly different growth responses to elevated [CO_2] (Fig. 3.33 and 3.34). Leaves from lower lateral branches were found to mature sooner in elevated [CO_2] than leaves in the upper canopy, in terms of growth, photosynthesis (Noormets et al., 2001) and respiration (Griffin et al., 2002). This might have been an effect of sun compared to shade leaves: an initial stimulation of individual leaf-area development by elevated [CO_2] was reduced in magnitude

as canopy shading and competition increased (Tricker et al., 2004). Higher stomatal conductance in shade leaves compared to sun leaves (Tjoelker et al., 1995) might also cause different responses to elevated $[CO_2]$ in different canopy positions. The higher biomass in the 1200 ppm treatment led to an increased shading, in particular in lower branches (Murthy et al., 2005, see also Fig. 3.45 and 3.46).

The increase in leaf area was caused mainly by accelerated leaf development with a higher RGR at emergence as shown for the tree tip (Fig. 3.32). The result that the increase in FLA in elevated $[CO_2]$ is caused by an accelerated RGR and hence accelerated leaf development, is consistent with results reported in literature (Seneweera et al., 1995; Wait et al., 1999). Accelerated leaf development does not only affect leaf area but is also connected with an altered establishment of the structure and function of the photosynthetic apparatus. Miller et al. (1997) examined the effect of 950 ppm $[CO_2]$ on tobacco photosynthesis and found a shifted course of photosynthetic rates during leaf development towards earlier developmental stages, associated with reduced Rubisco activity. Leadley and Reynolds (1989) found close correlations between leaf growth dynamics and photosynthesis in soybean. Leaf size did not change with $[CO_2]$ but initial rates of leaf expansion were more rapid and the period of expansion declined with increasing $[CO_2]$. Thus, accelerated leaf development does not always result in higher leaf area. As the responses are highly dependent on cultivation conditions it is important to distinguish between short-term and long-term exposures and to keep the limitations of the respective studies in mind when comparing results with other findings.

The relationship between relative leaf area (RLA) and RGR did not show a significant dependence on the CO_2 treatment with only slightly higher RGRs at a respective RLA in 1200 ppm (Fig. 3.35). This result indicates that accelerated leaf development does not change intrinsic mechanisms of development. The relationship between RLA and RGR was different in *P. deltoides* compared to previously studied herbs like *Nicotiana tabacum* (Walter, 1997; Christ, 2001) or soybean (Fig. 3.62). Poplar trees reached final leaf area more slowly than tobacco and leaves grew longer with medium growth rates between 20 and 40 % d^{-1}.

Specific leaf area (SLA) decreased in elevated $[CO_2]$, mainly due to an accumulation of starch in the leaves (e.g. Fig. 3.55). This is consistent with the findings of e.g. Radoglou and Jarvis (1990a,b); Ceulemans (1996); Ceulemans et al. (1997) or Barron-Gafford et al. (2005). The increased assimilates are not completely utilized for e.g. growth. This result indicates that other factors may have limited the transfer of the increased C-gain into biomass. Due to the stimulation of plant growth in elevated $[CO_2]$, annual removal of aboveground biomass led to a marked depletion of soluble soil P, Ca^{2+} and K^+ (11 – 26 % in 800 and 24 – 46 % in 1200 ppm in the upper 25 cm, Barron-Gafford et al., 2005). Similar effects were observed for the distribution of Mg^{2+}, Na^+ and NO_3^-, whereas NH_4^+, total N and C remained unchanged (Kudeyarov et al., 2002). This decline in nutrient availability might also be responsible for an altered transfer of C-gain into biomass.

Most of the published studies worked with a $[CO_2]$ elevation of approximately 550 – 700 ppm; concentrations that are predicted for the middle or end of this century (Prentice, 2001). Only a few studies were performed at higher $[CO_2]$ (Jolliffe and Ehret, 1985; Ehret and Jolliffe, 1985; Wang et al., 1999), often with the background of how plants would grow in life support systems for space missions (Wheeler et al., 1993; Reuveni and Bugbee, 1997), where $[CO_2]$ can rise up to 5000 – 10000 ppm. $[CO_2]$ >1000 ppm was found to be supra-optimal for soybean, bean and wheat, (Jolliffe and Ehret, 1985; Wheeler et al., 1993; Reuveni and Bugbee, 1997).

However, for the context of this study it is reasonable to consider higher CO_2 concentrations (1200 instead of 600 ppm): the achieved results can lead to conclusions about mechanisms, which will be more pronounced in extreme than in moderate conditions. If, for example, a reduction of the RGR in the afternoon should be important to decelerate growth in elevated $[CO_2]$, this should also be investigated on the level of starch metabolism at 600 – 800 ppm.

4.2 Elevated CO$_2$: Small-Scale Spatio-Temporal Leaf Growth Patterns

Leaves from all investigated species show diel growth rhythms. These rhythms differ in phasing between species (Lecharny et al., 1985; Jouve et al., 1998; Walter and Schurr, 2000). Furthermore, most key enzymes and metabolic processes within a plant are governed by diel or circadian rhythms and can be switched on and off within short time frames. The dynamics of some of those regulatory mechanisms are affected by external [CO$_2$] (Geiger et al., 1998; Matt et al., 2001). Cell division and expansion are also stimulated by elevated [CO$_2$] (Taylor et al., 1994).
The diel growth cycle was found to be affected by the diel carbohydrate metabolism (Kehr et al., 1998; Walter et al., 2002a). It is likely that additional carbohydrates, produced in elevated [CO$_2$], enhance cell production and cell expansion (Masle, 2000). Thus, the hypothesis was made that elevated [CO$_2$] affects the amplitude and phasing of the diel leaf growth cycle.

Beside temporal growth patterns, spatial patterns of leaf RGR have been described. The most prominent spatial growth pattern is a gradient between leaf base and tip, observed e.g for *Nicotiana tabacum* (Avery, 1933; Walter and Schurr, 2005) or *Ricinus communis* (Walter et al., 2002a). Furthermore, dicot leaves tend to grow more along the midvein with a gradient to the leaf sides (Avery, 1933; Dale, 1988). Another anatomical feature responsive to [CO$_2$] is stomatal density. Stomata are sensitive to CO$_2$ (Freudenberger, 1940; Heath, 1948) and apparent stomatal conductance is altered by elevated [CO$_2$] (Morison, 1987), via stomatal aperture and via stomatal density (Weyers and Lawson, 1997; Poole et al., 2000). Small spatial heterogeneities of stomata movements could be found in several species (Küppers et al., 1999; Osmond et al., 1999). Transpiration rate can alter turgor (Mott and Buckley, 2000) and as such growth (Lockhart, 1965). On the basis of these facts the hypothesis was formulated that also leaf growth proceeds with small heterogeneities. Elevated [CO$_2$] may thus also alter spatial patterns of leaf growth.

The improvements of the DISP method throughout the last years allowed a closer look to small-scale spatio-temporal patterns of the leaf RGR, including differences in the diel cycle or spatial heterogeneity to test these hypotheses.

4.2.1 Temporal Leaf Growth Patterns: Diel Growth Cycle

The RGR of *P. deltoides* leaves rose during the day, reaching a maximum at the end of the day, declined then only slightly and after midnight more rapidly in both, ambient and elevated [CO$_2$]. In the afternoon, growth declined transiently at approximately 4 pm in elevated [CO$_2$]. This growth decline was also present throughout the growing season in 2002 (Walter et al., 2005) and was analyzed in more detail in terms of assimilation rate and carbohydrate concentration. Only one reference in literature on effects of elevated [CO$_2$] on phasing and amplitude of the diel leaf growth cycle could be found (Seneweera et al., 1995). They did not detect clear responses that were attributable to the [CO$_2$] treatments beside the fact that single leaf RGR was increased initially by elevated [CO$_2$] but after longer exposure declined below that of comparable leaves in ambient conditions. Seneweera et al. (1995) however, used lower [CO$_2$] and worked on a monocotyledonous plant (rice).

Secondary effects of increased [CO$_2$] may also have affected the diel growth course. Trees had higher biomass in 1200 ppm and therefore, shading, in particular of lower side branches increased. Light can influence cell division and expansion (Mühling et al., 1995; Granier and Tardieu, 1999; Stiles and van Volkenburgh, 2002) and thus whole-leaf growth. The influence of fluctuating environmental factors in contrast to steady state in controlled conditions on diel leaf growth will be discussed in more detail in section 4.5.
The osmotic potential that is jointly responsible for cell growth (Lockhart, 1965) is temperature de-

pendent and temperature changes were found to alter e.g. root diameter (Genárd et al., 2001). It is unlikely, however, that the observed growth decline has been caused by the slightly higher afternoon temperature conditions in the elevated [CO_2] treatment in the west bay, as these were only in the range of 1 °C on average.

Correlations between changes in the diel course of carbohydrates and of growth were observed. Glucose concentrations were reduced in elevated [CO_2], whereas starch accumulated relative to ambient conditions (Fig. 3.55). Since glucose is the central substrate for respiration, starch and cellulose synthesis, decreases of glucose concentration below a certain threshold could have dramatic effects on cell and leaf expansion (Kemp, 1981).
A first indicator for a relation between glucose and the short-term growth rates is the transient decline of the growth rate during the afternoon in elevated [CO_2]. This leads to the hypothesis, that glucose availability might be an important regulatory factor that can dampen the growth response under elevated [CO_2] and hence explain the difference between the large increase in net CO_2 exchange rate (2.4 times) and the relatively small (1.2 times) increase in leaf growth. The increased starch concentration at the same time as the decrease in glucose concentration (Fig. 3.49) indicates effects of [CO_2] on the balance of the carbohydrate metabolism and points on the necessity of analyzing pathways of starch synthesis in this context. Carbohydrates diverted to starch in the light are evidently not rapidly remobilized, leading to a reduction in afternoon growth rate. Indeed, starch concentration continues to increase in the first hours of the night, after assimilation has ceased.

A second indicator for the role of glucose availability has been observed during the night. Glucose availability, but not concentration, might be increased in growing leaves in the second half of the night under elevated [CO_2], when the starch concentration decreases rapidly (Fig. 3.49) and when the afternoon growth decline is compensated slightly by a higher RGR.

Interactions between the endogenous diel course of the growth rate and carbohydrate metabolism may also be of great importance for different responses to [CO_2] in different species. The diel growth cycle in *P. deltoides*, characterized by highest growth rates in the afternoon, is markedly different from that of other dicot shrubs and herbs that have been investigated (see also Fig. 3.26). In *Nicotiana tabacum* (Fig. 3.26, D) or *Ricinus communis*, maximal leaf growth activity is found at dawn (see Schmundt et al., 1998; Walter et al., 2002a), and is thought to be driven by remobilization of glucose from starch at night. The diel pattern in *P. deltoides* clearly places leaf growth in competition with other demands for products of contemporary photosynthesis. Leaf growth is regulated by a network of factors (Dale, 1988; Cosgrove, 1999), including diel patterns of enzyme regulation. Unfortunately, most of the investigations of elevated [CO_2] effects on enzyme activities have been conducted with tobacco (Geiger et al., 1998; Matt et al., 2001), which shows low growth rates in the afternoon. Although it is known that the diel performance of several key enzymes can be altered by elevated [CO_2], further studies of the diel regulation of carbohydrate metabolism are needed in *P. deltoides*.
In contrast to the findings of several other reports (Ludewig et al., 1998; Grimmer et al., 1999), sucrose concentrations were higher in mature than in growing leaves, but did not respond to the [CO_2] treatment (e.g. Fig. 3.49). This may reflect the long acclimation of these plants to elevated [CO_2], compared to plants in other investigations.

An enhancement of photosynthesis by a factor of 2 − 3 and of a comparable production of assimilates could not be transferred completely to growth processes as plant structures are not "designed" for such "increased input" situations, which would need further changes in function and structures for increased stability or water and nutrient transport. From the results of this study, it can be hypothesized that *P. deltoides* decelerates growth in elevated [CO_2] by control of glucose availability.

4.2.2 Spatial Leaf Growth Patterns: Heterogeneity

In the last paragraph, temporal growth patterns were discussed. Beside temporal patterns, the RGR of *P. deltoides* leaves can show a high spatial patchiness (see e.g. Fig. 3.37) and heterogeneity was increased by elevated [CO$_2$] by a factor of 1.7 (Fig. 3.39).

The results obtained on carbohydrate distribution under elevated [CO$_2$] also hint for a role in spatial heterogeneity of growth. The increased heterogeneity of leaf growth in elevated [CO$_2$] was accompanied by an increased heterogeneity of the spatial distribution of hexose concentrations (Fig. 3.53), which are the central substrates for growth processes as cell wall production. Correlations between spatial carbohydrate concentrations and growth rates are common for e.g. base-tip growth gradients (*Nicotiana tabacum* or *Ricinus communis*, Walter et al., 2002a; Walter and Schurr, 2005) and the finding that the base-to-tip gradient is not as pronounced as in tobacco, associated with the absence of a gradient in the distribution of carbohydrates (see also Sect. 3.2.1) supports this idea.

An alternative explanation would be an effect of [CO$_2$] on the spatial distribution of stomatal aperture. It was already discussed at the beginning of this section that stomata movements can alter growth by turgor changes. Investigated leaves were photosynthetically active and stomatal conductance was decreased by elevated [CO$_2$] (e.g. Fig. 3.45). The increase in heterogeneity could be caused by altered patterns of stomata movements across the leaf lamina but this hypothesis would need further investigations of stomatal patchiness due to elevated [CO$_2$], e.g. by an infiltration method as used by Küppers et al. (1999). The connection between heterogeneities in growth and stomata movements may also be supported by the comparison of leaf growth in the IFB and the growth chamber (Sect. 3.2.1). In the growth chamber, where environmental conditions were constant, heterogeneities were smaller than in the IFB-grown plants. In constant conditions, stomata were found to oscillate periodically in many plant species (Upadhyaya et al., 1988; Yang et al., 2003) with wavelengths that can range between 10 and 30 – 50 min (Ryde-Pettersson, 1992) and that are under the control of CO$_2$ and water status (Raschke, 1975). The effects of other fluctuating conditions will be discussed in more detail below. Further support comes from the study of Rascher et al. (2001) on spatio-temporal heterogeneity patterns of photosynthesis (relative quantum efficiency) in *Kalanchoë daigremontiana*. They found increased heterogeneity in times of low c_i (high rate of net CO$_2$ fixation) and low heterogeneity when stomata were closed. Sometimes these dynamic patterns of spatial and temporal heterogeneity initiated over vascular tissue, but could not be correlated with anatomical structures. Differences between vascular and interveinal tissue will also be discussed below.

Thus, the investigations on spatio-temporal patterns of growth and their relationship to photosynthesis and assimilate contents with a high resolution are important to understand complex regulatory mechanisms in plants.

4.3 Elevated CO$_2$: Photosynthesis

The stimulation of photosynthesis by elevated [CO$_2$] is often thought to be short-lived because other factors, in particular nitrogen, might become limiting in most ecosystems (Bazzaz, 1990; Schimel, 1990). Alternatively, elevated [CO$_2$] allows increased efficiency of nitrogen use (Drake et al., 1996). At Biosphere 2 Center, photosynthesis was still stimulated significantly after four years under elevated [CO$_2$], although soil nutrient availability was declining in the elevated treatment due to stimulation of plant growth and annual removal of aboveground biomass (Barron-Gafford et al., 2005). In contrast to P, Ca^{2+} and K$^+$, however, soil N was not changed at B2C (Barron-Gafford et al., 2005).

4.3.1 Gas Exchange at Elevated CO_2

Net CO_2 exchange rate of *P. deltoides* trees was significantly stimulated after four years in elevated [CO_2], by a factor of 1.6 in mature and by a factor of 2.4 in growing leaves (1200 ppm compared to 400 ppm). Stomatal conductance in mature leaves was decreased in elevated [CO_2], resulting in an increased relationship between stomatal conductance and net CO_2 exchange rate. In contrast to most of the published literature (e.g. Bunce, 1990; Griffin et al., 1996), dark respiration was increased in elevated [CO_2] (Tab. 3.7), and this finding was consistent with increased stand respiration at B2C: Barron-Gafford et al. (2005) and Murthy et al. (2005) found both, net ecosystem CO_2 uptake and respiratory CO_2 release, stimulated by elevated [CO_2], whereas belowground respiration (soil and roots) did not change.

Dark respiration measurements, in particular in elevated [CO_2] were found to be highly sensitive to artefacts (Jahnke, 2001; Jahnke and Krewitt, 2002). Therefore even a recent study of Davey et al. (2004), indicating that dark respiration may indeed increase in many species by long-term elevation of [CO_2], has to be interpreted very carefully. Up to now, it was thought that the calculated decrease in foliar respiration might increase the potential of terrestrial vegetation to sequester carbon into biomass (for review see Gonzalez-Mehler and Siedow, 1999), as terrestrial plant respiration releases 10 times more carbon per annum than fossil fuel combustion (Amthor, 1997).

Shading and fluctuating light conditions may have been the reason that mean net CO_2 exchange rates were lower when measurements were performed with the open leaf chamber (e.g. Fig. 3.45). Furthermore, light intensities at measured leaves in 1200 ppm were lower than in 400 ppm. Self-shading in elevated [CO_2] was mainly caused by increased biomass and LAI (leaf area index) of the trees. Nevertheless, maximum net CO_2 exchange rates were approximately three times higher in elevated [CO_2]. Net CO_2 exchange rates were increased in elevated [CO_2] not only in CO_2-limiting but also in light-limiting conditions (Fig. 3.47). This might have been caused by a higher carboxylase activity of Rubisco, due to the increased c_i (internal [CO_2]). Quantum yield (the initial slope of the light response curve) of single leaf photosynthesis increased in response to [CO_2] (Fig. 3.47). This could also be found for whole-stand photosynthesis (efficiency of light use by the stand) at B2C (Murthy et al., 2005). However, canopy photosynthesis might respond differently than leaf-level photosynthesis since canopies may close faster, and leaf area growth may stagnate or even be reduced due to faster initial growth and competition under increased atmospheric [CO_2] (Gielen and Ceulemans, 2001). Whole-system maximum net CO_2 influx at B2C was significantly stimulated by an average of 21 and 83 % in years 3 and 4 of the experiment (Barron-Gafford et al., 2005).

Stomata are known to be sensitive to CO_2 (Freudenberger, 1940; Heath, 1948) and aperture generally declines in elevated [CO_2] (Morison, 1987, 1998; Mansfield et al., 1990). Acclimation of stomatal numbers to elevated [CO_2] seems to be common but not universal (Drake et al., 1997; Herrick et al., 2004; Long et al., 1992). As a result of decreased stomatal conductance, transpiration was reduced in elevated [CO_2] (Fig. 3.45 or Fig. 3.46). Thus, water-use efficiency (WUE), the amount of water lost during the production of biomass of the fixation of CO_2 in photosynthesis (Lambers et al., 1998), was increased by a factor of 2 in 1200 ppm (Tab. 3.6). Values that were found are consistent with the literature (see e.g. Morison, 1985). Under normal conditions, WUE of woody C_3 plants was found to be between 2 and 11 (reviewed in Lambers et al., 1998). Reduced water loss of trees in elevated [CO_2] would also explain why trees in 400 ppm were more water stressed than trees in elevated [CO_2] in June 2003 (low LWP, Fig. 3.50).

4.3.2 Electron Transport at Elevated CO_2

Chlorophyll a fluorescence relates to the photochemical process of photosynthesis (Krause and Weis, 1988). Potential quantum yield of PS II in dark-adapted leaves, F_v/F_m, was dependent on the devel-

opmental stage but not on [CO$_2$], although higher values were found e.g. in aspen after one growing season (Ceulemans et al., 1995) . The effective quantum yield in light-adapted leaves, $\Delta F/F_m\prime$, as well as the electron transport rate (ETR), measured on attached, fully expanded leaves, were slightly increased by elevated [CO$_2$]. This is consistent with results from soybean grown under elevated [CO$_2$] (Rogers et al., 2004).

Chlorophyll fluorescence can show different limitations of photosynthesis by carbon metabolism (Hymus et al., 1999; Long and Bernacchi, 2003). The relationship between ETR and net CO$_2$ exchange rate at a given light intensity (Fig. 3.48) refers to the amount of electrons that are used per fixed molecule CO$_2$. Measurements of assimilation and electron transport could not be done on the same leaves at the same time and should be interpreted with care. However, assuming that light response curves did not change between measurements (cp. Hymus et al., 1999), and keeping limitations in mind, the relationship of the two parameters can be used to discuss general trends in elevated [CO$_2$]: In light-limiting conditions, approximately 7.1 e$^-$ were utilized per molecule CO$_2$ in fully expanded leaves. Elevated [CO$_2$] shifted the ratio to 8.4 e$^-$ per molecule CO$_2$, but due to the high variance, the difference was not significant. If the photosynthetic apparatus would have been acclimated to elevated [CO$_2$] by reduced Rubisco contents, one would have expected an even more decreased initial slope compared to ambient conditions. When light intensities were not limiting, CO$_2$ was limiting in 400 ppm, but not in 1200 ppm, where the net CO$_2$ exchange rate still rose with increasing ETR. Despite these limitations, these results indicate that photosynthesis did not show acclimation even after four years of growth under highly elevated [CO$_2$].

4.3.3 Acclimation to Elevated CO$_2$

Acclimation due to long-term elevation of [CO$_2$] is attributed to e.g. increased non-structural carbohydrate concentration within leaves (Drake et al., 1997; Rogers et al., 2004), repressing the expression of specific photosynthetic genes (Harley and Sharkey, 1991; Drake et al., 1997; Moore et al., 1999; Pego et al., 2000), commonly associated with a limitation in the capacity to utilize the additional photosynthate produced under elevated [CO$_2$] (Rogers et al., 1998; Ainsworth et al., 2003a).

However, after four years in elevated [CO$_2$], photosynthesis and growth were still stimulated significantly in *P. deltoides* and results do not indicate acclimation. The indeterminate growth habit of poplar and maintained high sink strength might be the reason for the lack of photosynthetic down-regulation (Gaudillere and Mousseau, 1988; Ceulemans et al., 1997; Gielen and Ceulemans, 2001). The hypothesis that high sink strength might reduce or even inhibit acclimation processes are supported by results of Ainsworth et al. (2003a) on *Lolium perenne* after 10 years FACE.

4.4 Impact of Elevated O$_3$ on Photosynthesis and Growth

Soybean was grown in the field in a FACE facility near Champaign-Urbana, IL, USA. Ozone concentration was elevated during daytime for the whole growing season by 20 % above ambient [O$_3$]. Ozone enters the plant through the stomata. Inside the plant, it can dissolve in water of exposed cell walls where it can stimulate the formation of reactive oxygen species (ROS) that might attack the plasma membranes (Long and Naidu, 2002).

In this study, elevated [O$_3$] did not increase necroses or chloroses compared to soybean grown in ambient conditions. This is consistent with findings reported by Fiscus et al. (1997) and Long and Naidu (2002). However, at chronic background [O$_3$] concentrations (40–80 ppb) plants can show invisible damage as decreased photosynthetic rates, before visible symptoms occur that normally manifest at higher levels of ozone (200 ppb; for review, see Ashmore, 2002; Long and Naidu, 2002).

It was shown, that during pod-filling, photosynthesis was reduced in both, mature and growing leaves, in chronically elevated [O_3]. The reduction of photosynthesis resulted in reduced carbohydrate concentrations and subsequently altered leaf growth.

4.4.1 Primary Effects of Elevated O_3: Photosynthesis

At the end of the growing season, when pod-filling had started and measurements were performed, photosynthesis was reduced in mature and growing leaves of soybean, associated with a reduction in stomatal conductance, g_S (Fig. 3.63). Stomatal density, however, was not altered by elevated [O_3] (Tab. 3.12).

The observed reduction of photosynthesis (approximately 30 % in mid August and 10 – 24 % at the end of the month) was in the range of reported reductions (Noormets et al., 2001; Hassan, 2004). A meta-analysis on elevated [O_3] effects on soybean revealed that an average elevated [O_3] of 70 ppb caused a 17 % decrease in stomatal conductance and a 23 % decrease in net carbon assimilation with parallel decreases in leaf nonstructural carbohydrates (Morgan et al., 2003).

Prior studies with soybean and other plants have suggested that the effects of elevated [O_3] on photosynthesis accumulate with leaf age (Mulchi et al., 1992; McKee et al., 1995, 2000; Zheng et al., 2002; Morgan et al., 2004). However, in this study net CO_2 exchange rate at saturating light conditions (A_{sat}) and stomatal conductance were also reduced in newly emerged leaves, and to a similar percentage as in fully expanded leaves (approximately 30 %). In determinate cultivars, this might have been explained by altered development during flowering and pod-fill, however, Spencer is an indeterminate cultivar that puts new leaves after flowering (E.A. Ainsworth, personal communication). As leaves are exposed to full sunlight and usually show maximal stomatal conductance during pod-fill (Morgan et al., 2003), more ozone can enter the leaves. This might explain why losses are highest during final stages of plant development (Morgan et al., 2003). Another possible reason is discussed below.

4.4.2 Secondary Effects of Elevated O_3: Leaf Growth and Yield

Soluble carbohydrates like glucose, fructose and sucrose were not affected by O_3 in early August, but were reduced one month later, when pod-fill was in progress. At that time of the year, starch was accumulated in mature leaves, indicating altered sugar transport. Impact of elevated [O_3] on C-transport has previously been shown for wheat (Roeb, 2001) or cotton, in which the capacity for phloem-loading was reduced (Grantz and Farrer, 1999). Accumulation of starch was also found by Mulchi et al. (1992), but also decreases or no change of starch concentrations have been reported (Britz and Robinson, 2001).

Leaf growth was affected slightly by [O_3] when pod-filling had started. The principle leaf development of soybean was not impaired by elevated [O_3], as indicated by the fact that the relationship between RLA and RGR was not affected. Final leaf area was smaller at the end of August than at the beginning of the month. This might have been caused by the shift of assimilates away from vegetative towards reproductive growth. Furthermore, a short cold period in mid August (see Fig. 2.8) caused a sharp decrease in the RGR (Fig. 3.59 and 3.60), but this would only explain the strong reduction of the final leaf area of leaf 4, as leaf 3 was already fully expanded at that time. The shift of assimilates away from vegetative growth may also explain the reduced photosynthesis rate in growing leaves, as mechanisms to repair damages caused by ozone might have been inhibited by reduced carbohydrate availability.

Reported results of effects on leaf growth show a high variability, caused by species or cultivar differences, nutrient and moisture conditions or the developmental stage. In soybean, responses range between 0 and > 80 % loss of green leaf area (Heagle et al., 1991, 1998), whereas seed yield responses

vary between losses of > 40 % and stimulation of > 50 % (Heggestad et al., 1988; Miller et al., 1994).

As photosynthesis was decreased in elevated [O_3] but not yield, it can be speculated that yield could be maintained at the mild ozone concentrations of this study at the expense of leaf growth. This hypothesis is supported by findings from the literature. Elevated [O_3] decreased photosynthesis in fully expanded leaves over the entire growing season, with the greatest decreases occurring during pod filling (Mulchi et al., 1992; Reid and Fiscus, 1998). Reductions in leaf area index and percent green leaf tissue were also greatest during pod-filling (Morgan et al., 2003). Therefore, decreased photosynthetic capacity appears to be a critical change driving yield losses in soybean subjected to elevated [O_3] (Morgan et al., 2003). Due to the importance of soybean as a crop, cultivars are bred for high yields. This might explain why yield was not affected by reduced photosynthesis rates, at the expense of leaf growth.

4.4.3 Short-term Elevation of O_3: Leaf Growth

Short-term elevation of [O_3] for two weeks in the growth chamber (70 ppb $\pm$ 10 %) had no significant effect on leaf growth; neither on leaf area nor on the diel growth course. However, the spatial RGR pattern showed increased heterogeneity in elevated [O_3], consistent with increased heterogeneity of photosynthetic rates under elevated [O_3] (C. Chen, personal communication).

As discussed already for elevated [CO_2], spatially altered stomatal conductance could alter spatial growth patterns (Sect. 4.2) and thus increase heterogeneities in growth due to local closure of stomata. As ozone enters the plant through stomata, it is further conceivable that heterogeneity of leaf RGR increases due to local damage inside the leaf, caused by reactive oxygen species (ROS) that are produced in presence of ozone.

4.5 Spatial and Temporal Growth Patterns

The importance of the relationship between small-scale effects on growth, carbohydrate contents, and photosynthesis in understanding regulatory mechanisms of growth and effects of ecofactors on plant development has already been shown. In the following section, the effects of fluctuating versus constant light and temperature conditions on leaf growth of *P. deltoides* cuttings and their relation with carbohydrate concentrations are discussed as well as differences in spatial growth of veinal and interveinal tissue.

Basically all investigated leaves and shoots in various plant species show diel growth rhythms (Walter and Schurr, 2005). To understand the control mechanisms of growth it is important to investigate the impact of changing environmental conditions on patterns of the diel RGR course, in particular if one considers that different species show different phasing in their growth rhythms. Whereas leaves of *Nicotiana tabacum* (Fig. 3.26 or Walter and Schurr, 2000, controlled conditions), *Ricinus communis* (Walter et al., 2002a, controlled conditions), *Helianthus annuus* (Boyer, 1968, controlled conditions) or *Glycine max* (Fig. 3.68, GC; Bunce, 1977, controlled and field conditions) have their growth maximum at night or the end of the night, *Phaseolus vulgaris* (Davies and van Volkenburgh, 1983) or monocots like *Zea mays* (Watts, 1974; Acevedo et al., 1979, field), *Triticum* (Christ, 1978; Kemp, 1980, controlled and field conditions, respectively) and *Oryza* (Seneweera et al., 1995) were found to grow more during daytime or at the end of the day. The diel growth rhythm was found to be endogenously controlled (e.g. Walter, 2001), but underlying mechanisms are still not fully understood and further studies are needed.

Leaves also show spatial growth patterns. The most prominent pattern is a growth gradient from

the leaf base to the leaf tip (Avery, 1933), accompanied with a gradient in cell division and/or cell expansion (Taylor et al., 1994). Surprisingly, *P. deltoides* did not show this pronounced growth gradient, however, it also does not show spatial differences in epidermal cell size across the lamina (Matsubara et al., 2005). This was also found for other poplar species (Taylor et al., 2003) and suggests that for poplar, rate and timing of cell production is more important in determining leaf shape (Matsubara et al., 2005). Also for soybean no distinct growth gradient could be found (E. A. Ainsworth, personal communication).

4.5.1   Cultivation Conditions and Diel Rhythm of Leaf Growth

The effect of fluctuating environmental factors in contrast to steady levels in controlled conditions on the diel growth cycle of *P. deltoides* was investigated on cuttings that were grown in either the IFB or a growth chamber (Sect. 3.2.1). The aim was to see to what extent environmental- and species-dependent factors determine the diel leaf growth of *P. deltoides*. The general diel leaf growth pattern of *P. deltoides* did not differ between cuttings grown in the growth chamber or the IFB, but slight differences were found in the way the RGR rose or declined. During the day, the RGR of leaves in the IFB showed high fluctuations and at midday (between 12 and 1 pm) reflections of the sun sometimes disturbed the DISP measurements.

In the growth chamber, leaf RGR did not match that of leaves in the IFB. It is possible that these differences were a result of the different temperature conditions that were stable in the growth chamber but declined in the IFB during the night. Experiments with *Ricinus communis* showed that differences in the temperature course of the air and soil could alter the growth pattern (unpublished data, Walter et al.). In wheat, the diel leaf growth rhythm seemed to be more stable in the growth chamber (Christ, 1978) and showed a reduced amplitude compared to in the field (Kemp, 1981). In contrast to the small difference in temperature of 1°C between East Bay (400 ppm) and West Bay (1200 ppm, Sect. 4.2), day temperature could differ up to 10°C between the East Bay and the growth chamber, making effects of temperature more likely. However, contrasting studies exist in literature concerning the effect of temperature on leaf growth. Whereas diel leaf growth rhythm could be inhibited by keeping the shoot apical meristem of maize at a constant temperature of 30 – 34°C (Watts, 1974), no relationship between temperature and the diel rhythm of cell division could be found for chlorophyllous root tips of *Epidendron radicans* (Bünning, 1952).

A very interesting and important question is, why different species differ in the phasing of their diel rhythms. As already mentioned, diel leaf growth is driven by endogenous control (Walter, 2001; Walter and Schurr, 2005), with processes of cell division, cell expansion, and aquaporin expression involved (Harmer et al., 2000). Circadian rhythms confer higher levels of fitness, as shown for *Arabidopsis* plants (Green et al., 2002). Endogenous oscillators that drive the rhythms are balanced permanently by exogenous environmental factors (Harmer et al., 2000).

In dicot leaves, the processes of cell division and expansion may overlap spatially as well as temporally to a considerable extent (Dale, 1988). Cell division was found to be highest at night for e.g. soybean (Bünning, 1952). On the other hand, cell expansion is known to be enhanced by light (van Volkenburgh and Cleland, 1980; Staal et al., 1994; Mühling et al., 1995). It might be possible, that the shifted phasing of diel leaf growth in different species is caused by differences in the interaction of cell division and cell expansion (see also discussion on spatial growth patterns, Sect. 4.5.2). However, to answer this question, further analyses are needed.

As carbohydrates, in particular glucose, are important substrates for growth processes like cell wall production and for energy supply, one could expect that their concentrations would correlate with the growth rate. This was the case only for starch (Fig. 3.22, D) that showed a similar diel course as the RGR. Unfortunately, this correlation would be inverse for plants like tobacco that show the same

starch course but an opposite RGR course (e.g. Christ, 2001). Hexose concentrations varied more, but were in general lower at times of high RGR (Fig. 3.22 and 3.51). Kemp (1980) found maximum carbohydrate levels in field-grown wheat in the afternoon, after the maxima in PAR, temperature, or LER (leaf elongation rate), but consistent with the findings of *P. deltoides*, no correlation between diel hexose concentrations and LER was present. Thus, it might be important to investigate carbon fluxes instead of steady-state levels, that can be several times greater than the size of the carbohydrate pool itself (Kemp, 1980). One could assume that diel hexose concentrations only limit and thus correlate with growth when they are extremely low, as can happen in deep shade, which was shown by Kemp (1981) or in section 4.2.

In fluctuating environmental conditions, an increased regulation of photosynthesis is needed compared to steady-state conditions. Kühlein et al. (2002) examined the effect of lacking feedback de-excitation (ΔpH dependent NPQ) of two *Arabidopsis* mutants in fluctuating light conditions and found no effect in constant light but decreased fitness in fluctuating light either in the field or growth chamber. In the IFB, cuttings had more leaves and as a result a larger total leaf area, but carbohydrate concentrations were lower than those of plants in the growth chamber. Thus, in the growth chamber, growth might have been inhibited more than photosynthesis, which led to an accumulation of carbon in the plants.

The temporal growth pattern of the cuttings was analyzed using a Fast Fourier Transformation (FFT). In the growth chamber, small periodic wavelengths were more pronounced than in the IFB. In particular wavelengths in the range of oscillating stomata movements were present (15 min) which often occur in constant conditions (see Sect. 4.2). Endogenous periodic patterns might not have been disturbed as under field conditions, where high non-periodic fluctuations in the environment, especially shading events, might be superimposed on periodic oscillations, in particular of stomata movements, that have to respond continuously to external ecofactors.

4.5.2 Spatial Patterns: Base-Tip-Gradient

Leaves of *P. deltoides* show a base-to-tip growth gradient with a slightly higher RGR in the middle part of the leaf (Fig. 3.20). However, the gradient is not as distinct as the gradient in tobacco (Avery, 1933). Tobacco is the only species that was investigated to a similar extent and it was thought that the base-tip-gradient was similar in all leaves of dicot plants. However, different from tobacco, *P. deltoides* (Matsubara et al., 2005) and also other poplar species or hybrids (Taylor et al., 2003) do not show a gradient in epidermal cell size along the lamina. In contrast to e.g. *P. trichocarpa*, cell division in *P. deltoides* continues until 80 – 90 % of final leaf area (van Volkenburgh and Taylor, 1996). It was thus discussed that for *P. deltoides* leaves, the lack of a pronounced base-to-tip gradient is indicative of a continuation of proliferative growth (Matsubara et al., 2005).

Accompanied with the relatively homogeneous RGR from base to tip, *P. deltoides* does not show gradients in leaf photosynthesis, investigated with chlorophyll fluorescence (Sect. 3.2.3). Spatial distribution of chlorophyll fluorescence has been examined mainly for mature leaves (Siebke and Weis, 1995; Baker et al., 2001). A few studies, however, focused on growing leaves (Meng et al., 2001; Croxdale and Omasa, 1990) and found gradients in photosynthetic performance at the leaf base and tip as well as between different tissues for tobacco (Meng et al., 2001), which shows a distinct growth gradient (Avery, 1933). Additionally, the carbohydrate concentration along the midvein did not show a clear base-to-tip gradient either, although it was shown for *P. deltoides* (Larson and Dickson, 1973) and e.g. *Nicotiana tabacum* (Turgeon and Webb, 1973) by whole-leaf autoradiography that import of labelled translocate continues into the base of a *sink-source* transition leaf after it has terminated at the tip. With the DISP method, spatial growth differences could be found between veinal and interveinal tissue, that are discussed in the next section.

4.5.3   Comparison of Veinal and Interveinal Tissue

Veinal and interveinal tissue differ in their structure and composition and it is an interesting question how this balance occurs. After leaf emergence, interveinal tissue grows mainly two-dimensionally by increasing leaf area and nearly not in thickness during the period of rapid expansion, while veins still expand in diameter and in length (Avery, 1933).

It was shown that the midvein weight correlates with the weight of the interveinal tissue (Fig. 3.27) but that the relationship was not completely linear. The vein:intervein ratio was dependent on the developmental stage of the leaf, with a higher vein part in young, fast-growing leaves (high RGR).
The improvements of the DISP method facilitate a closer look to the growth of veinal and interveinal tissue. Midveins of *P. deltoides* cuttings grew with approximately 0.71 of the growth rate of interveinal tissue. However, the ratio between midvein and interveinal tissue was dependent on the RGR of the leaf and thus the developmental stage with a higher ratio for younger leaves (Fig. 3.19). This relationship between the growth rate of veinal and interveinal tissue is supported by theoretical assumptions: with an areal increase of a factor 2 and assuming a cylindrical growth of veins, in 2 dimensions veinal tissue should grow approximately 30 % less than interveinal tissue (A. Chavarría-Krauser, unpublished model). This becomes clearer with Figure 4.1: Increase in length L of veinal and interveinal tissue should be identical. This was also found for the volumetric increase, as the increase of veinal weight correlated with the increase in interveinal weight (Fig. 3.27). Thus, assuming that interveinal tissue would not expand to a large extent in thickness (Avery, 1933), veinal area would increase with $\sqrt{W/2}$ (with width $W = 2r$), in contrast to interveinal area increase.
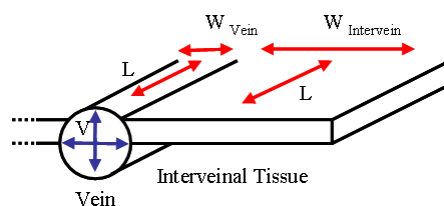
Figure 4.1: Scheme of the relationship between volumetric (V) and linear (L x W) growth of veinal and interveinal tissue.

Consistent with the results of Turgeon and Medville (1998), soluble sugar concentrations did not differ between phloem and mesophyll tissue in *P. deltoides* (Fig. 3.24 and Fig. 3.25). Starch, however, was accumulated more in interveinal tissue (photosynthetic active cells) than in veinal (transport/mechanical) tissue. Cells that surround veinal tissue have first access to sucrose that is unloaded from phloem in growing leaves and it is not surprising that veinal tissue differentiates earlier than the rest of the leaf (Avery, 1933; Esau, 1965). (1) Growth and development depend on import of nutrients and thus functional vascular bundles, and (2) veinal tissue lends stability to the still growing and non-rigid lamina.
Chloroplast development in cells surrounding the vascular bundles was found to be accelerated in many C_3 plants compared to cells of the rest of the leaf (Kinsman and Pyke, 1998). Also stomata were found to develop first around veinal tissue in *P. deltoides* (S. Mastubara, personal communication). This accelerated development in tissue surrounding veins is consistent with the finding that the RGR decreases from the midvein to the marginal tissue (Avery, 1933) and findings from the photosynthetic apparatus (Sect. 3.2.3) that showed different developmental kinetics in vein-surrounding and interveinal tissue (Fig. 3.28 and 3.29). There has been evidence that chloroplasts around veins in C_3 plants perform C_4 photosynthesis and under similar c_i, C_3 chloroplasts will have a different F_v/F_m than C_4 chloroplasts. An even more distinct effect on the different development of this parameter in veinal and

interveinal tissue was found by Walter et al. (2004) with tropical plants (*Coccoloba* and *Sanchezia*).

Support for accelerated development comes also from fluorescence induction kinetics. After dark-adaptation, leaves are exposed to light. The initial slope of $\Delta F/F_m\prime$ can reveal indications for fast processes like the electron transport and formation of a proton gradient across the thylakoid membrane. In mature leaves of *P. deltoides*, these processes start faster in the interveinal tissue, that is already fully photosynthetically active, than in the midvein (see Fig. 3.30), whereas in growing leaves, tissue surrounding the midvein showed a faster response. Walter et al. (2004) used the same protocol to study leaves of two tropical trees and found similar trends, although the differences between veinal and interveinal tissue they found were much greater than for poplar. These results show again the complexity of spatio-temporal dynamics of plant processes.

4.6 Conclusions

In this thesis the effects of the atmospheric gases $[CO_2]$ and $[O_3]$ on spatio-temporal patterns of leaf growth, photosynthesis and assimilate concentrations were investigated.
It was found that elevated $[CO_2]$ as well as elevated $[O_3]$, but also other ecofactors as light and temperature could alter spatial as well as temporal patterns of these processes:

- Elevated $[CO_2]$ induced a transient decline in the diel growth rate that was accompanied by reduced glucose concentration, indicating the importance of its availability in controlling diel growth patterns.

- Elevated $[CO_2]$ increased the heterogeneity of spatial growth patterns, accompanied with altered stomatal conductance, and again increased heterogeneity of hexose concentrations.

- Elevated $[O_3]$ also increased spatial RGR heterogeneity, which was correlated with increased heterogeneity of photosynthetic efficiency.

- Fluctuating light and temperature conditions altered temporal as well as spatial growth patterns.

It was shown, that plant growth, one of the most central processes and of crucial importance for plant development and plant performance in variable environments, was highly sensitive in terms of spatio-temporal dynamics. These complex growth dynamics are coupled with dynamics in spatio-temporal patterns of photosynthesis and assimilate availability. For a better understanding of this complexity and control of regulatory mechanisms, further studies, however, are necessary.

Further experiments should involve the connection of methods that investigate spatio-temporal dynamics of growth, photosynthesis and molecular biology. First experiments were already started that coupled the DISP method with chlorophyll fluorescence imaging (Walter et al., 2004), micro-array analysis (Matsubara et al., 2005), and theoretical growth models (Chavarría-Krauser et al., *unpublished*) but despite the improvements of the DISP method, further refining of the spatio-temporal resolution is essential for investigations of small-scale connections between the mentioned processes.

Bibliography

Acevedo, E., Fereres, E., Hsiao, T. C., Henderson, D. W., 1979. Diurnal growth trends, water potential and osmotic adjustment of maize and sorghum leaves in the field. Plant Physiology 64, 476–480.

Ainsworth, E. A., Davey, P. A., Bernacchi, C. J., Dermody, O. C., Heaton, E. A., Moore, D. J., Morgan, P. B., Naidu, S. L., Ra, H. S. Y., Zhu, X. G., Curtis, P. S., Long, S. P., 2002. A meta-analysis of elevated [CO_2] effects on soybean (*Glycine max*) physiology, growth and yield. Global Change Biology 8, 695–709.

Ainsworth, E. A., Davey, P. A., Hymus, G. J., Osborne, C. E., Rogers, A., Blum, H., Nosberger, J., Long, S. E., 2003a. Is stimulation of leaf photosynthesis by elevated carbon dioxide concentration maintained in the long term? A test with *Lolium perenne* grown for 10 years at two nitrogen fertilization levels under Free Air CO_2 Enrichment (FACE). Plant, Cell and Environment 26, 705–714.

Ainsworth, E. A., Rogers, A., Blum, H., Nosberger, J., Long, S. P., 2003b. Variation in acclimation of photosynthesis in *Trifolium repens* after eight years of exposure to Free Air CO_2 Enrichment (FACE). Journal of Experimental Botany 54, 2769–2774.

Amthor, J. S., 1997. Plant respiratory responses to elevated CO_2 partial pressure. In: Allen, L. H., Kirkham, M. B., Olszyk, D. M., Whitman, C. E. (Eds.), Advances in Carbon Dioxide Effects Research. American Society of Agronomy Special Publication, Madison, WI, pp. 35–77.

Arnon, D., 1949. Copper enzymes in isolated chloroplasts. Polyphenole oxidase in *Beta vulgaris*. Plant Physiology 24, 1–15.

Ashmore, M. R., 2002. Effects of oxidants at the whole plant and community level. In: Bell, J. N. B., Treshow, M. (Eds.), Air Pollution and Plant Life. Vol. 2. John Wiley, London, UK, pp. 89–118.

Avery, G., 1933. Structure and development of the tobacco leaf. American Journal of Botany 20, 565–592.

Baker, N. R., Oxborough, K., Lawson, T., Morison, J. I. L., 2001. High resolution imaging of photosynthetic activities of tissues, cells and chloroplasts in leaves. Journal of Experimental Botany 52, 615–621.

Barron-Gafford, G., Martens, D., Grieve, K., McLain, J. E. T., Lipson, D., Murthy, R., 2005. Growth of eastern cottonwoods (*Populus deltoides*) in elevated CO_2 stimulates stand-level respiration and rhizodeposition of carbohydrates, accelerates soil nutrient depletion, yet stimulates above and belowground biomass production. Global Change Biology 11, 1220–1233.

Bazzaz, F. A., 1990. The response of natural ecosystems to the rising global CO_2 levels. Annual Review of Ecology and Systematics 21, 167–196.

Bilger, W., Björkman, O., 1990. Role of the xanthophyl cycle in photoprotection elucidated by measurements of light-induced absorbancy changes, fluorescence and photosynthesis in leaves of *Hedera canariensis*. Photosynthesis Research 25, 173–185.

Bilger, W., Schreiber, U., Bock, M., 1995. Determination of the quantum efficiency of photosystem II and non-photochemical quenching of chlorophyll fluorescence in the field. Oecologia 102, 425–432.

Björkman, O., Demmig, B., 1987. Photon yield of O_2 evolution and chlorophyll fluorescence at 77 K among vascular plants of diverse origins. Planta 170, 489–504.

Bosac, C., 1995. Elevated CO_2 and hybrid poplar: A detailed investigation of root and shoot growth and physiology of *Populus euramericana*, 'Primo'. Forest Ecology & Management 74, 1–3.

Boyer, J. S., 1968. Relationship of water potential to growth of leaves. Plant Physiology 43, 1056–1062.

Britz, S. J., Robinson, J. M., 2001. Chronic ozone exposure and photosynthate partitioning into starch in soybean leaves. International Journal of Plant Sciences 162, 111–117.

Bunce, J. A., 1977. Leaf elongation in relation to leaf water potential in soybean. Journal of Experimental Botany 28, 156–161.

Bunce, J. A., 1990. Short- and long-term inhibition of respiratory carbon dioxide efflux by elevated carbon dioxide. Annals of Botany 65, 637–´642.

Bünning, E., 1952. Über den Tagesrhytmus der Mitosehäufigkeit in Planzen. Zeitschrift für Botanik 40, 193–199.

Calfapietra, C., Gielen, B., Sabatti, M., Angelis, P. D., Miglietta, F., Scarascia-Mugnozza, G., Ceulemans, R., 2003. Do above-ground growth dynamics of poplar change with time under CO_2 enrichment? New Phytologist 160, 305–318.

Ceulemans, R., 1996. A comparison among eucalypt, poplar and willow characteristics with particular reference to a coppice, growth-modelling approach. Biomass & Bioenergy 11.

Ceulemans, R., Jiang, X. N., Shao, B. Y., 1995. Growth and physiology of one-year old poplar (*Populus*) under elevated atmospheric CO_2 levels. Annals of Botany 75, 609–617.

Ceulemans, R., Leroux-Perez, A., Shao, B. Y., 1994. Physiology, growth and development of young poplar plants under elevated atmospheric CO_2 levels. In: Veroustraete, F., Ceulemans, R. J. M., Impens, I. I. P., Rensbergen, J. B. H. F. V. (Eds.), Vegetation Modelling and Climate Change Effects. SPB Academic Publishing, pp. 81–98.

Ceulemans, R., Mousseau, M., 1994. Effects of elevated atmospheric CO_2 on woody-plants. New Phytologist 127, 425–446.

Ceulemans, R., Taylor, G., Bosac, C., Wilkins, D., Besford, R. T., 1997. Photosynthetic acclimation to elevated CO_2 in poplar grown in glasshouse cabinets or in open top chambers depends on duration of exposure. Journal of Experimental Botany 48, 1681–1689.

Chameides, W. L., Kasibhatla, P. S., Yienger, J., Levy, H., 1994. Growth of continental-scale metro-agro-plexes, regional ozone pollution, and world food-production. Science 264, 74–77.

Christ, M. M., 2001. Interaktion von Wachstum und Kohlenhydratgehalten bei Blättern von *Nicotiana tabacum* unter Variation der Lichtverhältnisse. Diplomarbeit, Universität Heidelberg.

Christ, R. A., 1978. The elongation rate of wheat leaves. I. The elongation rates during night and day. Journal of Experimental Botany 29, 603–610.

Cosgrove, D. J., 1999. Enzymes and other agents that enhance cell wall extensibility. Annual Reviews of Plant Physiology 50, 391–417.

Croxdale, J. G., Omasa, K., 1990. Patterns of chlorophyll fluorescence kinetics in relation to growth and expansion in cucumber leaves. Plant Physiology 93, 1083–1088.

Curtis, P. S., Wang, X., 1998. A meta-analysis of elevated CO_2 effects on woody plant mass, form, and physiology. Oecologia 113, 299–313.

Dale, J. E., 1988. The control of leaf expansion. Annual Review of Plant Physiology and Plant Molecular Biology 39, 267–295.

Dann, M. S., Pell, E. J., 1989. Decline of activity and quantity of ribulose bisphosphate carboxylase/oxygenase and net photosynthesis in ozone-treated potato foliage. Plant Physiology 91, 427–432.

Darrall, N. M., 1989. The effect of air pollutants on physiological processes in plants. Plant, Cell and Environment 12, 1–30.

Davey, P. A., Hunt, S., Hymus, G. J., DeLucia, E. H., Drake, B. G., Karnosky, D. F., Long, S. P., 2004. Respiratory oxygen uptake is not decreased by an instantaneous elevation of $[CO_2]$, but is increased with long-term growth in the field at elevated $[CO_2]$. Plant Physiology 134, 520–527.

Davies, W. J., van Volkenburgh, E., 1983. The influence of water deficit on the factors controling the daily pattern of growth of *Phaseolus* trifoliates. Journal of Experimental Botany 34, 987–999.

Demmig-Adams, B., Adams III, W. W., Barker, D. H., Logan, B. A., Bowling, D. R., Verhoeven, A. S., 1996. Using chlorophyll fluorescence to assess the fraction of absorbed light allocated to thermal dissipation of excess excitation. Physiologia Plantarum 98, 253–264.

Dempster, W. F., 1999. Biosphere 2 engineering design. Ecological Engineering 13, 31–42.

Dixon, R. K., Brown, S., Houghton, R. A., Soloman, A. M., Trexler, M. C., Wisniewski, J., 1994. Carbon pools and flux of global forest ecosystems. Science 263, 185–190.

Drake, B. G., Gonzalez-Meler, M. A., Long, S. P., 1997. More efficient plants: A consequence of rising atmospheric CO_2? Annual Review of Plant Physiology and Plant Molecular Biology 48, 609–139.

Drake, B. G., Peresta, G., Beugeling, E., Matamala, R., 1996. Long term elevated CO_2 exposure in a chesapeake bay wetland: Ecosystem gas exchange, primary production, and tissue nitrogen. In: Koch, G. W., Mooney, H. A. (Eds.), Carbon Dioxide and Terrestrial Ecosystems. San Diego: Academic, pp. 197–214.

Ehleringer, J., Björkman, O., 1977. Quantum yields for CO_2 uptake in C_3 and C_4 plants. Dependence on temperture, CO_2 and O_2 concentrations. Plant Physiology 59, 86–90.

Ehret, D. L., Jolliffe, P. A., 1985. Photosynthetic carbon dioxide exchange of bean plants grown under elevated carbon dioxide concentrations. Canadian Journal of Botany 63, 2026–2030.

Esau, K., 1965. Plant Anatomy. John Wiley & Sons, Inc., NY.

Farquhar, G., Sharkey, T., 1982. Stomatal conductance and photosynthesis. Annual Review of Plant Physiology 33, 317–345.

Ferris, R., Sabatti, M., Miglietta, F., Mills, R. F., Taylor, G., 2001. Leaf area is stimulated in *Populus* by free air CO_2 enrichment (POPFACE), through increased cell expansion and production. Plant, Cell and Environment 24, 305–315.

Fiscus, E. L., Reid, C. D., Miller, J. E., Heagle, A. S., 1997. Elevated CO_2 reduces O_3 flux and O_3 induced yield losses in soybeans: Possible implications for elevated CO_2 studies. Journal of Experimental Botany 48, 307–313.

Freudenberger, H., 1940. Die Reaktion der Schliesszellen auf Kohlensäure und Sauerstoffentzug. Protoplasma 35, 15–34.

Fuhrer, J., Skarby, L., Ashmore, M. R., 1997. Critical levels for ozone effects in europe. Environmental Pollution 97, 91–106.

Gaudillere, J. P., Mousseau, M., 1988. Short-term effect of CO_2 enrichment on leaf development and gas exchange of young poplars (*Populus euramericana* cv. I 214). Oecologia Plantarum 10, 81–90.

Geiger, M., Walch-Liu, P., Engels, C., Harnecker, J., Schulze, E. D., Ludewig, F., Sonnewald, U., Scheible, W. R., Stitt, M., 1998. Enhanced carbon dioxide leads to a modified diurnal rhythm of nitrate reductase activity in older plants, and a large stimulation of nitrate reductase activity and higher levels of amino acids in young tobacco plants. Plant Cell and Environment 21, 253–268.

Genárd, M., Fishman, S., Vercambre, G., Huguet, J.-G., Bussi, C., Besset, J., Habib, R., 2001. A biophysical analysis of stem and root diameter variations in woody plants. Plant Physiology 126, 188–202.

Genty, B., Briantais, J. M., Baker, N. R., 1989. The relationship between the quantum yield of photosynthetic electron transport and quenching of chlorophyll fluorescence. Biochimica et Biophysica Acta 990, 87–92.

Gielen, B., Ceulemans, R., 2001. The likely impact of rising atmospheric CO_2 on natural and managed *Populus*: A literature review. Environmental Pollution 115, 335–358.

Golden, S. S., Ishiura, M., Johnson, C. H., Kondo, T., 1997. Cyanobacterial circadian rhythms. Annual Review of Plant Physiology and Plant Molecular Biology 48, 327–354.

Gonzalez-Mehler, M. A., Ribas-Carbo, M., Siedow, J. N., Drake, B. G., 1997. The direct inhibition of plant mitochondrial respiration by elevated CO_2. Plant Physiology 112, 1349–1355.

Gonzalez-Mehler, M. A., Siedow, J. N., 1999. The direct inhibition of mitochondrial respiratory enzymes by elevated CO_2: Does it matter at the tissue or whole-plant level? Tree Physiology 19, 253–259.

Grams, T. E. E., Anegg, S., Haberle, K. H., Langebartels, C., Matyssek, R., 1999. Interactions of chronic exposure to elevated CO_2 and O_3 levels in the photosynthetic light an dark reactions of European beech (*Fagus sylvatica*). New Phytologist 144, 95–107.

Granier, C., Tardieu, F., 1999. Leaf expansion and cell division are affected by reducing absorbed light before but not after the decline in cell division rate in the sunflower leaf. Plant, Cell & Environment 22, 1365–1376.

Grantz, D. A., Farrer, J. F., 1999. Acute exposure to ozone inhibits rapid carbon translocation from source leaves of Pima cotton. Journal of Experimental Botany 50, 1253–1262.

Green, R. M., Tingay, S., Wang, Z.-Y., Tobin, E. M., 2002. Circadian rhythms confer a higher level of fitness to *Arabidopsis* plants. Plant Physiology 129, 576–584.

Griffin, K. L., Ball, T. J., Strain, B. R., 1996. Direct and indirect effect of elevated CO_2 on whole-shoot respiration in ponderosa pine seedlings. Tree Physiology 16, 33–41.

Griffin, K. L., Turnbull, M. H., Murthy, R., Lin, G., Adams, J., Farnsworth, B., Mahato, T., Bazin, G., Potasnak, M., Yospin, M., Sachs, L., Thompson, A., Berry, J. A., 2002. *Populus deltoides* leaf respiration is differentially affected by leaf vs. ecosystem warming, results from short-term temperature manipulations. Global Change Biology 8, 479–485.

Grimmer, C., Bachfischer, T., Komor, E., 1999. Carbohydrate partitioning into starch in leaves of *Ricinus communis* L. grown under elevated CO_2 is controlled by sucrose. Plant, Cell & Environment 22, 1275–1280.

Gunderson, C. A., Wullschleger, S. D., 1994. Photosynthetic acclimation in trees to rising atmospheric CO_2: A broader perspective. Photosynthesis Research 39, 369–388.

Harley, P. C., Sharkey, T., 1991. An improved model of C_3 photosynthesis at high CO_2- reversed O_2 sensitivity explained by lack of glycerate reentry into the chloroplast. Photosynthesis Research 27, 169–178.

Harmer, S. L., Hogenesch, J. B., Straume, M., Chang, H.-S., Han, B., Zhu, T., Wang, X., Kreps, J. A., Kay, S. A., 2000. Orchestrated transcription of key pathways in *Arabidopsis* by the circadian clock. Science 290, 2110–2113.

Hassan, I. A., 2004. Interactive effects of salinity and ozone pollution on photosythesis, stomatal conductance, growth, and assimilate partitioning of wheat (*Triticum aestivum* L.). Photosynthetica 42, 111–116.

Hättenschwiler, S., Handa, I. T., Egli, L., Asshoff, R., Ammann, W., Körner, C., 2002. Atmospheric CO_2 enrichment of alpine treeline conifers. New Phytologist 156, 363–375.

Heagle, A. S., Miller, J. E., Pursley, W. A., 1998. Influence of ozone stress on soybean response to carbon dioxide enrichment: III. Yield and seed quality. Crop Science 38, 128–134.

Heagle, A. S., Miller, J. E., Rawlings, J. O., Vozzo, S. F., 1991. Effect of growth stage on soybean response to chronic ozone exposure. Journal of Environmental Quality 20, 562–570.

Heath, O. V. S., 1948. Control of stomatal movement by a reduction in the normal carbon dioxide content of the air. Nature 161, 179–181.

Heggestad, H. E., Anderson, E. L., Gish, T. J., Lee, E. H., 1988. Effects of ozone and soil water deficit on roots and shoots of field-grown soybeans. Environmental Pollution 50, 250–278.

Herrick, J. D., Maherali, H., Thomas, T. B., 2004. Reduced stomatal conductance in sweetgum (*Liquidamber styraciflua*) sustained over long-term CO_2 enrichment. New Phytologist 162, 837–396.

Houghton, J. T., Ding, Y., Griggs, D. J., Noguer, M., van der Linden, P. J., Xisaosu, D., 2001. Climate Change 2001, The scientific basis. Cambridge University Press, Cambridge, UK.

Hütt, M.-T., Neff, R., 2001. Quantification of spatiotemporal phenomena by means of cellular automata techniques. Physica A 289, 498–516.

Hymus, G. J., Ellsworth, D. S., Baker, N. R., Long, S. P., 1999. Does free-air carbon dioxide enrichment affect photochemical energy use by evergreen trees in different seasons? A chlorophyll fluorescence study of mature loblolly pine. Plant Physiology 120, 1183–1191.

IPCC, 2001. Contribution of working group I to the third assessment report of the intergovernmental panel on climate change. In: Houghton, J. T., Ding, Y., Griggs, D. J., Noguer, M., van der Linden, P. J., Xisaosu, D. (Eds.), Climate Change 2001, The scientific basis. Cambridge University Press, Cambridge, UK, p. 881pp.

Jähne, B., Haussecker, H., Geissler, P., 1999. Handbook of Computer Vision and Applications. Vol. 1–3. Academic Press, San Diego, London.

Jahnke, S., 2001. Atmospheric CO_2 concentration does not directly affect leaf respiration in bean or poplar. Plant, Cell and Environment 24, 1139–1151.

Jahnke, S., Krewitt, M., 2002. Atmospheric CO_2 concentration may directly affect leaf respiration measurement in tobacco, but not respiration itself. Plant, Cell and Environment 25, 641–651.

Jolliffe, P. A., Ehret, D. L., 1985. Growth of bean plants grown at elevated carbon dioxide concentrations. Canadian Journal of Botany 63, 2021–2025.

Jones, M. G. K., Outlaw, W. H., Lowry, O. H., 1977. Enzymatic assay of 10^{-7} to 10^{-14} moles of sucrose in plant tissue. Plant Physiology 60, 379–383.

Jouve, L., Greppin, H., Agosti, R. D., 1998. *Arabidopsis thaliana* floral stem elongation: Evidence for an endogenous circadian rhythm. Plant Physiology and Biochemistry 36, 469–472.

Kangasjärvi, J., Talvinen, J., Utriainen, M., Karjalainen, R., 1994. Plant defense systems induced by ozone. Plant, Cell and Environment 17, 783–794.

Keeling, C. D., Whorf, T. P., 2002. Atmosheric CO_2 records from sites in the SIO air sampling network. In: Trends: a compedium of data on global change. Oak Ridge, TN, USA: Carbon Dioxide Information Analysis Center, Oak Ridge National Laboratory, US Department of Energy, (http://cdiac.ornl.gov/trends/co2/sio-mlo.htm).

Kehr, J., Hustiak, F., Walz, C., Willmitzer, L., Fisahn, J., 1998. Transgenic plants changed in carbon allocation pattern display a shift in diurnal growth pattern. The Plant Journal 16, 497–503.

Kemp, D. R., 1980. Diurnal extension rates of wheat leaves in relation to temperntures and carbohydrate concentrations of the expansion zone. Journal of Experimental Botany 31, 821–828.

Kemp, D. R., 1981. The growth rate of wheat leaves in relation to the extension zone sugar concentration manipulated by shading. Journal of Experimental Botany 32, 141–150.

Kerstiens, G., 2001. Meta-analysis of the interaction between shade-tolerance,light environment and growth response of woody species to elevated CO_2. Acta Oecologica 22, 61–69.

Kinsman, E. A., Pyke, K. A., 1998. Bundle sheath cells and cell-specific plastid development in *Arabidopsis* leaves. Development 125, 1815–1822.

Kley, D., Kleinmann, M., Sanderman, H., Krupa, S., 1999. Photochemical oxidants: State of the science. Environmental Pollution 100, 19–42.

Kohut, R. J., Amundson, R. G., Laurence, J. A., Colavito, L., Van, L. P., King, P., 1987. Effects of ozone and sulphur dioxide on yield of winter wheat. Phytopathology 77, 71–74.

Körner, C., 2003a. Ecological impacts of atmospheric CO_2 enrichment on terrestrial ecosystems. Philosophical Transactions of the Royal Society of London Series A – Mathematical, Physical and Engeneering Sciences 361, 2023–2041.

Körner, C., 2003b. Nutrients and sink activity drive plant CO_2 responses – Caution with literature-based analysis. New Phytologist 159, 537–538.

Kozlowski, T. T., Kramer, P. J., Pallardy, S. G., 1991. The physiological ecology of woody plants. Academic Press, New York.

Kramer, J., 1981. Carbon dioxide concentration, photosynthesis and dry matter production. Bioscience 31, 29–30.

Krause, G. H., Weis, E., 1988. The photosynthetic apparatus and chlorophyll fluorescence. An introduction. In: Lichtenthaler, H. K. (Ed.), Applications of Chlorophyll Fluorescence in Photosynthesis Research, Stress Physiology, Hydrobiology and Remote Sensing. Kluwer Academic Publishers, pp. 3–11.

Krause, G. H., Weis, E., 1991. Chlorophyll fluorescence and photosynthesis - The basics. Annual Review of Plant Physiology and Plant Molecular Biology 42, 313–349.

Kruse, J., Hetzger, I., Mai, C., Polle, A., Rennenberg, H., 2003. Elevated pCO$_2$ affects N-metabolism of young poplar plants (*Populus tremolo* XP. alba) differently at deficient and sufficient N-supply. New Phytologist, , 157, 65–81.

Kudeyarov, V. N., Ponizovski, A. A., Bil, K. Y., Blagodatsky, S. A., Semenov, V. M., Kuznetsova, T. V., Alekseev, A. O., Kudeyarova, A. Y., Murthy, R., 2002. Soil in the intensive forestry biome at the Biosphere 2 station, Columbia University (Arizona, United States). Eurasian Soil Sciences 35 (Suppl. 1), 34–45.

Kühlein, C., Agren, J., Jansson, S., 2002. Rapid regulation of light harvestingand plant fitness in the field. Science 297, 91–93.

Küppers, M., Heiland, I., Schneider, H., Neugebauer, P. J., 1999. Light-flecks cause non-uniform stomatal opening – studies with special emphasis on *Fagus sylvatica* L. Trees 14, 130–144.

Lai, I.-L., Scharr, H., Chavarria-Krauser, A., Küsters, R., Wu, J.-T., Chou, C.-H., Schurr, U., Walter, A., 2005. Leaf growth dynamics of two congener gymnosperm tree species reflect the heterogeneity of light intensities given in their natural ecological niche. Plant, Cell and Environment doi: 10.1111/j.1365-3040.2005.01386.x.

Lambers, H., Chapin, F. S., Pons, T. L., 1998. Plant Physiological Ecology. Springer Verlag, New York.

Landau, L. D., Lifschitz, E. M., 1987. Statistische Physik I. Vol. 5 of Lehrbuch der Theoretischen Physik. Akademie-Verlag Berlin.

Larson, P. R., Dickson, R. E., 1973. Distribution of imported ^{14}C in developing leaves of eastern cottonwood according to phyllotaxy. Planta 111, 95–112.

Leadley, P. W., Reynolds, J. F., 1989. Effect of carbon-dioxide enrichment on development of the 1st 6 mainstem leaves in soybean. American Journal of Botany 76, 1551–1555.

Lecharny, A., Schwall, M., Wagner, E., 1985. Stem extension rate in light-grown plants – Effects of photoperiod and thermoperiod on the engogenous circadian-rhythm in *Chenopodium rubrum*. Plant Physiology 79, 625–629.

Lee, T. T., 1968. Effect of ozone on swelling of tobacco mitochondria. Plant Physiology 43, 133–139.

Lockhart, J., 1965. An analysis of irreversible plant cell elongation. Journal of Theoretical Biology 8, 264–275.

Long, S. P., Ainsworth, E. A., Rogers, A., Ort, D., 2004. Rising atmospheric carbon dioxide: Plants face the future. Annual Review of Plant Biology 55, 591–628.

Long, S. P., Bernacchi, C. J., 2003. Gas exchange measurements, what can they tell us about the underlying limitations to photosynthesis? Procedures and sources of error. Journal of Experimental Botany 54, 2393–2401.

Long, S. P., Drake, B. G., 1992. Photosynthetic CO_2 assimilation and rising atmospheric CO_2 concentrations. In: Baker, N. R., Thomas, H. (Eds.), Topics in Photosynthesis. Crop Photosynthesis: Spatial and Temporal Determinants, 2nd Edition. Elsevier Sci., pp. 69–107.

Long, S. P., Naidu, S. L., 2002. Effects of oxidants at the biochemical, cell and physiological levels, with particular reference to ozone. In: Bell, J. N. B., Treshow, M. (Eds.), Air Pollution and Plant Life. Vol. 2. John Wiley, London, UK, pp. 69–88.

Long, S. P., Nie, G. Y., Baker, N. R., Drake, B. G., Farage, P. K., Hendrey, G., Lewin, K. H., 1992. The implications of concurrent increases in temperature, CO_2 and tropospheric O_3 for terrestrial C_3 photosynthesis. Photosynthesis Research 34, 108–108.

Ludewig, F., Sonnewald, U., Kauder, F., Heineke, D., Geiger, M., Stitt, M., Muller-Rober, B. T., Gillissen, B., Kuhn, C., Frommer, W. B., 1998. The role of transient starch in acclimation to elevated atmospheric CO_2. Febs Letters 429, 147–151.

Lui, W. P., Kozovits, A. R., Grams, T. E. E., Blaschke, H., Rennenberg, H., Matyssek, R., 2004. Competition modifies effects of enhanced ozone/carbon dioxide concentrations on carbohydrate and biomass accumulation in juvenile Norway spruce and European beech. Tree Physiology 24, 1045–1055.

Maksymowych, R., 1973. Analysis of leaf development. Cambridge University Press, Cambridge.

Mansfield, T. A., Hetherington, A. M., Atkinson, C. J., 1990. Some current aspects of stomatal physiology. Annual Review of Plant Physiology and Plant Molecular Biology 41, 55–75.

Masle, J., 2000. The effects of elevated CO_2 on cell division rate, growth patterns and blade anatomy in young wheat plants are modulated by factors related to leaf position, vernalization and genotype. Plant Physiology 122, 1399–1415.

Matsubara, S., Hurry, V., Druart, N., Benedict, C., Chavarría-Krauser, A., Walter, A., Janzik, I., Schurr, U., 2005. Nocturnal changes in leaf growth rate are controlled by cell proliferation in *Populus deltoides*. Planta *submitted*.

Matt, P., Geiger, M., Walch-Liu, P., Engels, C., Krapp, A., Stitt, M., 2001. Elevated carbon dioxide increases nitrate uptake and nitrate reductase activity when tobacco is growing on nitrate, but increases ammonium uptake and inhibits nitrate reductase activity when tobacco is growing on ammonium nitrate. Plant Cell and Environment 24, 1119–1137.

Maxwell, K., Johnson, G. N., 2000. Chlorophyll fluorescence – A practical guide. Journal of Experimental Botany 51, 659–668.

McKee, I. F., Farage, P. K., Long, S. P., 1995. The interactive effects of elevated CO_2 and O_3 concentration on photosynthesis in spring wheat. Photosynthesis Research 45, 111–119.

McKee, I. F., Mulholland, B. J., Craigon, J., Black, C. R., Long, S. P., 2000. Elevated concentrations of atmospheric CO_2 protect against and compensate for O_3 damage to photosynthetic tissues of field-grown wheat. New Phytologist 146, 427–435.

McLeod, A. R., Long, S. P., 1999. Free-air carbon dioxide enrichment (FACE) in global change research: A review. Advances in Ecological Research 28, 1–55.

Mehlhorn, H., O'Shea, J. M., Wellburn, A. R., 1991. Atmospheric ozone interacts with stress ethylene formation by plants to cause visible plant injury. Journal of Experimental Botany 42, 17–24.

Melillo, J. M., McGuire, A. D., Kicklighter, D. W., Moore III, B., Vorosmarty, C. J., Schloss, A. L., 1993. Global climate change and terrestrial net primary production. Nature 363, 234–240.

Meng, Q. W., Siebke, K., Lippert, P., Baur, B., Mukherjee, U., Weis, E., 2001. Sink-source transition in tobacco leaves visualized using chlorophyll fluorescence imaging. New Phytologist 151, 585–595.

Meyer, W. B., Turner, B. L., 1992. Human population growth and global land-use/cover change. Annual Review of Ecology and Systematics 23, 39–61.

Miglietta, F., Peressotti, A., Vaccari, F. P., Zaldei, A., deAngelis, P., Scarascia-Mugnozza, G., 2001. Free-air CO_2 enrichment (FACE) of a poplar plantation: the POPFACE fumigation system. New Phytologist 150, 465–476.

Miller, A., Tsai, C. H., Hemphill, D., Endres, M., Rodermel, S., Spalding, M., 1997. Elevated CO_2 effects during leaf ontogeny (A new perspective on acclimation). Plant Physiology 115, 1195–1200.

Miller, J. E., Booker, F. L., Fiscus, E. L., Heagle, A. S., Pursley, W. A., Vozzo, S. F., Heck, W. W., 1994. Ultraviolet-B radiation and ozone effects on growth, yield and photosynthesis of soybean. Journal of Environmental Quality 23, 83–91.

Mills, G., Hayes, F., Buse, A., Reynolds, B., 2000. Air pollution and vegetation. In: Annual Report 1999/2000 of UN/ECE ICP Vegetation. Center for Ecology and Hydrology, Bangor, ME.

Moore, B. D., Cheng, S. H., Sims, D., Seemann, J. R., 1999. The biochemical and molecular basis for photosynthetic acclimation to elevated atmospheric CO_2. Plant, Cell and Environment 22, 567–582.

Morgan, P. B., Ainsworth, E. A., Long, S. P., 2003. How does elevated ozone impact soybean? A meta-analysis of photosynthesis, growth and yield. Plant, Cell and Environment 26, 1317–1328.

Morgan, P. B., Bernacchi, C. J., Ort, D. R., Long, S. P., 2004. An in vivo analysis of the effect of season-long open-air elevation of ozone to anticipated 2050 levels on photosynthesis in soybean. Plant Physiology 135, 2348–2357.

Morison, J. I. L., 1985. Sensitivity of stomata and water-use efficiency to high CO_2. Plant, Cell and Environment 8 (6), 467–474.

Morison, J. I. L., 1987. Intercellular CO_2 concemtration and stomatal response to CO_2. In: Zeiger, E., Cowan, I., Farquhar, G. (Eds.), Stomatal function. Stanford University Press, pp. 229–251.

Morison, J. I. L., 1998. Stomatal response to increased CO_2 concentration. Journal of Experimental Botany 49, 443–452.

Mott, K., Buckley, T. N., 2000. Patchy stomatal conductance: emergent collective behaviour of stomata. Trends in Plant Science 5, 258–262.

Mousseau, M., Saugier, B., 1992. The direct effect of increased CO_2 on gas exchange and growth of forest tree species. Journal of Experimental Botany 43, 1121–1130.

Mühling, K. H., Plieth, C., Hansen, U.-P., Sattelmacher, B., 1995. Apoplastic ph of intact leaves of *Vicia faba* as influenced by light. Journal of Experimental Botany 46, 377–382.

Mulchi, C. L., Slaughter, L., Saleem, M., Lee, E., Pausch, R., Rowland, R., 1992. Growth and physiological-characteristics of soybean in open-top chambers in response to ozone and increased atmospheric CO_2. Agriculture Ecosystems and Environment 38, 107–118.

Murthy, R., Barron-Gafford, G., Dougherty, P. M., Engel, V. C., Grieve, K., Handley, L., Potosnak, C. K. M. J., Zarnoch, S. J., Zhang, J., 2005. Increased leaf area dominates carbon flux response to elevated CO_2 in stands of *Populus deltoides* (Bartr.). Global Change Biology 11, 716–731.

Murthy, R., Griffin, K. L., Zarnoch, S. J., Dougherty, P. M., Watson, B., v. Haren, J., Patterson, R. L., Mahato, T., 2003. Carbon dioxide efflux from a 550 m^3 soil across a range of soil temperatures. Forest Ecology & Management 178, 311–327.

Nedbal, L., Soukopová, J., Kaftan, D., Whitmarsh, J., Trtílek, M., 2000. Kinetic imaging of chlorophyll fluorescence using modulated light. Photosynthesis Research 66, 3–12.

Noormets, A., McDonald, E. P., Dickson, R. E., Kruger, E. L., Sober, A., Isebrands, J. G., Karnosky, D. F., 2001. The effect of elevated carbon dioxide and ozone on leaf- and branch-level photosynthesis and potential plant-level carbon gain in aspen. Trees – Structure and Function 15, 262–270.

Norby, R. J., Kobayashi, K., Kimball, B. A., 2001. Rising CO_2 – Future ecosystems. New Phytologist 150, 215–221.

Norby, R. J., Wullschleger, S. D., Gunderson, C. A., Johnson, D. W., Ceulemans, R., 1999. Tree responses to rising CO_2 in field experiments: implications for the future forest. Plant, Cell and Environment 22, 683–714.

Nowak, R. S., Ellsworth, D. S., Smith, S. D., 2004. Functional responses of plants to elevated atmospheric CO_2 – do photosynthetic and productivity data from FACE experiments support early predictions? New Phytologist 162, 253–280.

Osmond, C., Kramer, D., Lüttge, U., 1999. Reversible, water stress-induced non-uniform chlorophyll fluorescence quenching in wilting leaves of *Potentilla reptans* may not be due to patchy stomatal responses. Plant Biology 1, 618–624.

Pearson, M., Brooks, G. L., 1995. The influence of elevated CO_2 on growth and age-related-changes in leaf gas-exchange. Journal of Experimental Botany 46, 1651–1659.

Pego, J. V., Kortstee, A. J., Huijser, G., Smeekens, S. G. M., 2000. Photosynthesis, sugars and the regulation of gene expression. Journal of Experimental Botany 51, 407–416.

Pell, E. J., Dann, M. S., 1991. Multiple stress-induced foliar senescence and implications for whole-plant longevity. In: Mooney, H. A., Winner, W. E., Pell, E. J. (Eds.), Response of Plants to Multiple Stresses. Academic Press, San Diego, CA, pp. 189–204.

Poole, I., Lawson, T., Weyers, J. D. B., Raven, J. A., 2000. Effect of elevated CO_2 on the stomatal distribution and leaf physiology of *Alnus glutinosa*. New Phytologist 145, 511–521.

Poorter, H., Navas, M. L., 2003. Plant growth and competition at elevated CO_2: on winners, losers and functional groups. New Phytologist 157, 175–198.

Prather, M., Ehhalt, D., 2001. Atmospheric chemistry and greenhouse gases. In: Houghton, J. T., et al. (Eds.), Climate Change 2001: The Scientific Basis. Cambridge U. Press, Cambridge, UK, pp. 239–287.

Prather, M., Gauss, M., Berntsen, T., Isaksen, I., Sundet, J., Bey, I., Brasseur, G., Dentener, F., Derwent, R., Stevenson, D., Grenfell, L., Hauglustaine, D., Horowitz, L., Jacob, D., Mickley, L., Lawrence, M., von Kuhlmann, R., Muller, J. F., Pitari, G., Rogers, H., Johnson, M., Pyle, J., Law, K., van der Weele M, M., Wild, O., 2003. Fresh air in the 21st century? Geophysical Research Letters 30, art. no. 1100.

Prentice, I. C., 2001. The carbon cycle and atmospheric carbon dioxide. In: Houghton, J. T., Ding, Y., Griggs, D. J., Noguer, M., van der Linden, P., Dai, X., Maskell, K., Johnson, C. A. (Eds.), Climate Change 2001: The Scientific Basis. Cambridge University Press, Cambridge, UK, pp. 183–238.

Radoglou, K. M., Jarvis, P. G., 1990b. Effects of CO_2 enrichment on 4 poplar clones. 1. Growth and leaf anatomy. Annals of Botany 65, 617–626.

Radoglou, K. M., Jarvis, P. G., 1990a. Effects of CO_2 enrichment on 4 poplar clones. 2. Leaf surface-properties. Annals of Botany 65, 627–632.

Rascher, U., Hutt, M. T., Siebke, K., Osmond, B., Beck, F., Luttge, U., 2001. Spatiotemporal variation of metabolism in a plant circadian rhythm: The biological clock as an assembly of coupled individual oscillators. Proceedings of the National Academy of Sciences of the United States of America 98, 11801–11805.

Rascher, U., Liebig, M., Luettge, U., 2000. Evaluation of instant light-response curves of chlorophyll fluorescence parameters obtained with a portable chlorophyll fluorometer on site in the field. Plant, Cell & Environment 23, 1397–1405.

Raschke, K., 1975. Stomatal action. Annual Review of Plant Physiology 26, 309–340.

Reid, C. D., Fiscus, E. L., 1998. Effects of elevated [CO_2] and/or ozone on limitations to CO_2 assimilation in soybean (*Glycine max*). Journal of Experimental Botany 49, 885–895.

Reuveni, J., Bugbee, B. T., 1997. Very high CO_2 reduces photosynthesis, dark respiration and yield in wheat. Annals of Botany 80, 539–546.

Roeb, G. W., 2001. Allocation of ^{11}C-labelled photosynthates in wheat plants. In: Horst, W. J., et al. (Eds.), Plant nutrition – food security and sustainability of agro-ecosystems. Kluwer Academic Publishers, pp. 216–217.

Rogers, A., Allen, D. J., Davey, P. A., Morgan, P. B., Ainsworth, E. A., Bernacchi, C. J., Cornic, G., Dermody, O., Dohleman, F. G., Heaton, E. A., Mahoney, J., Zhu, X. G., DeLucia, E. H., Ort, D. R., Long, S. P., 2004. Leaf photosynthesis and carbohydrate dynamics of soybeans grown throughout their life-cycle under free-air carbon dioxide enrichment. Plant, Cell and Environment 27, 449–458.

Rogers, A., Fischer, B. U., Bryant, J., Frehner, M., Blum, H., Raines, C. A., Long, S. P., 1998. Acclimation of photosynthesis to elevated CO_2 under low-nitrogen nutrition is affected by the capacity for assimilate utilization. Perennial ryegrass under free-air CO_2 enrichment. Plant Physiology 118, 683–689.

Rosenthal, Y., Farnsworth, B., Romo, F. V. R., Lin, G., Marino, B. D. V., 1999. High quality, continuous measurements of CO_2 in Biosphere 2 to assess whole mesocosm carbon cycling. Ecological Engineering 13, 249–262.

Ryde-Pettersson, U., 1992. Oscillations in the photosynthetic Calvin cycle: Examination of a mathematical model. Acta Chem Scand 46, 406–408.

Sage, R. F., 1994. Acclimation of photosynthesis to increasing atmospheric CO_2 – The gas-exchange perspective. Photosynthesis Research 39, 351–368.

Scarascia-Mugnozza, G. E., Ceulemans, R., Heilman, P. E., Isebrands, J. G., Stettler, R. F., Hinckley, T. M., 1997. Production physiology and morphology of populus species and their hybrids grown under short rotation. 2. Biomass components and harvest index of hybrid and parental species clones. Canadian Journal of Forest Research 27, 285–294.

Scharr, H., 2005. Optimal filters for extended optical flow. In: International Workshop on Complex Motion, LNCS 3417.

Schimel, D., 1990. Biogeochemical feedbacks in the earth system. In: Leggett, J. (Ed.), Global warming. The Greenpeace report. Oxford University Press, pp. 68–82.

Schmundt, D., Stitt, M., Jaehne, B., Schurr, U., 1998. Quantitative analysis of local growth rates of dicot leaves at high temporal and spatial resolution, using image sequence analysis. Plant Journal 16, 505–514.

Schreiber, U., Bilger, W., 1993. Progress in chlorophyll fluorescence research: Major developments during the past years in retrospect. In: Behnke, H. D., et al. (Eds.), Progress in Botany. Vol. 54. Springer Verlag, Berlin Heidelberg, pp. 151–173.

Schurr, U., 1998. Growth physiology: Approaches to a spatially and temporarily varying problem. In: Behnke, H. D., Lüttge, U., Esser, K., Kadereit, J. W., Runge, M. (Eds.), Progress in Botany. Springer Verlag, Berlin, pp. 355–373.

Seneweera, S. P., Basra, A. S., Barlow, E. W., Conroy, J. P., 1995. Diurnal regulation of leaf blade elongation in rice by CO_2. Plant Physiology 108, 1471–1477.

Siebke, K., Weis, E., 1995. Imaging of chlorophyll-a-fluorescence in leaves: Topography of photosynthetic oscillations in leaves of *Glechoma hederacea*:. Photosynthesis Research 45, 225–237.

Staal, M., Elzenga, J. T. M., van Elk, A. G., Prins, H. B. A., van Volkenburgh, E., 1994. Red and blue light-stimulated proton efflux by epidermal leaf cells of the Argenteum mutant of *Pisum sativum*. Journal of Experimetnal Botany 45, 1213–1218.

Stiles, K. A., van Volkenburgh, E., 2002. Light-regulated leaf expansion in two *Populus* species: Dependence on developmentally controlled ion transport. Journal of Experimental Botany 53, 1651–1657.

Stitt, M., 1991. Rising CO_2 levels and their potential significance for carbon flow in photosynthetic cells. Plant, Cell and Environment 14, 741–762.

Stockwell, W. R., Kramm, G., Scheel, H.-E., Mohnen, V. A., Seiler, W., 1997. Ozone formation, destruction and exposure in Europe and the United States. In: Sandermann, H., Wellburn, A. R., Heath, R. L. (Eds.), Forest decline and ozone. Springer-Verlag, Berlin, Heidelberg, pp. 1–38.

Taylor, G., Ranasinghe, S., Bosac, C., Gardner, S. D. L., Ferris, R., 1994. Elevated CO_2 and plant-growth – Cellular mechanisms and responses of whole plants. Journal of Experimental Botany 45, 1761–1774.

Taylor, G., Tricker, P. J., Zhang, F. Z., Alston, V. J., Miglietta, F., Kuzminsky, E., 2003. Spatial and temporal effects of free-air CO_2 enrichment (POPFACE) on leaf growth, cell expansion, and cell production in a closed canopy of poplar. Plant Physiology 131, 177–185.

Tjoelker, M. G., Oleksyn, J., Reich, P. B., 1998. Seedlings of five boreal tree species differ in acclimation of net photosynthesis to elevated CO_2 and temperature. Tree Physiology 18, 715–726.

Tjoelker, M. G., Volin, J. C., Oleksyn, J., Reich, P. B., 1995. Interaction of ozone pollution and light effects on photosynthesis in a forest canopy experiment. Plant, Cell and Environment 18, 895–905.

Tricker, P. J., Calfapietra, C., Kuzminsky, E., Puleggi, R., Ferris, R., Nathoo, M., Pleasants, L. J., Alston, V., de Angelis, P., Taylor, G., 2004. Long-term acclimation of leaf production, development, longevity and quality following 3 yr exposure to free-air CO_2 enrichment during canopy closure in *Populus*. New Phytologist 162, 413–426.

Turgeon, R., Medville, R., 1998. The abscence of phloem loading in willow leaves. Proceedings of the National Academy of Sciences 95, 12055–12060.

Turgeon, R., Webb, J. A., 1973. Leaf development and phloem transport in *Cucurbita pepo*: Transition from import to export. Planta 113, 179–191.

Turnbull, M. H., Murthy, R., Griffin, K. L., 2002. The relative impact of daytime and night-time warming on photosynthetic capacity in *Populus deltoides*. Plant, Cell & Environment 25, 1729–1737.

Umweltbundesamt, 1991. Jahresbericht 1990. Berlin.

Upadhyaya, S. K., Rand, R. V., Crooke, J. R., 1988. Role of stomatal oscillations on transpiration, assimilation and water use efficiency of plants. Ecological Modelling 41, 27–40.

van der Weele, C. M., Jiang, H. S., Palaniappan, K. K., Ivanov, V. B., Palaniappan, K., Baskin, T. I., 2003. A new algorithm for computational image analysis of deformable motion at high spatial and temporal resolution applied to root growth. Roughly uniform elongation in the meristem and also, after an abrupt acceleration, in the elongation zone. Plant Physiology 132, 1138–1148.

van Kooten, O., Snel, J. F. H., 1990. The use of chlorophyll fluorescence nomenclature in plant stress physiology. Photosynthesis Research 25, 147–150.

van Volkenburgh, E., 1999. Leaf expansion – An integrating plant behaviour. Plant, Cell and Environment 22, 1463–1473.

van Volkenburgh, E., Cleland, R. E., 1980. Proton excretion and cell expansion in bean leaves. Planta 148, 273–278.

van Volkenburgh, E., Taylor, G., 1996. Leaf growth physiology. In: Stettler, R. F., Bradshaw, H. D. J., Heilman, P. E., Hinckley, T. M. (Eds.), Biology of *Populus*. Ottawa: NRC Research Press, pp. 283–299.

Vessey, J. K., Henry, L. T., Raper, C. D., 1990. Nitrogen nutrition and temporal effects of enhanced carbon-dioxide on soybean growth. Crop Science 30, 287–294.

Vogelmann, T. C., Larson, P. R., Dickson, R. E., 1982. Translocation pathways in the petioles and stem between source and sink leaves of *Populus deltoides* Bartr. ex. Marsh. Planta 156, 345–358.

Wait, D. A., Jones, C. G., Wynn, J., Woodward, F. I., 1999. The fraction of expanding to expanded leaves determines the biomass response of *Populus* to elevated CO_2. Oecologia 121, 193–200.

Walter, A., 1997. Quantitative Analyse des Wachstums von *Nicotiana tabacum* unter besonderer Berücksichtigung des Sink-Source-Verhaltens. Diplomarbeit, Universität Heidelberg.

Walter, A., 2001. Räumliche und zeitliche Wachstumsmuster in Wurzeln und Blättern dikotyler Pflanzen. Ph.d. thesis, Universität Heidelberg.

Walter, A., Christ, M. M., Barron-Gafford, G. A., Grieve, K. A., Paige, T., Murthy, R., Rascher, U., 2005. The effect of elevated CO_2 on diel leaf growth cycle, leaf carbohydrate content and canopy growth performance of *Populus deltoides*. Global Change Biology 11, 1207–1219.

Walter, A., Feil, R., Schurr, U., 2002a. Restriction of nyctinastic movements and application of tensile forces to leaves affects diurnal patterns of expansion growth. Functional Plant Biology 29, 1247–1258.

Walter, A., Lambrecht, S. C., 2004. Biosphere 2 Center as a unique tool for environmental studies. Journal of Environmental Monitoring 6, 267–277.

Walter, A., Rascher, U., Osmond, C. B., 2004. Transitions in photosynthetic parameters of midvein and interveinal regions of leaves and their importance during leaf growth and development. Plant Biology 6, 184–191.

Walter, A., Schurr, U., 1999. The modular character of growth in *Nicotiana tabacum* plants under steady-state nutrition. Journal of Experimental Botany 50, 1169–1177.

Walter, A., Schurr, U., 2000. Spatial variability of leaf development, growth and function. In: Marshall, B., Roberts, J. (Eds.), Leaf Development and Canopy Growth. Sheffield: Sheffield Academic Press, pp. 96–118.

Walter, A., Schurr, U., 2005. Dynamics of leaf and root growth – Endogenous control versus environmental impact. Annals of Botany 95, 891–900.

Walter, A., Spies, H., Terjung, S., Kusters, R., Kirchgessner, N., Schurr, U., 2002b. Spatio-temporal dynamics of expansion growth in roots: Automatic quantification of diurnal course and temperature response by digital image sequence processing. Journal of Experimental Botany 53, 689–698.

Wang, Z., Pan, Q., Quebedeaux, B., 1999. Carbon partitioning into sorbitol, sucrose, and starch in source and sink apple leaves as affected by elevated CO_2. Environmental & Experimental Botany 41, 39–46.

Watts, W. R., 1974. Leaf extension in *Zea mays*. Journal of Experimental Botany 25, 1085–1096.

Weyers, J. D. B., Lawson, T., 1997. Heterogeneity in stomatal characteristics. Advances in botanical research incorporating advances in plant pathology 26, 317–352.

Wheeler, R. M., Mackowiak, C. L., Siegriest, L. M., Sager, J. C., 1993. Supraoptimal carbon dioxide effects on growth of soybean [*Glycine max* (L.) Merr.]. Journal of Plant Physiology 142, 173–178.

Wolf, S., Silk, W., Plant, R., 1986. Quantitative patterns of leaf expansion: comparision of normal and malformed leaf growth in *Vitis vinifera* cv. Ruby Red. American Journal of Botany 73, 832–846.

Wong, S. C., 1990. Elevated atmospheric partial-pressure of CO_2 and plant growth. 2. Nonstructural carbohydrate content in cotton plants and its effect on growth-parameters. Photosynthesis Research 23, 171–180.

Yang, H.-M., Zhang, X.-Y., Wang, G.-X., Li, Y., Wei, X.-P., 2003. Cytosolic calcium oscillations may induce stomatal oscillation in *Vicia faba*. Plant Science 165, 1117–1122.

Zabel, B., Hawes, P., Hewitt, S., Marino, B. D. V., 1999. Construction and engineering of a created environment: Overview of the Biosphere 2 closed system. Ecological Engineering 13, 43–63.

Zheng, Y., Shimizu, H., Barnes, J. D., 2002. Limitations to CO_2 assimilation in ozone-exposed leaves of *Plantago major*. New Phytologist 155, 67–78.

List of Figures

List of Tables

Appendix A

Parameters and Filter Settings for DISP Analysis

Parameters of DISP Analysis

tau: structure tensor parameter, when an *eigenwert* will be accepted as *zero* (e.g. 0.05)

noise: structure tensor parameter, must not be higher than three times *tau* (e.g. 0.149)

pyrstufe: Pyramid level used for calculation (0 = all data, 1 = 1/4 of image): 1

pyr_st: Pyramid level used in the structure tensor: 1

pyr_out: Pyramid level of the saved data: 1

threshold: Grey value threshold for the mask, that separates the background from the leaf structure: 15 – 35

hochpasssize: Size of the high pass filter, that is used to adjust the brightness of images: 21

b_rec_x and b_rec_y: Recursive filter value for regularization in x and y direction (smoothing fraction: 0,1 = nothing happens, 1,0 = only smoothing): 0.55,0.45 or 0.8,0.2

viter: Number of non-recursive iterations in regularization: 5

viter_rec: Number of recursive iterations in regularization: 10

vsmooth: Smoothness parameter in the regularization: 1000

Filter settings (auto)

For more information about filter settings see also Scharr (2005).

Dx: 0.0130 0.1190 0.2232 0 -0.2232 -0.1190 -0.0130

Dx_y: 0.0031 0.0583 0.2461 0.3845 0.2461 0.0583 0.0031

Dx_t: 0.0031 0.0583 0.2461 0.3845 0.2461 0.0583 0.0031

Dy: 0.0130 0.1190 0.2232 0 -0.2232 -0.1190 -0.0130

Dy_x: 0.0031 0.0583 0.2461 0.3845 0.2461 0.0583 0.0031

Dy_t: 0.0031 0.0583 0.2461 0.3845 0.2461 0.0583 0.0031

Dt: 0.0130 0.1190 0.2232 0 -0.2232 -0.1190 -0.0130

Dt_x: 0.0031 0.0583 0.2461 0.3845 0.2461 0.0583 0.0031

Dt_y: 0.0031 0.0583 0.2461 0.3845 0.2461 0.0583 0.0031

B_x: 0.00390625 0.03125 0.109375 0.21875 0.2734375 0.21875 0.109375 0.03125 0.00390625

B_y: 0.00390625 0.03125 0.109375 0.21875 0.2734375 0.21875 0.109375 0.03125 0.00390625

B_t: 0.0625 0.25 0.375 0.25 0.0625

pypre: 0.00390625 0.03125 0.109375 0.21875 0.2734375 0.21875 0.109375 0.03125 0.00390625

pypost: 0.25 0.5 0.25

pyipol: -0.0625 0.5625 0.5625 -0.0625

Filter Settings (small)

Dx: 0.5 0 -0.5

Dx_y: 0.1875 0.625 0.1875

Dx_t: 0.1875 0.625 0.1875

Dy: 0.5 0 -0.5

Dy_x: 0.1875 0.625 0.1875

Dy_t: 0.1875 0.625 0.1875

Dt: 0.5 0 -0.5

Dt_x: 0.1875 0.625 0.1875

Dt_y: 0.1875 0.625 0.1875

B_x: 0.0625 0.25 0.375 0.25 0.0625

B_y: 0.0625 0.25 0.375 0.25 0.0625

B_t: 0.0625 0.25 0.375 0.25 0.0625

pypre: 0.0625 0.25 0.375 0.25 0.0625

pypost: 0.25 0.5 0.25

pyipol: -0.0625 0.5625 0.5625 -0.0625

Acknowledgements

I thank my supervisors Prof. Uli Schurr and Achim Walter for the subject of this Ph.D. thesis, their support and the discussions, and PD Dirk Gansert for being my co-referee.

For discussions, help with measurements, programs and machines, as well as support for social life I want to thank Andreas Averesch, Lisa Ainsworth, Bernd Biskup, Andrés Chavarría, Charles Chen, Georg Dreissen, Michaela Ernst, Andreas Fischbach, Frank Gilmer, Katie Grieve, Liezel Gouws, Ingar Janzik, Norbert Kirchgessner, Ralf Küsters, I-Ling Lai, Andrew Leaky, Stephen Long, Annelie Lorenz, Shizue Matsubara, Kate Morrissey, Kerstin Nagel, Maria Naumann, Barry Osmond, Roland Pieruschka, Uwe Rascher, Hanno Scharr, Stefan Terjung, Liz Tilley, Beate Uhlig, Olivia Virnich, Anika Wiese, as well as the Biosphere 2 Team, the ICG III staff, and the good ol' Heidelberg group... Angelika Simons I want to thank for the great help with the officialism. My friends I thank for being my friends although they know me.

My family, in particular my parents, I want to thank for their support and that they helped me to become the person I am and of course for the way they led me to explore the secrets of plants from the very beginning on.

My special thanks go to Andrés for his love and for belaying me.
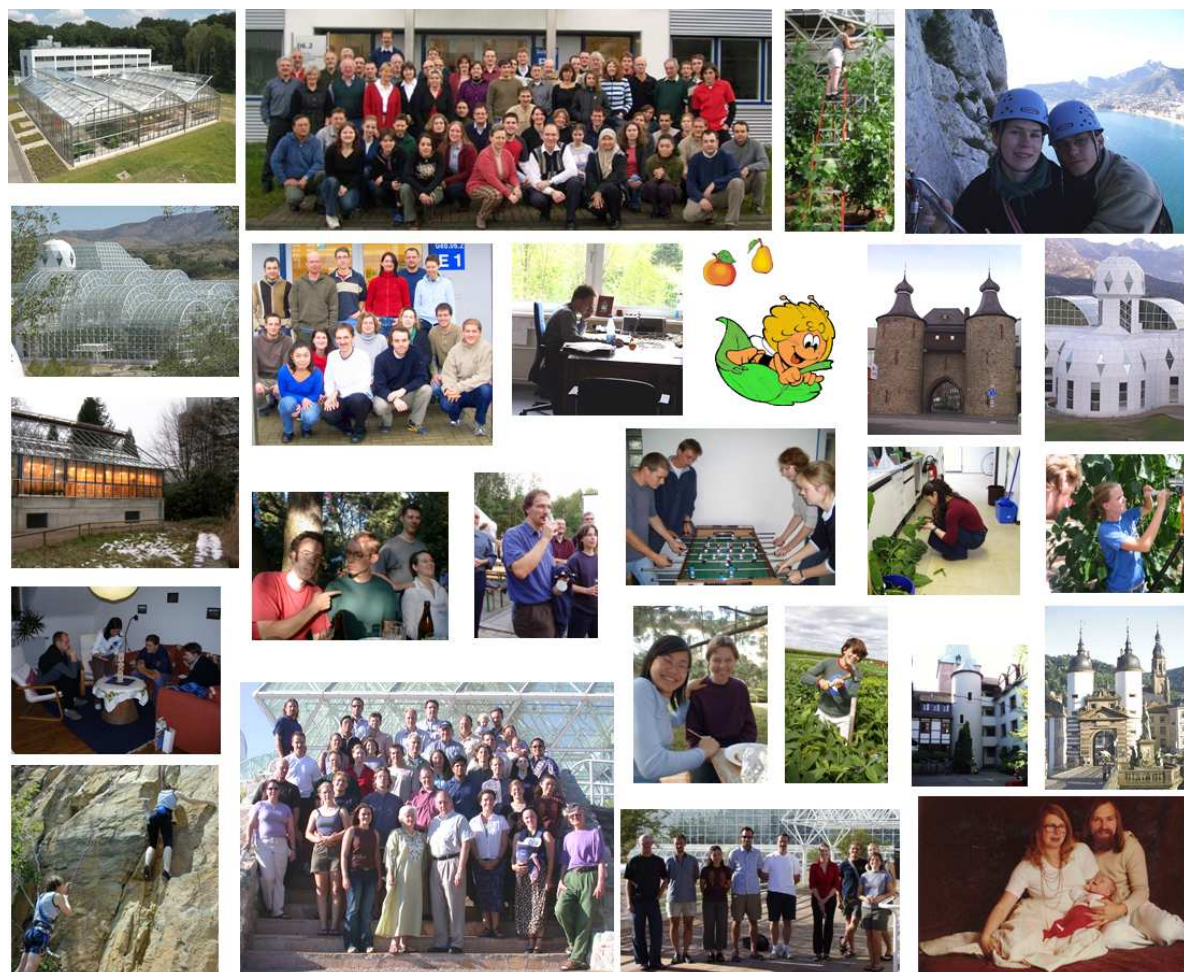
Many of the used programs were developed in our group and I thank the people for providing these programs: *algotest*: G. Dreissen and H. Scharr; *Aufnahme3.1*, *AufnahmeFire*, *energy*, *fft*, *GrowFlow* and *RGRFlow*: A. Chavarría-Krauser; Algorithms for DISP analysis: H. Scharr and A. Chavarría-Krauser